WCAP-10637

WESTINGHOUSE CLASS 3
CUSTOMER DESIGNATED DISTRIBUTION

ANALYSIS OF CAPSULES T-330 AND W-290 FROM THE CONSUMERS POWER COMPANY PALISADES REACTOR VESSEL RADIATION SURVEILLANCE PROGRAM

M. K. Kunka
C.A. Cheney

September 1984

Work performed under Shop Order Nos. ENVJ-106 and ENVJ-450

APPROVED: T A Meyer
T. A. Meyer, Manager
Structural Materials and Reliability Technology

Prepared by Westinghouse for the Consumers Power Company

Although information contained in this report is nonproprietary, no distribution shall be made outside Westinghouse or its licensees without the customer's approva'

WESTINGHOUSE ELECTRIC CORPORATION
Nuclear Energy Systems
P.O. Box 355
Pittsburgh, Pennsylvania 15230

PREFACE

This report has been technically reviewed and verified.

	Reviewer	
Sections 1 through 5 and 7	S. E. Yanichko	S. E. Yanichko
Section 6	S. L. Anderson	S. L. Anderson

TABLE OF CONTENTS

LIST OF TABLES

LIST OF TABLES (cont.)

LIST OF TABLES (cont.)

LIST OF TABLES (cont.)

LIST OF ILLUSTRATIONS

LIST OF ILLUSTRATIONS (cont.)

LIST OF ILLUSTRATIONS (cont.)

LIST OF ILLUSTRATIONS (cont.)

LIST OF ILLUSTRATIONS (cont.)

SECTION 1
SUMMARY OF RESULTS

The analysis of the material contained in Capsule T-330, the first thermal surveillance capsule removed from the Consumers Power Company's Palisades reactor pressure vessel, led to the following conclusions:

- o The weld and heat-affected zone metal has experienced a 60-70°F shift in the ductile to brittle transition temperatures due to exposure to elevated temperature.

The analysis of the material contained in Capsule W-290, the second irradiated surveillance capsule to be removed from the Consumers Power Company Palisades reactor pressure vessel, led to the following conclusions:

- o The capsule received an average fast neutron fluenc (E>1.0Mev) of 1.09×10^{19} n/cm^2.

- o Irradiation of the reactor vessel intermediate shell course plate D-3803-1, to 1.09×10^{19} n/cm, resulted in 30 and 50 ft-lb transition temperature increases of 155 and 160°F, respectively, for specimens oriented perpendicular to the principal rolling direction (transverse orientation), and 175°F and 180°F, respectively, for specimens oriented parallel to the principal rolling direction (longitudinal orientation).

- o Weld metal irradiated to 1.09×10^{19} n/cm^2 resulted in 30 and 50 ft-lb transition temperature increase of 290 and 300°F, respectively.

- o The average upper shelf energy of all the surveillance materials remained above 50 ft-lbs, thereby providing adequate toughness for continued safe plant operation.

- Comparison of the 30 ft-lb transition temperature increases for the Palisades surveillance material with predicted increases using the methods of NRC Regulatory Guide 1.99, Revision 1, shows that the weld metal transition temperature increase was greater than predicted. It is suspected that the relatively high nickel content of the weld metal contributed to the greater than predicted transition temperature increase experienced by the weld metal.

SECTION 2
INTRODUCTION

This report presents the results of the examinations of Capsule T-330, a thermal surveillance capsule, and Capsule W-290, an irradiated surveillance capsule, removed from the Palisades reactor vessel during a Fall of 1983 outage. Throughout the operating life of the Palisades Nuclear Plant the thermal capsule, Capsule T-330, was located above the reactor core and was exposed only to the elevated temperature of reactor operation. Capsule W-290, the second irradiated surveillance capsule to be removed from the Palisades reactor vessel, is part of the continuing program which monitors the effects of neutron irradiation, on the encapsulated materials, under actual operation conditions.

The Palisades nuclear reactor is a pressurized water reactor built by Combustion Engineering Inc. The surveillance program for the reactor pressure vessel was designed by Combustion Engineering Inc. to the requirements of ASTM E185-66. A complete description of the surveillance program has been reported by Combustion Engineering Inc.[1]. This report summarizes the testing of and postirradiation data obtained from Capsules T-330 and W-290 removed from the Palisades reactor vessel, and discusses the analysis of these data. The data are compared to the results of tests performed on unirradiated material as reported by Battelle Columbus Laboratories[2].

SECTION 3
BACKGROUND

The ability of the large steel pressure vessel containing the reactor core and its primary coolant to resist fracture constitutes an important factor in ensuring safety in the nuclear industry. The beltline region of the reactor pressure vessel is the most critical region of the vessel because it is subjected to significant fast neutron bombardment. The overall effects of fast neutron irradiation on the mechanical properties of low alloy ferritic pressure vessel steels such as SA-302 (Modified) Grade B (base material of the Palisades reactor pressure vessel beltline) are well documented in the literature. Generally, low alloy ferritic materials show an increase in hardness and tensile properties and a decrease in ductility and toughness under certain conditions of irradiation.

A method for performing analyses to guard against fast fracture in reactor pressure vessels has been presented in "Protection Against Non-ductile Failure," Appendix G to Section III of the ASME Boiler and Pressure Vessel Code. The method utilizes fracture mechanics concepts and is based on the reference nil-ductility temperature, RT_{NDT}.

The initial RT_{NDT} is defined as the greater of either the drop weight nil-ductility transition temperature (NDTT per ASTM E-208) or the temperature 60°F less than the 50 ft lb (and 35-mil lateral expansion) temperature as determined from Charpy specimens oriented normal (transverse) to the major working direction of the material. The RT_{NDT} of a given material is used to index that material to a reference stress intensity factor curve (K_{IR} curve) which appears in Appendix G of the ASME Code. The K_{IR} curve is a lower bound of dynamic, crack arrest, and static fracture toughness results obtained from several heats of pressure vessel steel. When a given material is indexed to the K_{IR} curve, allowable stress intensity factors can be obtained for this material as a function of temperature. Allowable operating limits can then be determined utilizing these allowable stress intensity factors.

RT_{NDT} and, in turn, the operating limits of nuclear power plants can be adjusted to account for the effects of radiation on the reactor vessel material properties. The radiation embrittlement or changes in mechanical properties of a given reactor pressure vessel steel can be monitored by a reactor surveillance program, in which a surveillance capsule is periodically removed from the operating nuclear reactor and the encapsulated specimens are tested. The increase in the average Charpy V-notch 30 ft-lb temperature (ΔRT_{NDT}) due to irradiation is added to the original RT_{NDT} to adjust the RT_{NDT} for radiation embrittlement. This adjusted RT_{NDT} (RT_{NDT} initial + ΔRT_{NDT}) is used to index the material to the K_{IR} curve and, in turn, to set operating limits for the nuclear power plant which take into account the effects of irradiation on the reactor vessel materials. RT_{NDT} can also be adjusted by using radiation damage trend curves such as those identified in NRC Regulatory Guide 1.99 Revision 1.

SECTION 4
DESCRIPTION OF PROGRAM

Eight surveillance capsules for monitoring the effects of neutron exposure on the Palisades reactor pressure vessel core region material were inserted in the reactor vessel prior to initial plant startup. Six of these capsules were positioned on the inner wall of the reactor vessel ("wall" capsules), while the other two capsules were positioned closer to the core, on the outer wall of the core support barrel ("accelerated" capsules). Figure 4-1 shows the location of the various irradiation surveillance capsule assemblies within the Palisades pressure vessel.

Two surveillance capsules for monitoring the effects of operating temperature on the Palisades reactor pressure vessel material were also inserted prior to plant startup. In Figure 4-1, note their location in relation to the reactor core.

Capsules T-330 and W-290 were removed after 4.975 effective full power years of plant operation. Per reference (1), the Combustion Engineering description of the Palisades surveillance program, each of these capsules contained Charpy V-notch impact and tensile test specimens (Figure 4-2) from the intermediate shell course plate, from submerged arc weld metal representative of the core region of the reactor vessel, and from the weld heat-affected zone (HAZ) material.

The chemistry of the surveillance materials, as reported by Combustion Engineering[1], are presented in Table 4-1. The chemical analyses reported in Table 4-1 were obtained from unirradiated material used in the surveillance program. The surveillance plate material was cut directly from the intermediate shell course plate, and thus received the same heat treatment. The surveillance material received 1 3/4 hours interstage and 30 hours final heat, at 1150 ± 25°F[1]. The base metal test material was fabricated from plate no. D-3803-1. The weld metal test material was fabricated by welding together intermediate shell plate nos. D-3803-1 and D-3803-2. The heat-affected zone test material was fabricated by welding together intermediate shell plate nos. D-3803-2 and D-3803-3. In their summary report on the Palisades surveillance program(1), Combustion Engineering explains that the root welds, of both the weld and HAZ surveillance material, were manually welded with an 8018-E Class 3 rod (note the backgroove area highlighted in Figure 4-3), and then chipped back after a given amount of face weld was established. The face welds were made by a submerged arc process, using a MIL-B4 electrode and a simultaneous 1/16" diameter Nickel-200 wire feed.

All the plate test specimens represent material taken at least one plate thickness from any water quenched edge. Charpy specimens were machined from the plate in both the longitudinal (major axis of specimen is parallel to the principal rolling direction) and transverse (major axis of the specimen is perpendicular to the principal rolling direction) orientations. Tensile specimens were machined from the plate with the major axis of the specimen parallel to the principal rolling direction. Charpy V-notch and tensile specimens from the heat-affected zone were oriented with the major axis of the specimens transverse to the welding direction. The root of the Charpy specimen notches were centered on the fusion line between the base metal and weld metal. For the weld metal specimens, the Charpy V-notch specimens were oriented with the major axis of the specimen transverse to the welding direction, while the tensile specimens were oriented with the major axis of the specimen parallel to the welding direction.

The flux monitors were fabricated using six materials as neutron threshold detectors -- uranium, sulfur, iron, nickel, copper and titanium. Two sets of flux monitors were installed in each tensile-monitor compartment. One set of flux monitors, consisting of the six different materials, are used to determine the neutron spectrum. Each detector was placed inside a grooved 1/8-inch sheath of 304 stainless steel (plain quartz in the case of sulfur) which is used to identify the material and to facilitate handling. Cadmium covers were used for those materials which have competing thermal activities (i.e., uranium, nickel and copper). The second set of monitors is composed of iron wires placed inside a grooved 1/16-inch sheath of 304 stainless steel, and they serve to evaluate the flux attenuation through the thickness of the Charpy specimen.

The temperature monitor assemblies consist of four separate monitors, each of a different composition and thus having a different melting point. The four alloys and their melting points are:

92.5% Pb, 5.0% Sn, 2.5% Ag	Melting Point of 536°F
90.0% Pb, 5.0% Sn, 5.0% Ag	Melting Point of 558°F
97.5% Pb, 2.5% Ag	Melting Point of 580°F
97.5% Pb, 0.75% Sn, 1.75% Ag	Melting Point of 590°F

TABLE 4-1
CHEMICAL COMPOSITION OF THE PALISADES REACTOR VESSEL SURVEILLANCE MATERIALS

Chemical Composition (WT-%)
(Combustion Engineering Analyses[1])

Element	Base Material,[a] Plate D-3803-1	Plate D-3803-2	Plate D-3803-3	HAZ Weld Material[b] Root	HAZ Weld Material[b] Face	Weld Metal[c] Root	Weld Metal[c] Face
Si	.23	.32	.24	.24	.25	.25	.22
S	.019	.021	.020	.009	.010	.010	.010
P	.011	.012	.010	.011	.012	.011	.011
Mn	1.55	1.43	1.56	1.08	1.03	1.01	1.02
C	.22	.23	.21	.098	.080	.088	.086
Cr	.13	.42	.13	.05	.04	.05	.03
Ni	.53	.55	.53	.43	1.28	.63	1.27
Mo	.58	.58	.59	.54	.53	.55	.52
Al	.037	.022	.037	Nil	Nil	Nil	Nil
V	.003	.003	.003	Nil	Nil	Nil	Nil
Cu	.25	.25	.25	.25	.20	.26	.22

(a) Used to fabricate base metal test specimens.

(b) Fabricated by welding plate D-3803-2 to plate D-3803-3.

(c) Fabricated by welding plate D-3803-1 to plate D-3803-2.

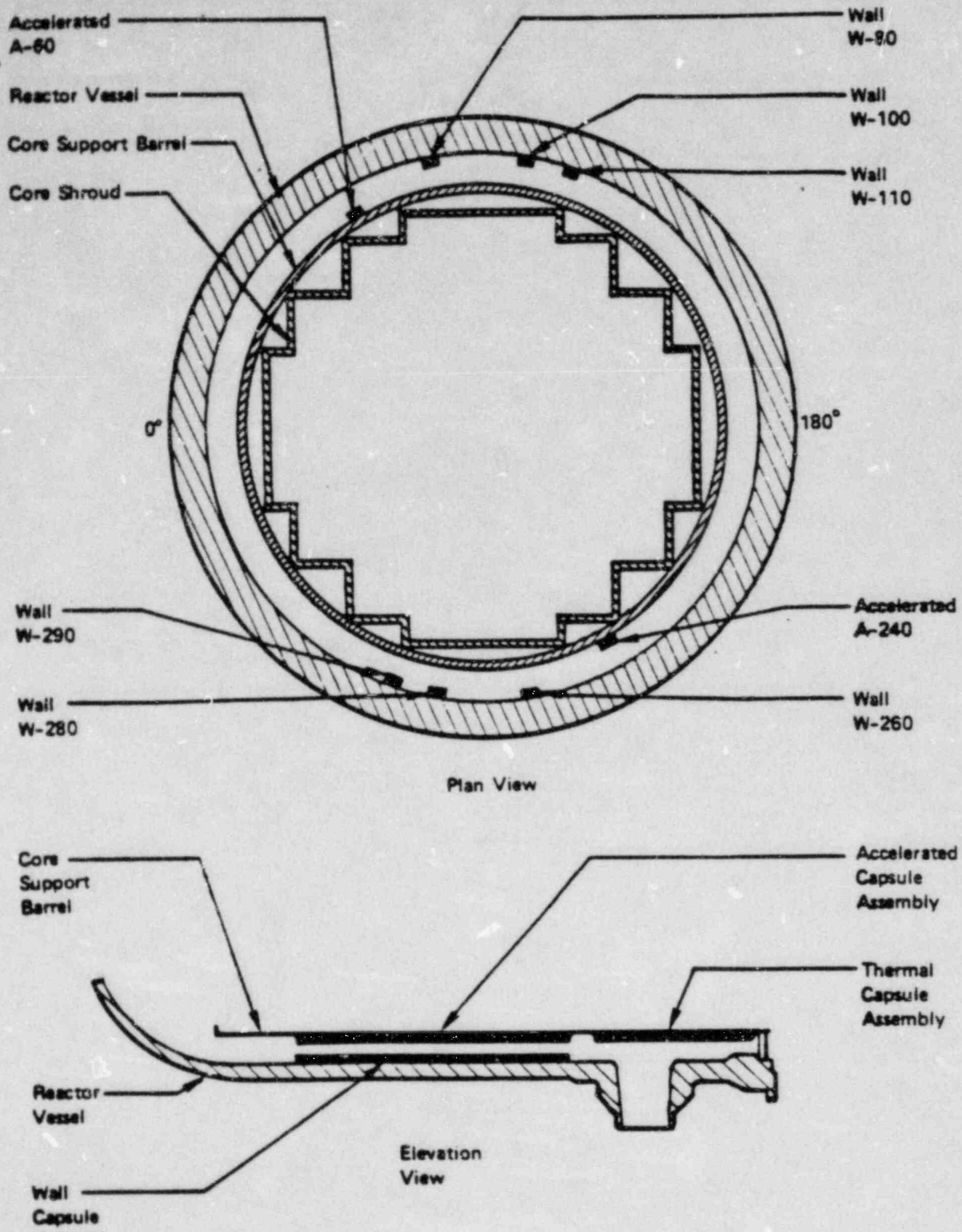

Figure 4-1 Arrangement of Surveillance Capsules in the Palisades Reactor Vessel

8092B:1b:091284

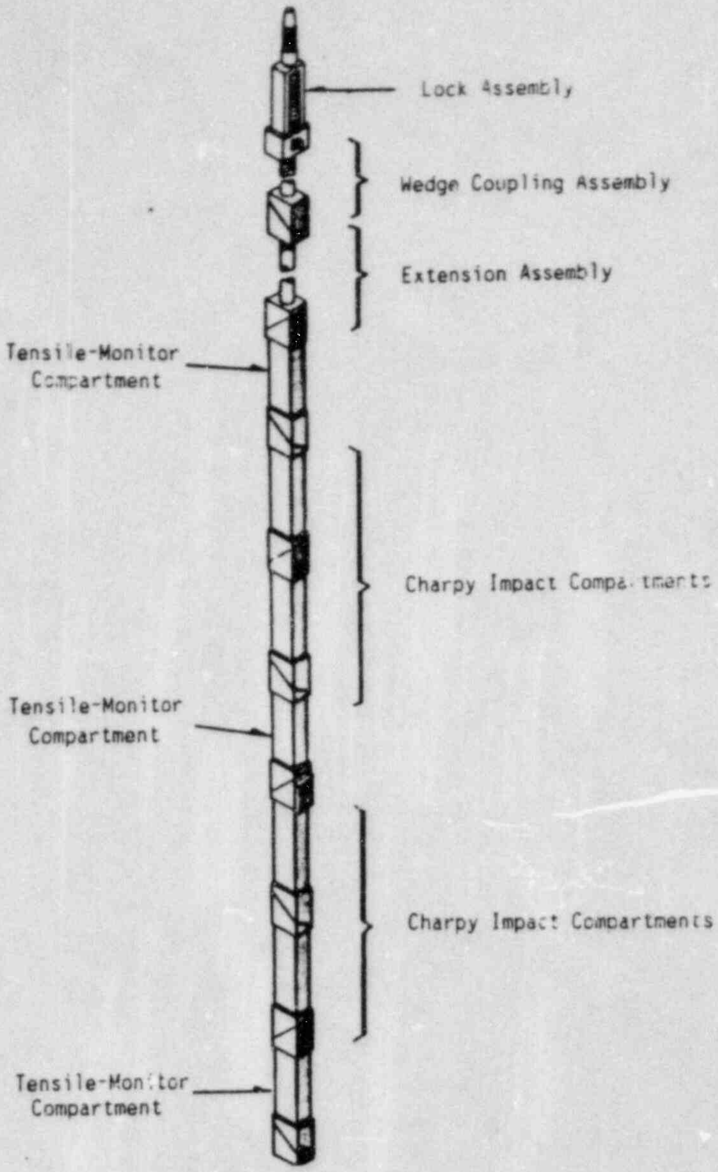

Compartment	Capsule W-290	Capsule T-330
1	HAZ Tensile I.D. #1A14	HAZ Tensile I.D. #1C14
2	HAZ Impact I.D. #1A24	HAZ Impact I.D. #1C24
3	Base (T) Impact I.D. #1A32	Base (T) Impact I.D. #1C32
4	Base (L) Tensile I.D. #1A41	Base (L) Tensile I.D. #1C41
5	Base (L) Impact I.D. #1A51	Base (L) Impact I.D. #1C51
6	Weld Impact I.D. #1A63	Weld Impact I.D. #1C63
7	Weld Tensile I.D. #1A73	Weld Tensile I.D. #1C73

Figure 4-2 Diagram Showing Location of Test Specimens, Thermal Monitors, and Dosimetry Monitors in the Palisades Surveillance Capsule Assemblies

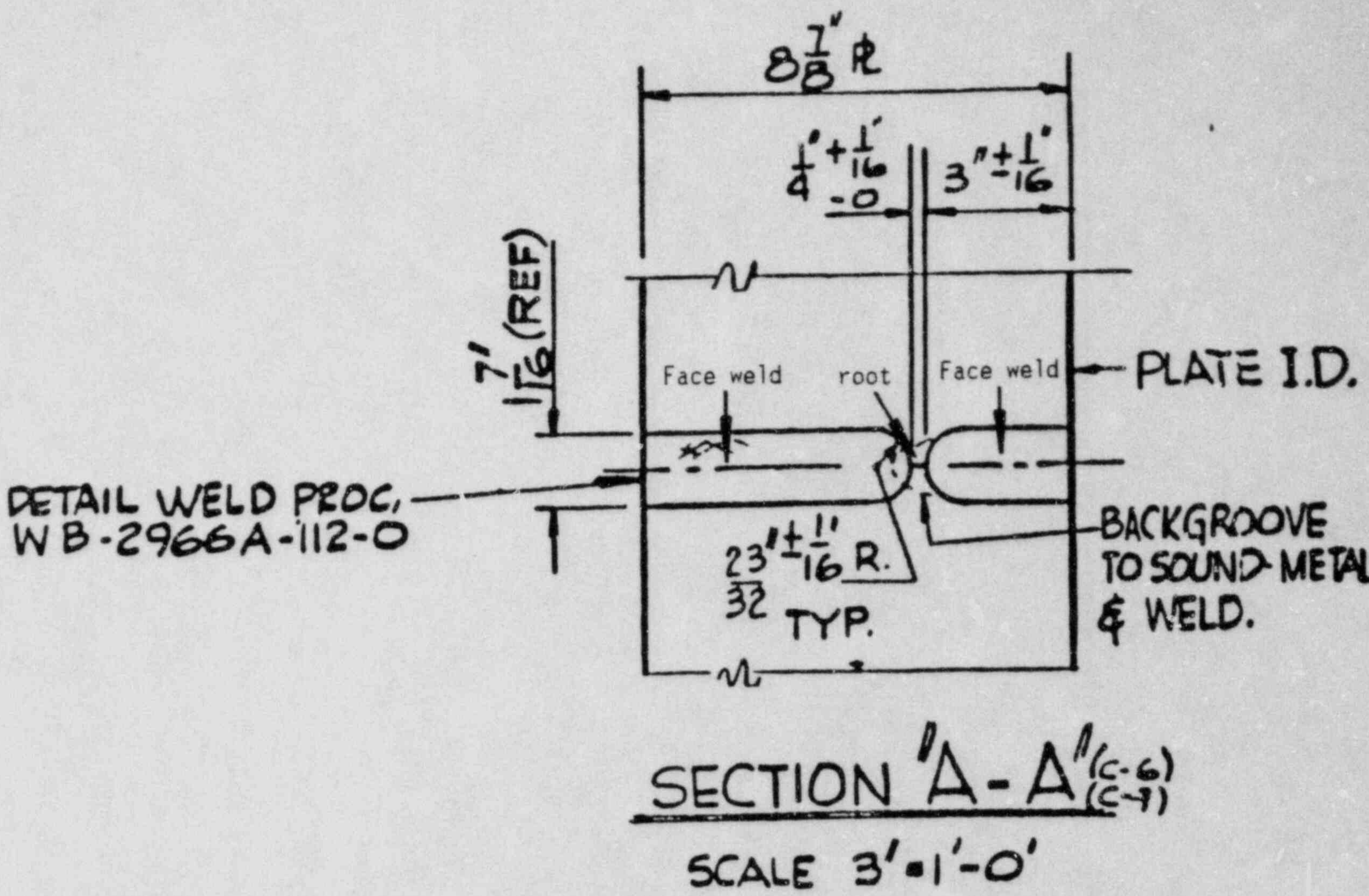

Figure 4-3 Palisades Weld Metal Surveillance Test Material Fabrication (From C-E Drawing No. C-245-321-1)

SECTION 5
TESTING OF SPECIMENS FROM CAPSULES T-330 AND W-290

5-1. OVERVIEW

The postirradiation mechanical testing of the thermal and irradiated capsules' Charpy V-notch and tensile specimens was performed at the Westinghouse Research and Development Laboratory, with consultation by Westinghouse Nuclear Energy Systems personnel. Testing was performed in accordance with 10CFR50, Appendices G and H, ASTM Specification E185-82 and Westinghouse Procedures RMFs 8402-0, 8102-0, and 8103-0.

Upon receipt of the capsules at the laboratory, they were opened in accordance with Westinghouse Procedure RMF 8404-0. The specimens and spacer blocks were carefully removed, inspected for identification number, and checked against the master list in C-E's summary report.[1] No discrepancies were found.

Examination of the four types of low-melting (536, 558, 580 and 590°F) alloys indicated no melting of any of the thermal monitors.

Samples of both the surveillance capsule plate and weld metal materials were chemically analyzed for the elemental content of Cr, Cu, Mn, Mo, and Ni (by an emission spectroscopy inductively coupled plasma method), and for P and Si (through wet analysis techniques).

The Charpy impact tests were performed per ASTM Specification E23-82 and RMF Procedure 8103 on a Tinius-Olsen Model 74, 359J machine. The tup (striker) of the Charpy machine is instrumented with an Effects Technology Model 500 instrumentation system. With this system, load-time and energy-time signals can be recorded in addition to the standard measurement of Charpy energy (E_D). From the load-time curve, the load of general yielding (P_{GY}), the time to general yielding (t_{GY}), the maximum load (P_M), and the time to maximum load (t_M) can be determined. Under some test conditions, a sharp drop in load indicative of fast fracture was observed. The load at which fast fracture was initiated is identified as the fast fracture load (P_F), and the load at which fast fracture terminated is identified as the arrest load (P_A).

The energy at maximum load (E_M) was determined by comparing the energy-time record and the load-time record. The energy at maximum load is roughly equivalent to the energy required to initiate a crack in the specimen. Therefore, the propagation energy for the crack (E_p) is the difference between the total energy to fracture (E_D) and the energy at maximum load.

The yield stress (σy) is calculated from the three point bend formula. The flow stress is calculated from the average of the yield and maximum loads, also using the three point bend formula.

Percentage shear was determined from postfracture photographs using the ratio-of-areas methods in compliance with ASTM Specification A370-77. The lateral expansion was measured using a dial gage rig similar to that shown in the same specification.

Tension tests were performed on a 20,000-pound Instron, split-console test machine (Model 1115) per ASTM Specifications E8-83 and E21-79, and RMF Procedure 8102. All pull rods, grips, and pins were made of Inconel 718 hardened to Rc45. The upper pull rod was connected through a universal joint to improve axiality of loading. The tests were conducted at a constant crosshead speed of 0.05 inch per minute throughout the test.

Deflection measurements were made with a linear variable displacement transducer (LVDT) extensometer. The extensometer knife edges were spring-loaded to the specimen and operated through specimen failure. The extensometer gage length is 1.00 inch. The extensometer is rated as Class B-2 per ASTM E83-67.

Elevated test temperatures were obtained with a three-zone electric resistance split-tube furnace with a 9-inch hot zone. All tests were conducted in air.

Because of the difficulty in remotely attaching a thermocouple directly to the specimen, the following procedure was used to monitor specimen temperature.

Chromel-alumel thermocouples were inserted in shallow holes in the center and each end of the gage section of a dummy specimen and in each grip. In test configuration, with a slight load on the specimen, a plot of specimen temperature versus upper and lower grip and controller temperatures was developed over the range room temperature to 550°F (288°C). The upper grip was used to control the furnace temperature. During the actual testing the grip temperatures were used to obtain desired specimen temperatures. Experiments indicated that this method is accurate to plus or minus 2°F.

The yield load, ultimate load, fracture load, total elongation, and uniform elongation were determined directly from the load-extension curve. The yield strength, ultimate strength, and fracture strength were calculated using the original cross-sectional area. The final diameter and final gage length were determined from postfracture photographs. The fracture area used to calculate the fracture stress (true stress at fracture) and percent reduction in area was computed using the final diameter measurement.

5-2. THERMAL MONITOR MELTING

Due to the lack of thermal monitor melting, questions arose as to whether the Palisades reactor was operating at a lower than design temperature, or whether the thermal monitor melting points were other than had been specified. To answer this, a system, consisting of a troughed brass block resting on a hot plate, was rigged for melting the capsule thermal monitors. A thermocouple was placed in the trough with the monitor wire, and upon gradual heating the temperature of visually observable melting was noted. To prevent oxide formation from visually concealing the point of monitor melting, the monitors were coated with flux.

Prior to testing the Palisades thermal monitors, controls were run of calibrated Westinghouse thermal monitors. Two Palisades thermal monitors (536 and 590°F) (from capsule T-330) were then tested. The 590°F monitor melted at its rated temperature. The 536°F monitor melted only upon reaching 572°F, which indicates that the 536°F monitor has a much higher melting point and therefore is not truly a 536°F monitor. A 558°F monitor from capsule W-290 was then tested and resulted in a melting temperature of 590°F. Based on these test results it appears that a mixup in monitors occurred during the initial loading of the capsules and therefore a reliable estimate of the capsule temperature cannot be determined from the thermal monitors.

5-3. CHEMICAL ANALYSIS

Chemical analyses were performed on fractured Charpy V-notch specimens in order to confirm the chemical composition of the surveillance plate and weld materials. The chemical analysis results are summarized in Table 5-1. The most notable feature of these analyses is the great variance measured in the nickel content, specifically from .95 to 1.60 wt. %. From the high nickel content, it is evident that a Nickel-200 addition was made to the surveillance weldment, and from the nickel variances observed it can be concluded that the rate of Nickel-200 addition was varied during welding.

5-4. CHARPY V-NOTCH IMPACT TEST RESULTS

Capsule T-330:

The results of the Charpy V-notch impact tests performed on the various materials contained in Capsule T-330, the thermal capsule, are presented in Tables 5-2 through 5-9 and Figures 5-1 through 5-4. From the Charpy V-notch plots based on best engineering judgement it appears that the weld and heat-affected zone metals have experienced a 60 to 70°F shift in the ductile to brittle transition temperatures due to exposure to elevated temperature, but no decrease in upper shelf energy.

The fracture appearance of each Charpy specimen from the various materials is shown in Figures 5-5 through 5-8, and show an increasing ductile or tougher appearance with increasing test temperature.

A typical instrumented Charpy curve, representing the curves of both Capsule T-330 and Capsule W-290, is presented in Figure 5-9.

Capsule W-290:

The results of the Charpy V-notch impact tests performed on the various materials contained in Capsule W-290, irradiated at 1.09×10^{19} n/cm^2, are presented in Tables 5-10 through 5-17 and Figures 5-10 through 5-13. A summary of the transition temperature increases and upper shelf energy decreases for the Capsule W-290 material is shown in Table 5-18.

Irradiation of the vessel intermediate shell course plate D-3803-1 (transverse orientation) to 1.09×10^{19} n/cm^2 (Figure 5-10) resulted in 30 and 50 ft-lb transition temperature increases of 155 and 160°F, respectively, and an upper shelf energy decrease of 18 ft-lb. Irradiation of the vessel intermediate shell plate material (longitudinal orientation) to 1.09×10^{19} n/cm^2 (Figure 5-11) resulted in 30 and 50 ft-lb transition temperature increases of 175 and 180°F, respectively, and an upper shelf energy decrease of 43 ft-lb.

Weld metal irradiated to 1.09×10^{19} n/cm^2 (Figure 5-12) resulted in 30 and 50 ft-lb transition temperature increases of 290 and 300°F, respectively, and an upper shelf energy decrease of 54 ft-lb.

Weld HAZ metal irradiated to 1.09×10^{19} n/cm^2 (Figure 5-13) resulted in 30 and 50 ft-lb transition temperature increases of 235 and 245°F, respectively, and an upper shelf energy decrease of 44 ft-lb.

The fracture appearance of each irradiated Charpy specimen from the various materials is shown in Figures 5-14 through 5-17 and show an increasing ductile or tougher appearance with increasing test temperature.

Figure 5-18 shows a comparison of the 30 ft-lb transition temperature increases for the various Palisades surveillance materials with predicted increases using the methods of NRC Regulatory Guide 1.99, Revision 1.[3]

The regulatory curves used for comparison were developed from the average copper and phosphorus contents (averages of the analyses presented in Tables 4-1 and 5-1) of plate D-3803-1 and the weld metal. This comparison shows that the plate transition temperature increases resulting from irradiation to 1.09 x 10^{19} n/cm^2 are less than predicted by the Guide for plate D-3803-1. The weld metal transition temperature increase resulting from 1.09 x 10^{19} n/cm^2 is greater than predicted by the Guide. This can be explained by the high nickel content of the weld metal. It is widely recognized today that nickel has a profound effect upon the irradiation damage of reactor vessel materials, whereas the current revision of Regulatory Guide 1 99 does not incorporate this important variable.

5-5. TENSION TEST RESULTS

Capsule T-330:

The results of the thermal capsule tension tests performed on plate D-3803-1 (longitudinal orientation) and weld metal are shown in Table 5-19 and Figures 5-19 and 5-20, respectively. These results show that the thermal environment produced little change in the 0.2 percent yield strength of the plate and weld material. Fractured tension specimens for each of the materials are shown in Figures 5-22 through 5-24. A typical stress-strain curve for the tension specimens, representing the curves of both Capsule T-330 and Capsule W-290, is shown in Figure 5-25.

Capsule W-290.

The results of the irradiated capsule tension tests performed on plate D-3803-1 (longitudinal orientation) and weld metal irradiated to 1.09 x 10^{19} n/cm^2 are show in Table 5-20 and Figures 5-26 and 5-27, respectively. These results show that irradiation produced an increase in the 0.2 percent yield strength of approximately 20 ksi for plate D-3803-1 and of approximately 30 ksi for the weld metal. Fractured tension specimens for each of the materials are shown in Figures 5-29 through 5-31.

TABLE 5-1

Results of Chemical Analyses Performed on Palisades

Charpy V-notch Specimens (WT-%)

Charpy Specimen	Cr	Cu	Mn	Mo	Ni	P	Si
37C (Weld Metal	.050	.25	1.28	.51	1.60	.013	.20
341 (Weld Metal)	.056	.30	1.20	.52	1.38	.014	.25
46D (Weld Metal Portion of HAZ Specimen)	.050	.26	1.22	.47	1.19	.015	.24
46E (Weld Metal Portion of HAZ Specimen)	.050	.25	1.09	.45	0.95	.014	.19
22J (Plate D-3803-1)	.11	.24	1.66	.45	0.53	.005	.20
25J (Plate D-3803-1)	.11	.24	1.61	.45	0.52	.004	.24

TABLE 5-2

CAPSULE T-330, THERMAL CAPSULE

CHARPY V-NOTCH IMPACT DATA FOR THE PALISADES INTERMEDIATE SHELL PLATE D-3803-1 (TRANSVERSE ORIENTATION)

Sample No.	Temperature (°F)	Impact Energy (ft-lb)	Lateral Expansion (mils)	Shear (%)
22M	-75	5	6.5	5
22L	-25	13	18	10
22J	25	28	20	26
22E	50	47	42.5	47
21L	60	48	47.5	45
22B	77	79	58	50
22C	100	71	60	56
21J	150	82	64.5	78
21K	200	112	78	100
22D	250	92	74	100
22K	300	117	80	100
21M	400	110	78	100

TABLE 5-3

CAPSULE T-330, THERMAL CAPSULE

CHARPY V-NOTCH IMPACT DATA FOR THE PALISADES
INTERMEDIATE SHELL PLATE D-3803-1 (LONGITUDINAL ORIENTATION)

Sample No.	Temperature (°F)	Impact Energy (ft-lb)	Lateral Expansion (mils)	Shear (%)
13M	-50	7	9	2
13P	0	13	13.5	14
13C	25	39	32.5	20
13B	35	50	47.2	27
13E	50	65	53	40
13J	77	112	74.5	66
13K	150	131	91.5	83
13Y	200	156	87.0	100
13D	300	158	77.5	100
13L	350	158	85.5	100
13T	400	215	67.5	100

*Specimen 13U was improperly centered on anvil.

TABLE 5-4

CAPSULE T-330, THERMAL CAPSULE

CHARPY V-NOTCH IMPACT DATA FOR THE PALISADES PRESSURE VESSEL WELD METAL

Sample No.	Temperature (°F)	Impact Energy (ft-lb)	Lateral Expansion (mils)	Shear (%)
33M	-100	12	17	18
33K	- 75	45	39	30
343	- 60	22	26	29
341	- 50	31	32	37
33L	- 50	23	26	42
33P	- 25	32	28.5	40
342	0	82	65.5	60
33Y	25	93	75.5	84
344	77	79	88.5	94
33T	150	120	94.5	100
33J	300	122	74.5	100
33U	350	155	79	100

TABLE 5-5

CAPSULE T-330, THERMAL CAPSULE

CHARPY V-NOTCH IMPACT DATA FOR THE PALISADES PRESSURE VESSEL WELD HEAT-AFFECTED ZONE METAL

Sample No.	Temperature (°F)	Impact Energy (ft-lb)	Lateral Expansion (mils)	Shear (%)
43D	-75	45	39	3
42D	-25	27	27.5	14
42E	-10	43	41.5	34
44D	0	55	47.5	44
43E	25	52	47	43
41E	40	88	57	62
46E	50	130	84	88
44E	60	115	81	84
46D	77	70	55	85
45E	150	125	80.5	100
41D	225	110	67	100
45D	300	121	77	100

TABLE 5-6

CAPSULE T-330, THERMAL CAPSULE
INSTRUMENTED CHARPY IMPACT TEST RESULTS FOR
PALISADES INTERMEDIATE SHELL
PLATE D-3803-1 (TRANSVERSE ORIENTATION)

Sample Number	Test Temp (F)	Charpy Energy (ft lbs)	Normalized Energies (ft-lbs/in^2) Charpy Ed/A	Maximum Em/A	Prop Ep/A	Yield Load (kips)	Time to Yield (uSec)	Maximum Load (kips)	Time to Maximum (uSec)	Fracture Load (kips)	Arrest Load (kips)	Yield Stress (ksi)	Flow Stress (ksi)
22M	-75	5.0	40	17	23			2.60	85	2.60			
22L	-25	13.0	105	70	34	3.30	90	3.55	195	3.55	.25	108	113
22J	25	28.0	225	139	87	3.10	85	3.75	350	3.75	.70	102	113
22E	50	47.0	378	198	180	2.95	160	3.95	560	3.95	1.95	97	114
21L	60	48.0	387	254	133	2.95	85	3.95	605	3.90	1.55	98	115
22B	77	79.0	636	307	329	2.85	80	4.00	725	3.85	1.95	94	113
22C	100	71.0	572	262	309	2.60	90	3.85	655	3.60	1.95	86	107
21J	150	82.0	660	193	467	2.70	80	3.60	500	3.00	2.50	89	104
21K	200	112.0	902	258	644	2.60	85	3.75	655			86	105
22D	250	92.0	741	226	515	2.25	50	3.50	610			74	95
22K	300	117.0	942	294	648	2.10	50	3.55	775			69	93
21M	400	110.0	886	249	637	2.20	85	3.45	675			73	94

8092B:1b/091984

TABLE 5-7

CAPSULE T-330, THERMAL CAPSULE

INSTRUMENTED CHARPY IMPACT TEST RESULTS FOR

PALISADES INTERMEDIATE SHELL

PLATE D-3803-1 (LONGITUDINAL ORIENTATION)

Sample Number	Test Temp (F)	Charpy Energy (ft lbs)	Normalized Energies (ft-lbs/in^2) Charpy Ed/A	Maximum Em/A	Prop Ep/A	Yield Load (kips)	Time to Yield (uSec)	Maximum Load (kips)	Time to Maximum (uSec)	Fracture Load (kips)	Arrest Load (kips)	Yield Stress (ksi)	Flow Stress (ksi)
13M	-50	7.0	56	24	32			3.35	85	3.35	.10		
13P	0	13.0	105	38	66	3.15	90	3.20	125	3.10	.35	104	105
13C	25	39.0	314	201	113	3.00	85	4.05	485	4.05	.70	99	117
13B	35	50.0	403	162	241	2.85	80	3.80	410	3.75	2.15	95	110
13E	50	65.0	523	314	209	2.90	90	4.00	740	3.95	.90	97	115
13J	77	112.0	902	350	552	2.80	80	4.10	815	3.25	1.60	93	114
13K	150	131.0	1055	332	723	2.45	70	3.90	815	2.30	1.70	81	105
13Y	200	156.0	1256	323	933	2.55	90	3.75	825			85	104
13D	300	158.0	1272	290	982	2.40	100	3.55	775			80	99
13L	350	158.0	1272	294	978	2.10	45	3.45	805			68	91
13T	400	215.0	1731	285	1446	2.10	60	3.50	770			69	92

8092B:1b/091984

TABLE 5-8
CAPSULE T-330, THERMAL CAPSULE
INSTRUMENTED CHARPY IMPACT TEST RESULTS FOR
PALISADES WELD METAL

Sample Number	Test Temp (F)	Charpy Energy (ft lbs)	Normalized Energies Charpy Ed/A (ft-lbs/in^2)	Maximum Em/A	Prop Ep/A	Yield Load (kips)	Time to Yield (uSec)	Maximum Load (kips)	Time to Maximum (uSec)	Fracture Load (kips)	Arrest Load (kips)	Yield Stress (ksi)	Flow Stress (ksi)
33M	-100	12.0	97	68	29	3.65	125	3.85	200	3.80	.30	121	124
33K	-75	45.0	362	218	144	3.35	90	4.15	500	4.05	.15	110	123
343	-60	22.0	177	139	38	3.35	95	3.85	345	3.85	.45	110	119
341	-50	31.0	250	176	74	3.25	95	3.95	425	3.95	.50	107	119
33L	-50	23.0	185	104	82	3.25	90	3.70	270	3.55	.55	108	115
33P	-25	32.0	258	181	77	3.15	95	3.85	445	3.80	.75	105	116
342	0	82.0	660	290	371	3.10	90	4.10	670	3.45	1.15	102	119
33Y	25	93.0	749	274	474	2.95	95	3.90	665	3.40	2.2	98	114
344	77	79.0	636	335	301	2.70	85	3.80	825	2.95	2.2	90	108
33T	150	120.0	966	300	666	2.50	75	3.65	770			83	102
33J	300	122.0	982	283	699	2.20	75	3.40	780			73	93
33U	350	155.0	1248	280	968	2.10	65	3.30	775			70	90

TABLE 5-9

CAPSULE T-330, THERMAL CAPSULE

INSTRUMENTED CHARPY IMPACT TEST RESULTS FOR PALISADES WELD HEAT AFFECTED ZONE METAL

Sample Number	Test Temp (F)	Charpy Energy (ft lbs)	Normalized Energies (ft-lbs/in^2): Charpy Ed/A	Normalized Energies (ft-lbs/in^2): Maximum Em/A	Normalized Energies (ft-lbs/in^2): Prop Ep/A	Yield Load (kips)	Time to Yield (uSec)	Maximum Load (kips)	Time to Maximum (uSec)	Fracture Load (kips)	Arrest Load (kips)	Yield Stress (ksi)	Flow Stress (ksi)
43D	-75	17.0	137	114	13	3.55	95	4.05	275	4.05		117	125
42D	-25	27.0	217	174	44	3.40	105	4.05	410	4.05	.35	112	123
42E	-10	43.0	346	222	125	3.30	90	4.15	505	4.15	1.15	110	124
44D	0	55.0	443	179	264	3.50	105	4.15	415	4.15	.25	116	127
43E	25	52.0	419	211	207	3.20	90	3.90	500	3.80	1.35	106	118
41E	40	88.0	709	347	362	3.15	90	4.30	770	3.75	1.75	105	124
46E	50	130.0	1047	326	721	3.10	95	4.10	750	2.15	1.40	103	119
44E	60	115.0	926	282	644	3.15	100	4.00	665	2.70	1.60	103	118
46D	77	70.0	564	209	354	3.05	85	4.00	495	3.85	2.25	101	117
45E	150	125.0	1007	313	693	2.80	85	3.75	770			92	108
41D	225	110.0	886	246	640	2.45	65	3.80	610			80	103
45D	300	121.0	974	312	662	2.25	75	3.55	820			74	96

TABLE 5-10

CAPSULE W-290, IRRADIATED CAPSULE

CHARPY V-NOTCH IMPACT DATA FOR THE PALISADES INTERMEDIATE SHELL PLATE D-3803-1 (TRANSVERSE ORIENTATION)

Sample No.	Temperature (°F)	Impact Energy (ft-lb)	Lateral Expansion (mils)	Shear (%)
25K	79	17	16	15
25P	150	23	25	27
24M	175	30	26.5	34
25J	200	33	30	41
25L	225	67	62.5	76
24E	225	72	61.5	79
25Y	250	84	60.5	89
24J	250	76	63.5	92
25M	275	78	71	100
24K	300	84	66.5	100
25T	350	88	71	100
25U	450	85	68.5	100

TABLE 5-11

CAPSULE W-290, IRRADIATED CAPSULE

CHARPY V-NOTCH IMPACT DATA FOR THE PALISADES
INTERMEDIATE SHELL PLATE D-3803-1 (LONGITUDINAL ORIENTATION)

Sample No.	Temperature (°F)	Impact Energy (ft-lb)	Lateral Expansion (mils)	Shear (%)
164	79	11	12	5
16D	150	20	21.5	23
1AU	150	25	24.5	27
162	175	22	23	29
163	175	34	31	34
1AT	200	47	36	39
1AP	200	49	33	36
1AY	225	71	59.5	67
165	250	110	75.5	89
166	300	116	80.5	100
161	350	109	84	100
16E	450	112	78.5	100

TABLE 5-12

CAPSULE W-290, IRRADIATED CAPSULE

CHARPY V-NOTCH IMPACT DATA FOR THE PALISADES PRESSURE VESSEL WELD METAL

Sample No.	Temperature (°F)	Impact Energy (ft-lb)	Lateral Expansion (mils)	Shear (%)
34A	79	8	8	5
34E	125	10	10.5	15
34D	150	18	14	25
37L	175	18	16	24
37C	200	28	22	33
37J	225	45	35.5	71
34B	250	36	38	67
37D	275	64	49	89
37B	300	61	49	95
37K	350	72	52.5	100
37A	450	67	67.5	100
34C	500	52	51.5	100

TABLE 5-13

CAPSULE W-290, IRRADIATED CAPSULE

CHARPY V-NOTCH IMPACT DATA FOR THE PALISADES
PRESSURE VESSEL WELD HEAT-AFFECTED ZONE METAL

Sample No.	Temperature (°F)	Impact Energy (ft-lb)	Lateral Expansion (mils)	Shear (%)
426	50	16	12.5	16
457	79	51	36.5	45
427	100	21	20.5	32
453	100	36	27.5	28
425	125	27	10.5	34
456	150	28	25.5	41
4AZ	150	35	32.5	49
451	175	35	35	59
4AA	200	62	47	74
455	250	79	53	91
454	350	73	60.5	100
452	450	71	60.5	100

8092B:1b/091984

TABLE 5-14

CAPSULE W-290, IRRADIATED CAPSULE
INSTRUMENTED CHARPY IMPACT TEST RESULTS FOR
PALISADES INTERMEDIATE SHELL
PLATE D-3803-1 (TRANSVERSE ORIENTATION)

Sample Number	Test Temp (F)	Charpy Energy (ft lbs)	Normalized Energies (ft-lbs/in^2) Charpy Ed/A	Maximum Em/A	Prop Ep/A	Yield Load (kips)	Time to Yield (uSec)	Maximum Load (kips)	Time to Maximum (uSec)	Fracture Load (kips)	Arrest Load (kips)	Yield Stress (ksi)	Flow Stress (ksi)
25K	79	17.0	137	69	68	3.10	85	3.40	200	2.90		102	107
25P	150	23.0	185	117	68	3.25	95	3.80	295	3.80	.55	107	117
24M	175	30.0	242	134	107	3.15	90	3.90	335	3.85	1.00	104	117
25J	200	33.0	266	144	121	3.05	90	3.85	360	3.85	1.60	101	114
25L	225	67.0	540	219	320	3.15	90	4.20	495	3.90	3.10	104	121
24E	225	72.0	580	220	360	3.15	85	4.15	500			104	120
25Y	250	84.0	676	212	465	2.70	70	4.00	495			90	111
24J	250	76.0	612	214	398	2.95	85	4.05	505			98	116
25M	275	78.0	628	189	439	3.05	95	4.00	450			101	117
26K	300	84.0	676	214	463	2.85	80	4.10	500			95	115
25T	350	88.0	709	260	449	2.55	65	3.95	605			84	108
25U	450	85.0	684	195	490	2.45	75	3.70	500			82	102

TABLE 5-15

CAPSULE W-290, IRRADIATED CAPSULE

INSTRUMENTED CHARPY IMPACT TEST RESULTS FOR

PALISADES INTERMEDIATE SHELL

PLATE D-3803-1 (LONGITUDINAL ORIENTATION)

Sample Number	Test Temp (F)	Charpy Energy (ft lbs)	Normalized Energies Charpy Ed/A	(ft-lbs/in^2) Maximum Em/A	Prop Ep/A	Yield Load (kips)	Time to Yield (uSec)	Maximum Load (kips)	Time to Maximum (uSec)	Fracture Load (kips)	Arrest Load (kips)	Yield Stress (ksi)	Flow Stress (ksi)
164	79	11.0	89	60	28	3.30	95	3.60	175	3.55	.15	110	114
16D	150	20.0	161	101	60	3.25	90	3.85	260	3.85	.65	107	117
1AU	150	25.0	201	147	54	3.20	95	4.00	360	3.95	.25	106	120
162	175	22.0	177	103	74	3.15	90	3.80	270	3.70	.85	104	114
163	175	34.0	274	204	70	3.00	95	3.90	495	3.90	.75	99	114
1AT	200	47.0	378	258	120	3.15	95	4.20	585	4.20	1.50	104	122
1AP	200	49.0	395	277	118	2.95	85	4.10	640	4.05	1.35	98	117
1AY	225	71.0	572	282	290	2.80	80	4.05	650	3.80	2.20	93	114
165	250	110.0	886	292	593	2.60	65	4.25	650	3.50	2.95	86	113
166	300	116.0	934	276	658	2.75	80	4.00	650			91	112
161	350	109.0	878	258	619	2.65	75	4.05	605			87	111
16E	450	112.0	902	251	651	2.50	70	3.85	605			82	105

TABLE 5-16

CAPSULE W-290, IRRADIATED CAPSULE

INSTRUMENTED CHARPY IMPACT TEST RESULTS FOR

PALISADES WELD METAL

Sample Number	Test Temp (F)	Charpy Energy (ft lbs)	Normalized Energies (ft-lbs/in^2): Charpy Ed/A	Normalized Energies (ft-lbs/in^2): Maximum Em/A	Normalized Energies (ft-lbs/in^2): Prop Ep/A	Yield Load (kips)	Time to Yield (uSec)	Maximum Load (kips)	Time to Maximum (uSec)	Fracture Load (kips)	Arrest Load (kips)	Yield Stress (ksi)	Flow Stress (ksi)
34A	79	8.0	64	42	22	3.50	90	3.75	125	3.75		116	121
34E	125	10.0	81	60	20	3.40	95	3.75	170	3.75		113	119
34D	150	18.0	145	109	36	3.55	95	4.20	260	4.20		117	128
37L	175	18.0	145	94	51	3.60	95	3.95	230	3.95	.25	119	125
37C	200	28.0	225	157	68	3.45	95	4.20	360	4.15	.65	115	127
37J	225	45.0	362	189	173	3.50	85	4.40	405	4.35	3.00	116	130
34B	250	36.0	290	145	145	3.45	85	4.15	330	4.00	2.25	113	125
37D	275	64.0	515	203	313	3.40	85	4.25	445			112	126
37B	300	61.0	491	179	312	3.40	85	4.15	405			112	124
37K	350	72.0	580	182	398	3.30	105	4.05	430			109	121
37A	450	67.0	540	170	370	3.15	85	3.95	400			104	118
34C	500	52.0	419	183	236	3.00	85	3.75	445			99	111

TABLE 5-17

CAPSULE W-290, IRRADIATED CAPSULE

INSTRUMENTED CHARPY IMPACT TEST RESULTS FOR

PALISADES WELD HEAT AFFECTED ZONE METAL

Sample Number	Test Temp (F)	Charpy Energy (ft lbs)	Normalized Energies Charpy Ed/A	(ft-lbs/in^2) Maximum Em/A	Prop Ep/A	Yield Load (kips)	Time to Yield (uSec)	Maximum Load (kips)	Time to Maximum (uSec)	Fracture Load (kips)	Arrest Load (kips)	Yield Stress (ksi)	Flow Stress (ksi)
426	50	16.0	129	104	25	3.25	85	3.95	260	3.95		108	120
457	79	51.0	411	222	188	3.20	85	4.30	495	4.20	.90	106	124
427	100	21.0	169	108	61	3.30	90	3.95	270	3.95	.80	109	120
453	100	36.0	290	237	53	3.65	90	4.45	500	4.35		120	134
425	125	27.0	217	134	84	3.10	90	3.85	335	3.80	.85	103	115
456	150	28.0	225	138	88	3.25	95	4.00	335	4.00	1.35	108	120
4A2	150	35.0	282	136	146	3.30	95	3.95	330	3.85	1.30	110	121
451	175	35.0	282	133	149	3.15	95	3.90	335	3.85	1.65	104	116
4AA	200	62.0	499	252	247	2.85	85	3.95	605	3.80	2.15	94	113
455	250	79.0	636	218	418	3.15	85	4.10	495	3.95	3.15	105	120
454	350	73.0	588	164	424	2.65	75	3.85	405			87	107
452	450	71.0	572	170	401	2.30	50	3.55	445			76	96

TABLE 5-18

EFFECT OF IRRADIATION AT 1.09 x 10^{19} (E > 1 MeV) ON THE NOTCH TOUGHNESS PROPERTIES OF THE PALISADES SURVEILLANCE VESSEL MATERIALS

Material	Average 30 ft-lb Temp (°F)			Average 35 mil Lateral Expansion Temp (°F)			Average 50 ft-lb Temp (°F)			Average Energy Absorption at Full Shear (ft-lb)		
	Unirradiated	Irradiated	ΔT	Unirradiated	Irradiated	ΔT	Unirradiated	Irradiated	ΔT	Unirradiated	Irradiated	Δ (ft-lb)
Plate D-3803-1 (Transverse)	25	180	155	25	195	170	55	215	160	102	84	18
Plate D-3803-1 (Longitudinal)	0	175	175	5	190	185	20	200	180	155	112	43
Weld Metal	-85	205	290	-75	240	315	-50	250	300	118	64	54
HAZ Metal	-90	145	235	-55	150	215	-65	180	245	116	72	44

8092B:1b/091984

TABLE 5-19

Thermal Capsule Tensile Properties for Palisades Surveillance Material

SAMPLE NUMBER	MATERIAL	TEST TEMPERATURE F	.2% YIELD STRENGTH ksi	ULTIMATE STRENGTH ksi	FRACTURE LOAD kip	FRACTURE STRESS ksi	FRACTURE STRENGTH ksi	UNIFORM ELONGATION %	TOTAL ELONGATION %	REDUCTION in AREA %
1DK	PLATE	65	64.2	86.6	2.65	179.8	54.0	12.0	27.3	70
1DL	PLATE	120	62.1	82.5	2.45	179.0	49.9	11.4	26.2	72
1DJ	PLATE	550	57.0	83.5	2.80	156.4	57.0	9.9	21.3	64
3DK	WELD	-10	75.9	94.2	3.10	198.5	63.2	13.5	27.1	[illegible]8
3DJ	WELD	74	74.4	91.7	3.25	186.4	66.2	12.0	25.5	64
3DL	WELD	550	63.2	85.1	3.25	159.6	66.2	10.0	19.2	59
4DK	HAZ	25	66.7	88.6	2.85	180.0	58.1	9.9	22.7	68
*4DJ	HAZ	74	64.7	84.5				9.9		
*4DL	HAZ	550	57.4	81.5				7.8		

* These specimens fractured outside the gage length.

TABLE 5-20

Irradiated Capsule Tensile Properties for Palisades Surveillance Material, Irradiated to 1.12×10^{19} n/cm^2

SAMPLE NUMBER	MATERIAL	TEST TEMPERATURE F	.2% YIELD STRENGTH ksi	ULTIMATE STRENGTH ksi	FRACTURE LOAD kip	FRACTURE STRESS ksi	FRACTURE STRENGTH ksi	UNIFORM ELONGATION %	TOTAL ELONGATION %	REDUCTION in AREA %
1EL	PLATE	210	81.9	97.8	3.30	202.6	67.2	10.1	21.2	67
1EM	PLATE	245	79.5	97.8	3.30	223.9	67.2	9.9	21.0	70
1EK	PLATE	550	73.9	96.4	3.45	224.1	70.3	9.0	19.2	69
3J6	WELD	210	95.7	109.4	4.00	235.7	81.5	11.1	20.8	65
3J1	WELD	300	92.7	105.9	4.00	198.9	81.5	10.2	19.8	59
3J7	WELD	550	87.6	104.9	4.10	187.2	83.5	8.7	17.1	55
4EL	HAZ	165	82.0	98.8	3.25	191.5	66.2	8.1	19.5	65
4EM	HAZ	225	78.9	96.8	3.35	237.5	68.2	7.1	17.5	71
4EK	HAZ	550	73.9	94.7	3.60	172.5	73.3	6.0	14.7	57

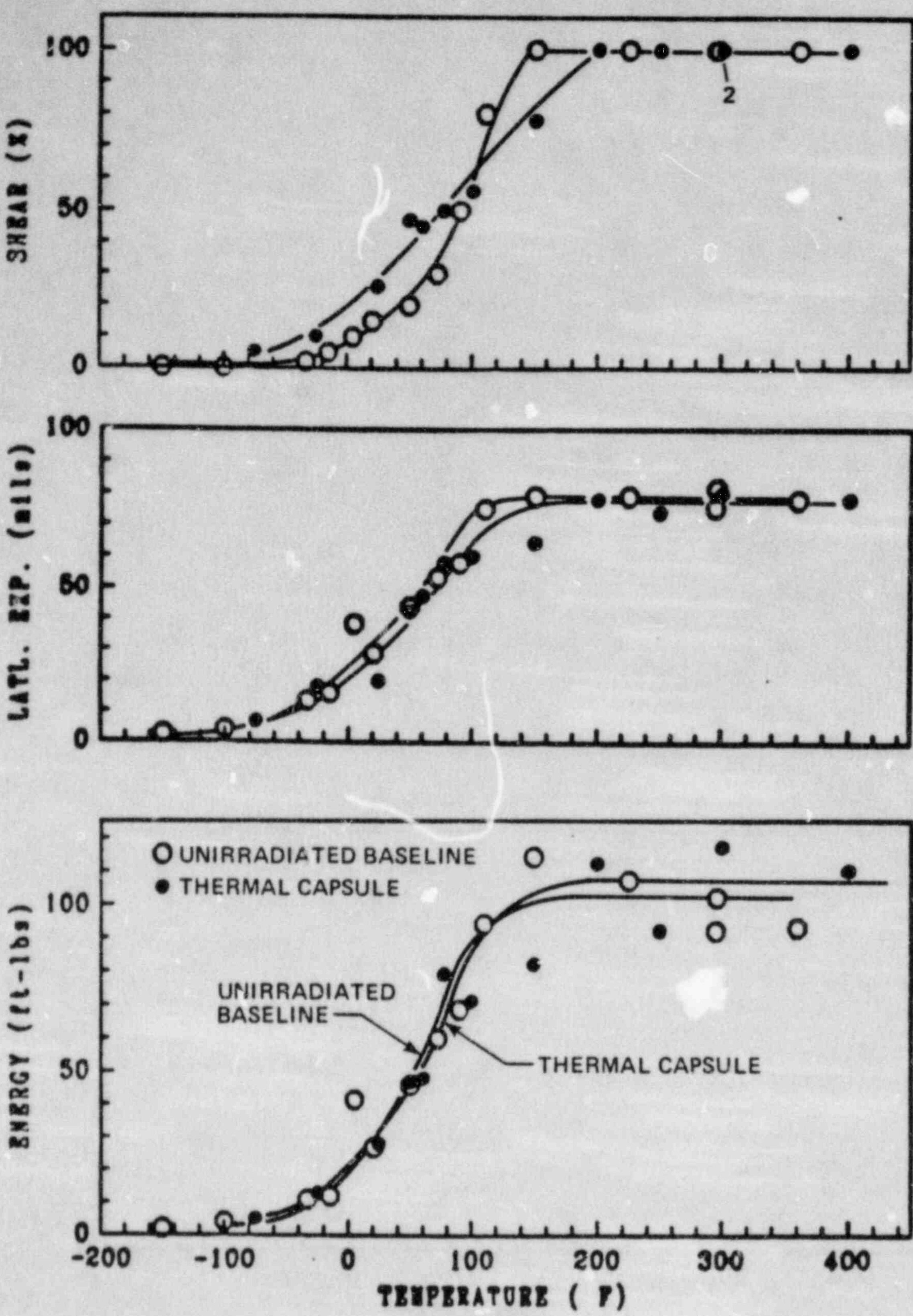

Figure 5-1. Thermal Capsule Charpy V-Notch Impact Properties for Palisades Intermediate Shell Plate D 3803-1 (Transverse Orientation)

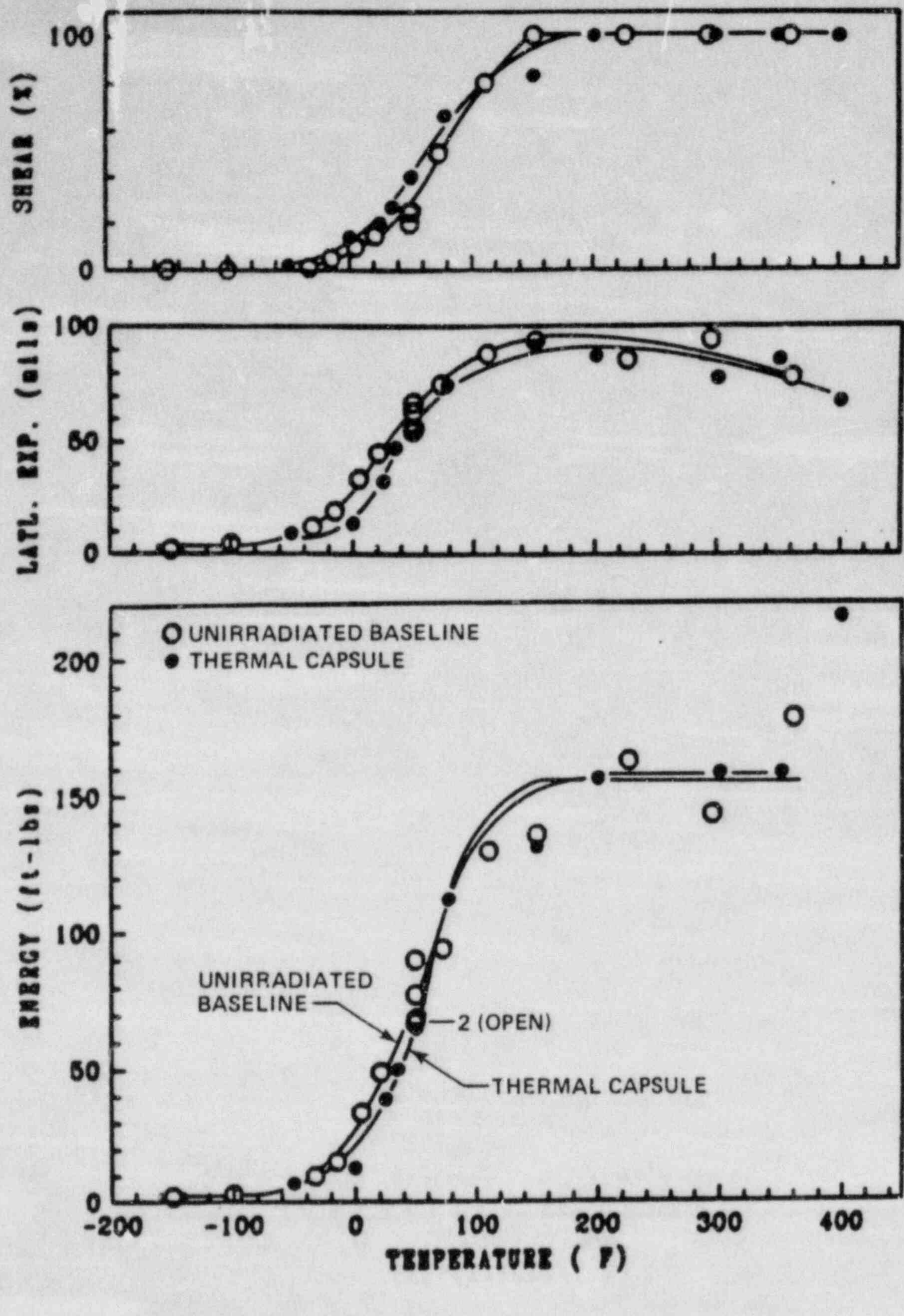

Figure 5-2. Thermal Capsule Charpy V-Notch Impact Properties for Palisades Intermediate Shell Plate D-3803-1 (Longitudinal Orientation)

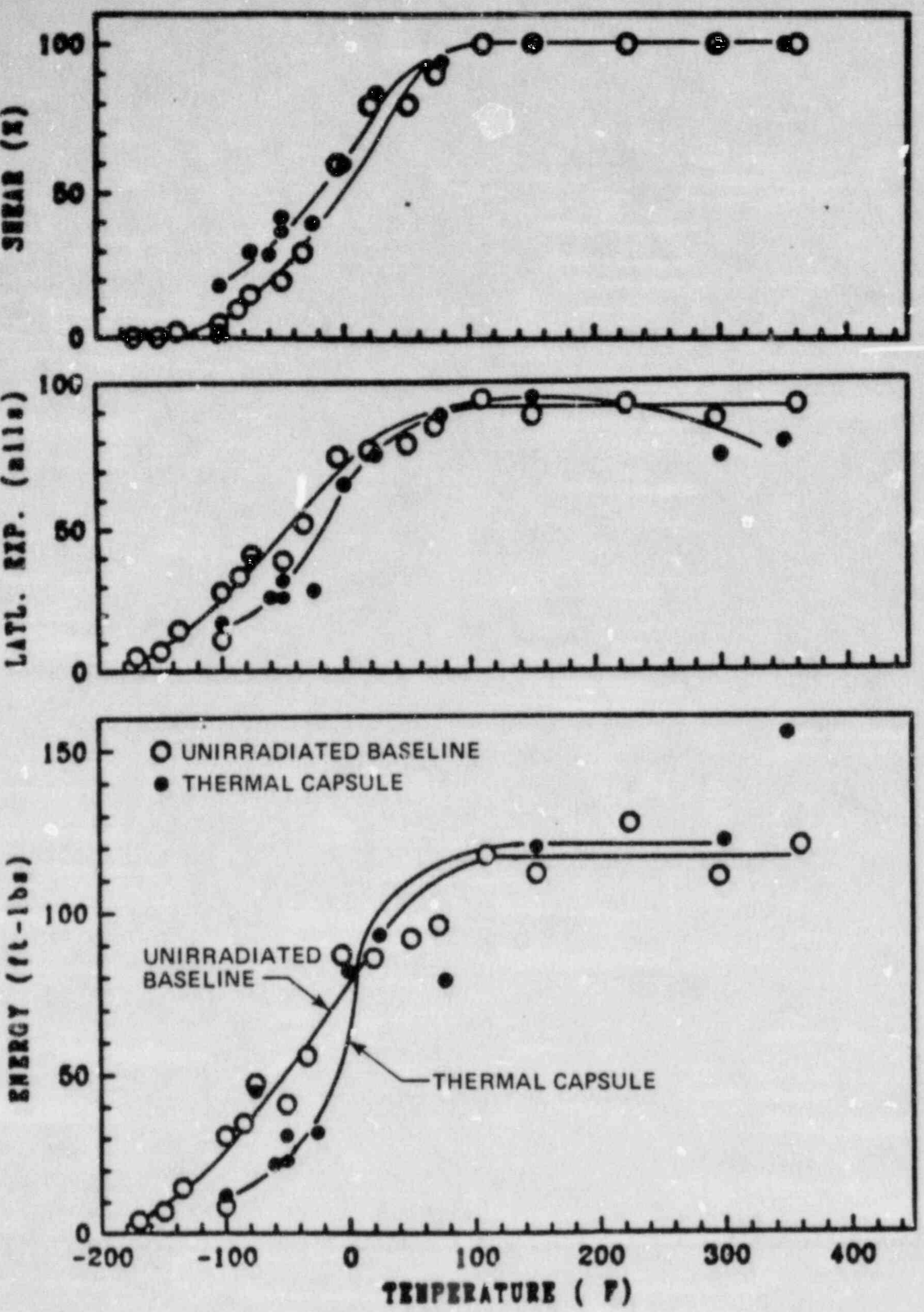

Figure 5-3. Thermal Capsule Charpy V-Notch Impact Properties for Palisades Weld Metal

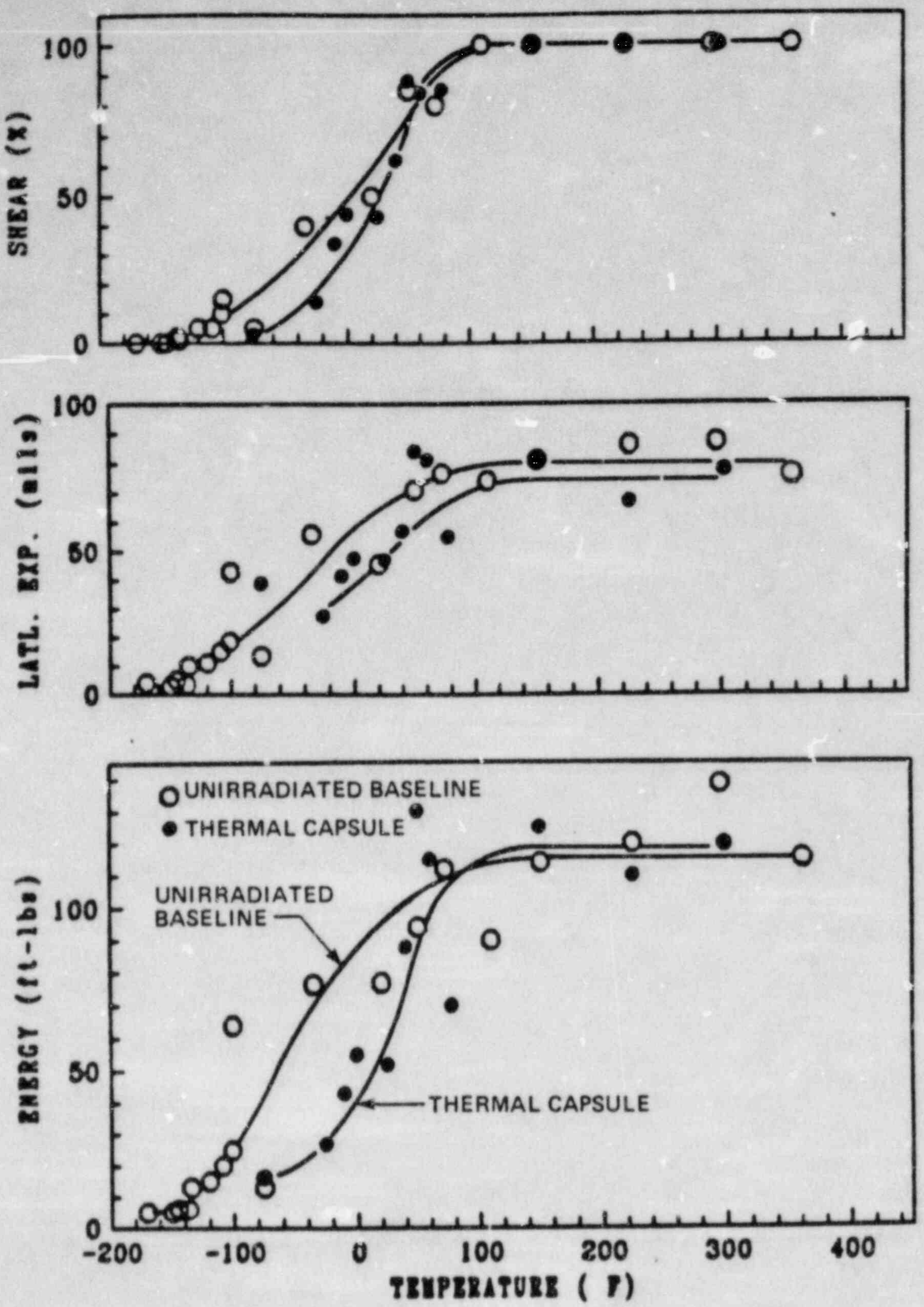

Figure 5-4. Thermal Capsule Charpy V-Notch Impact Properties for Palisades Weld Heat Affected Zone Metal

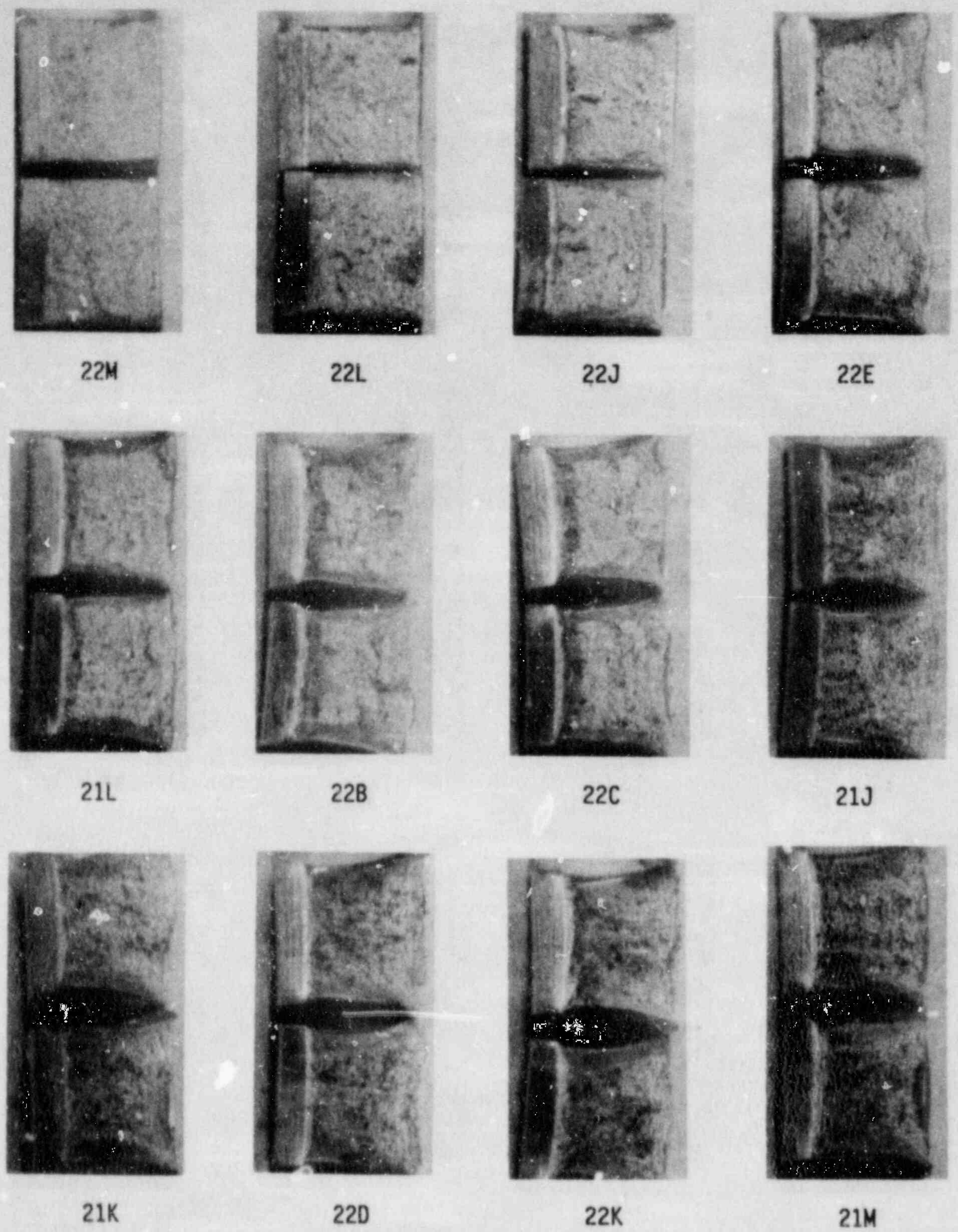

Figure 5-5. Thermal Capsule (T-330) Charpy Impact Specimen Fracture Surfaces for Palisades Intermediate Shell Plate D-3803-1 (Transverse Orientation)

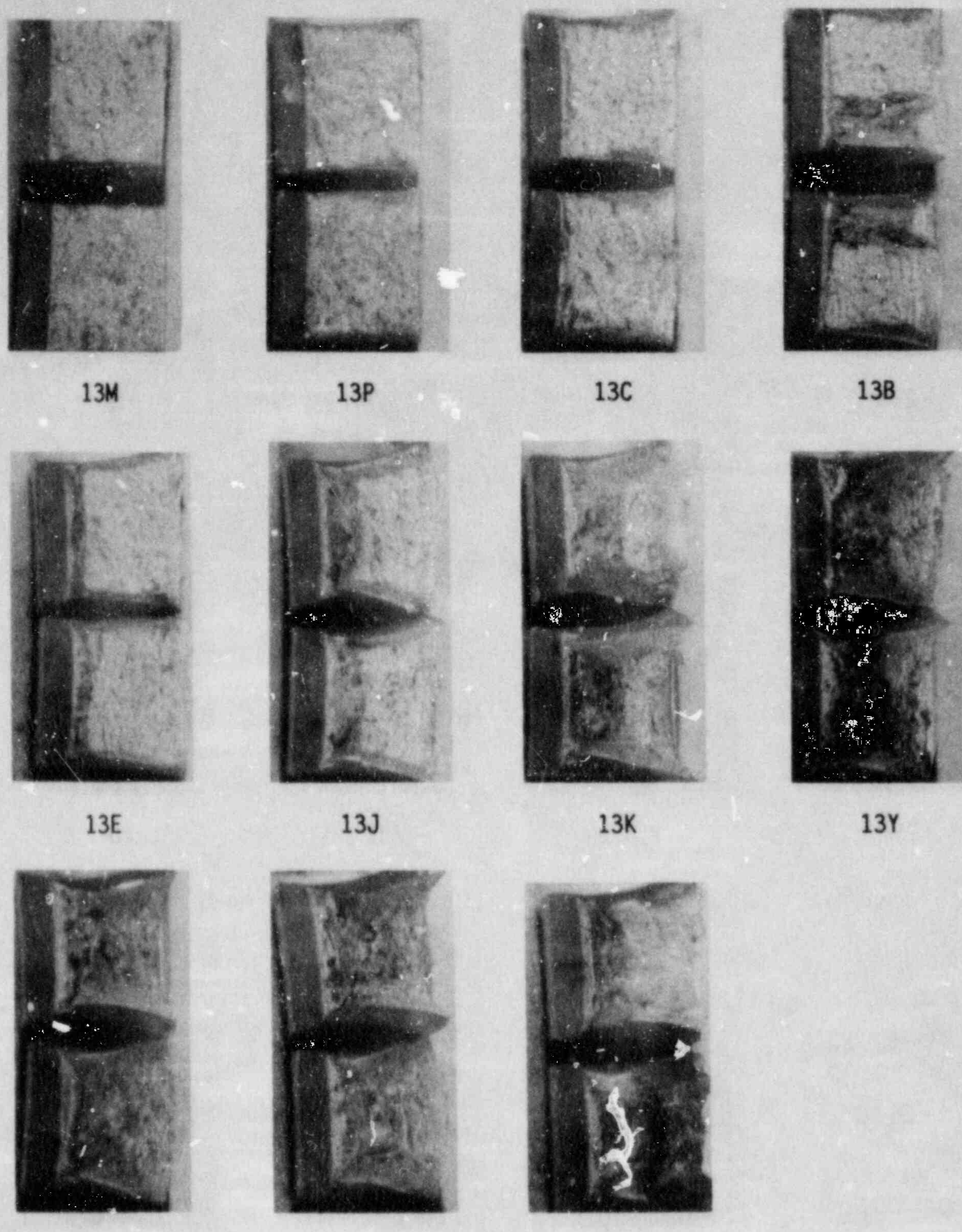

Figure 5-6. Thermal Capsule (T-330) Charpy Impact Specimen Fracture Surfaces for Palisades Intermediate Shell Plate D-3803-1 (Longitudinal Orientation)

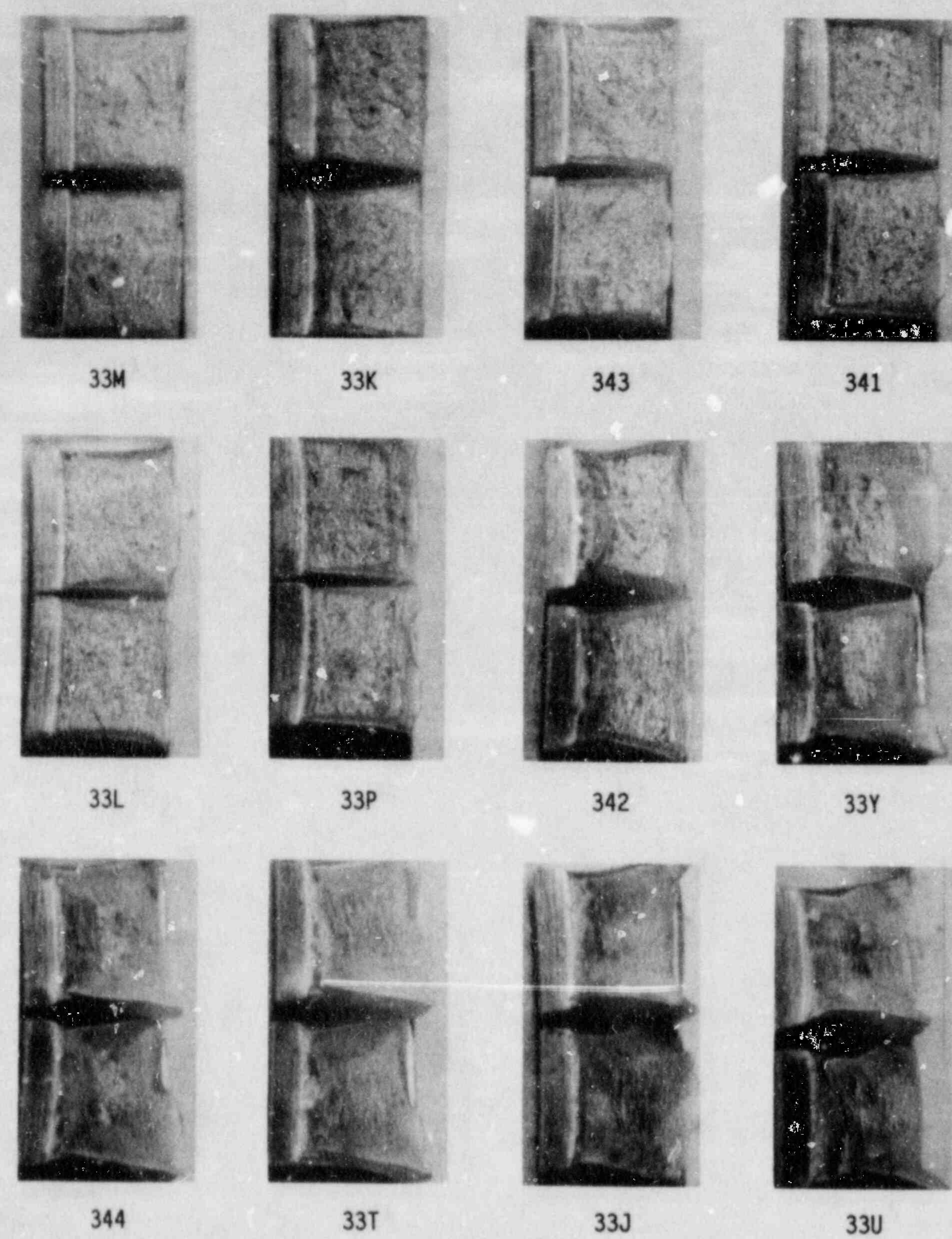

Figure 5-7. Thermal Capsule (T-330) Charpy Impact Specimen Fracture Surfaces for Palisades Weld Metal

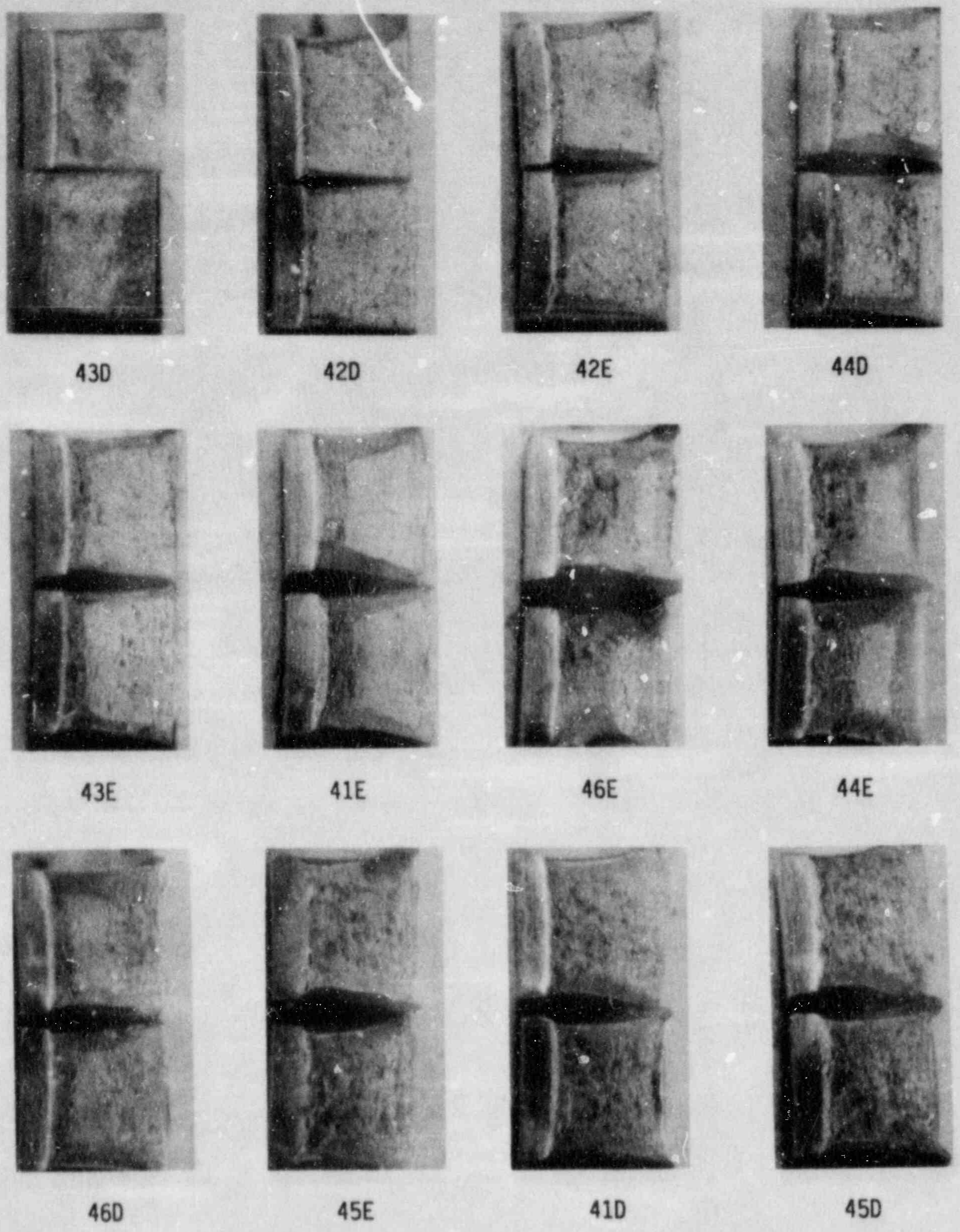

Figure 5-8. Thermal Capsule (T-330) Charpy Impact Specimen Fracture Surfaces for Palisades Weld Heat Affected Zone Metal

Figure 5-9
Typical Curve for Instrumented Charpy Specimens

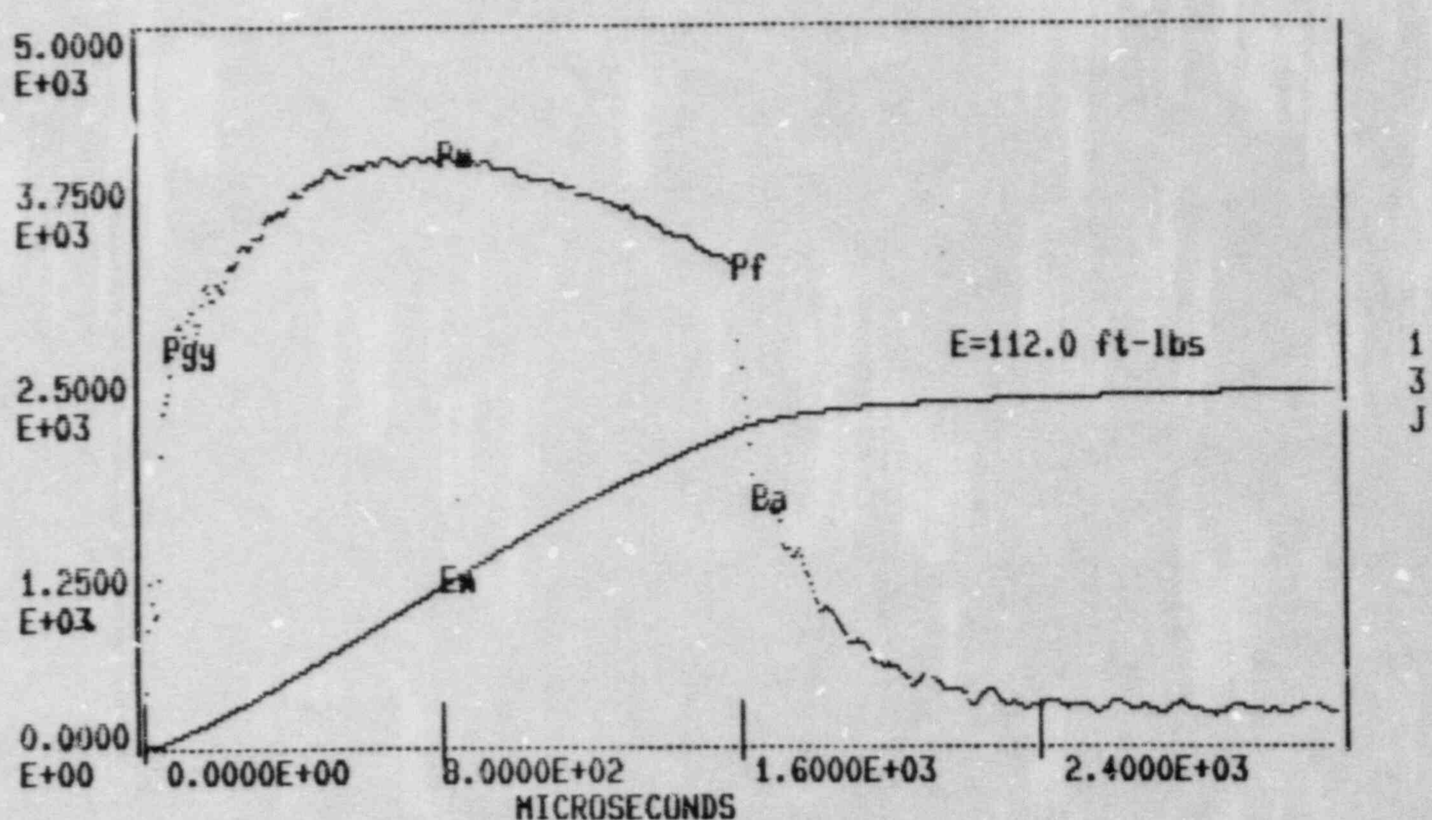

SAMPLE NO. 13J TESTED AT 77 F, DIAL ENERGY =112.0 ft-lbs

General Yielding ***Maximum Load*** ***Fast Fracture***

P=2.82klb t= 80uS P=4.09klb E= 45.4ft-lbs t= 815uS Pf=3.24klb Pa=1.62klb

8092B:1b/092084

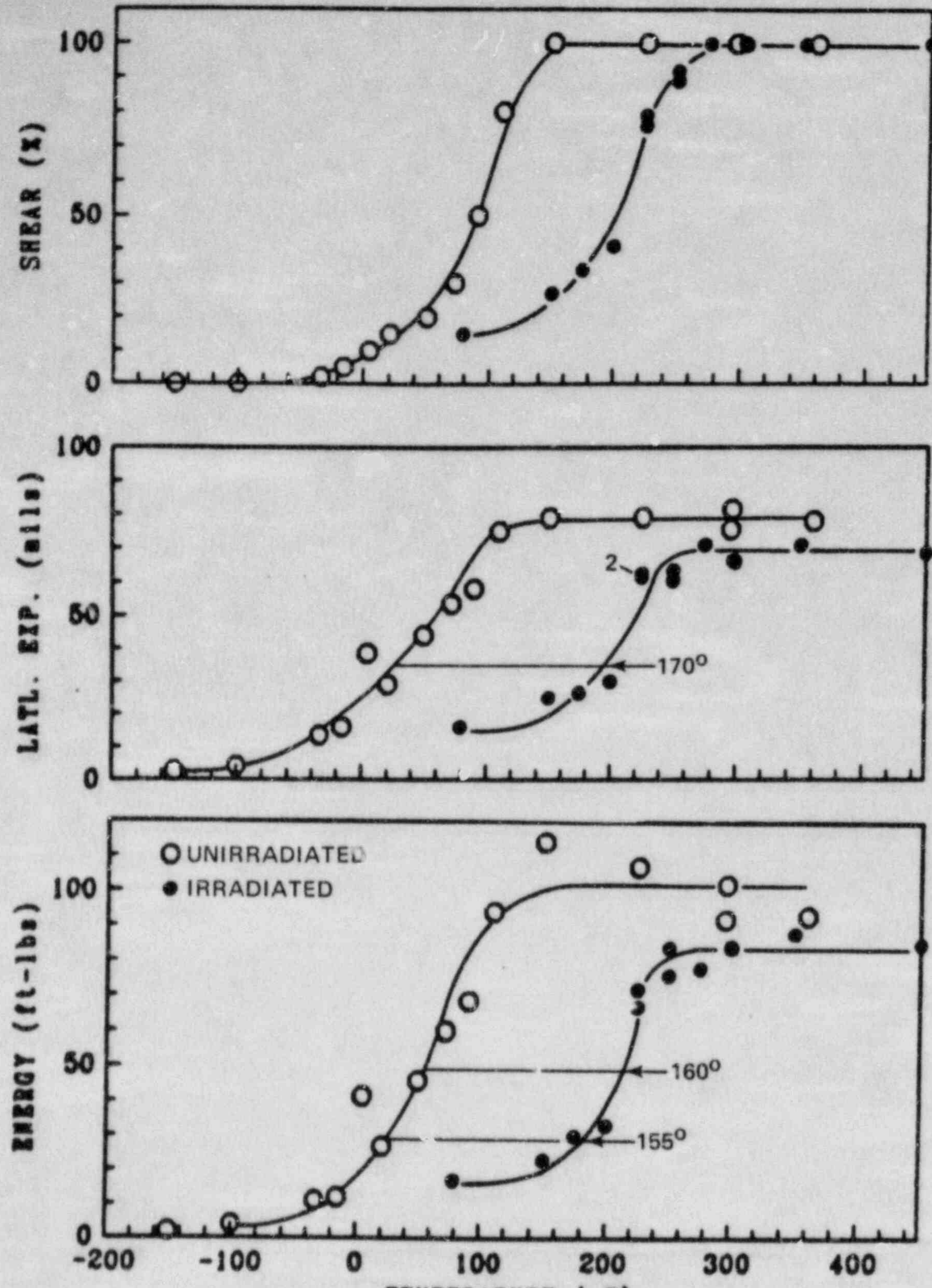

Figure 5-10. Irradiated Capsule Charpy V-Notch Impact Properties for Palisades Intermediate Shell Plate D-3803-1 (Transverse Orientation)

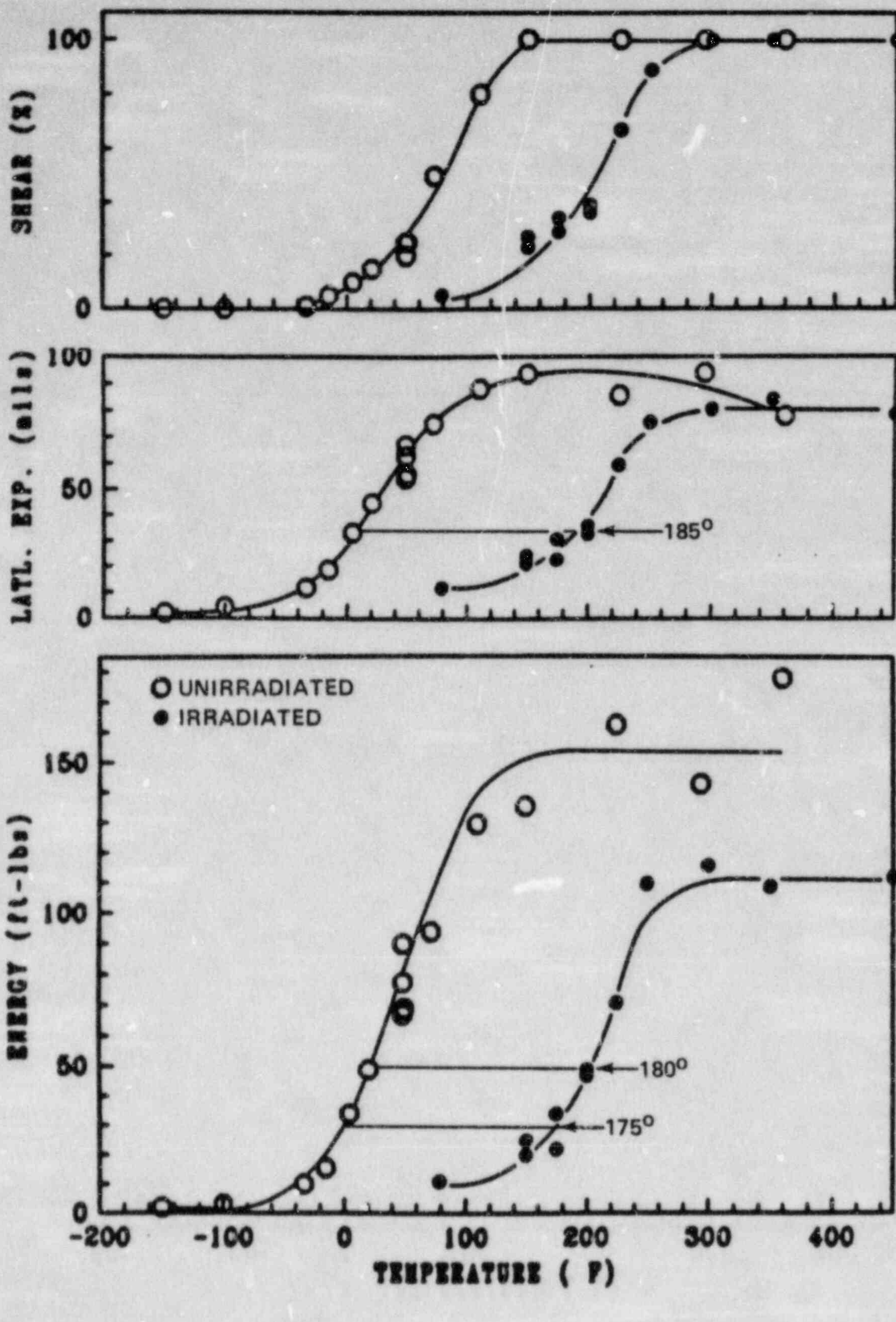

Figure 5-11. Irradiated Capsule Charpy V-Notch Impact Properties for Palisades Intermediate Shell Plate D-3803-1 (Longitudinal Orientation)

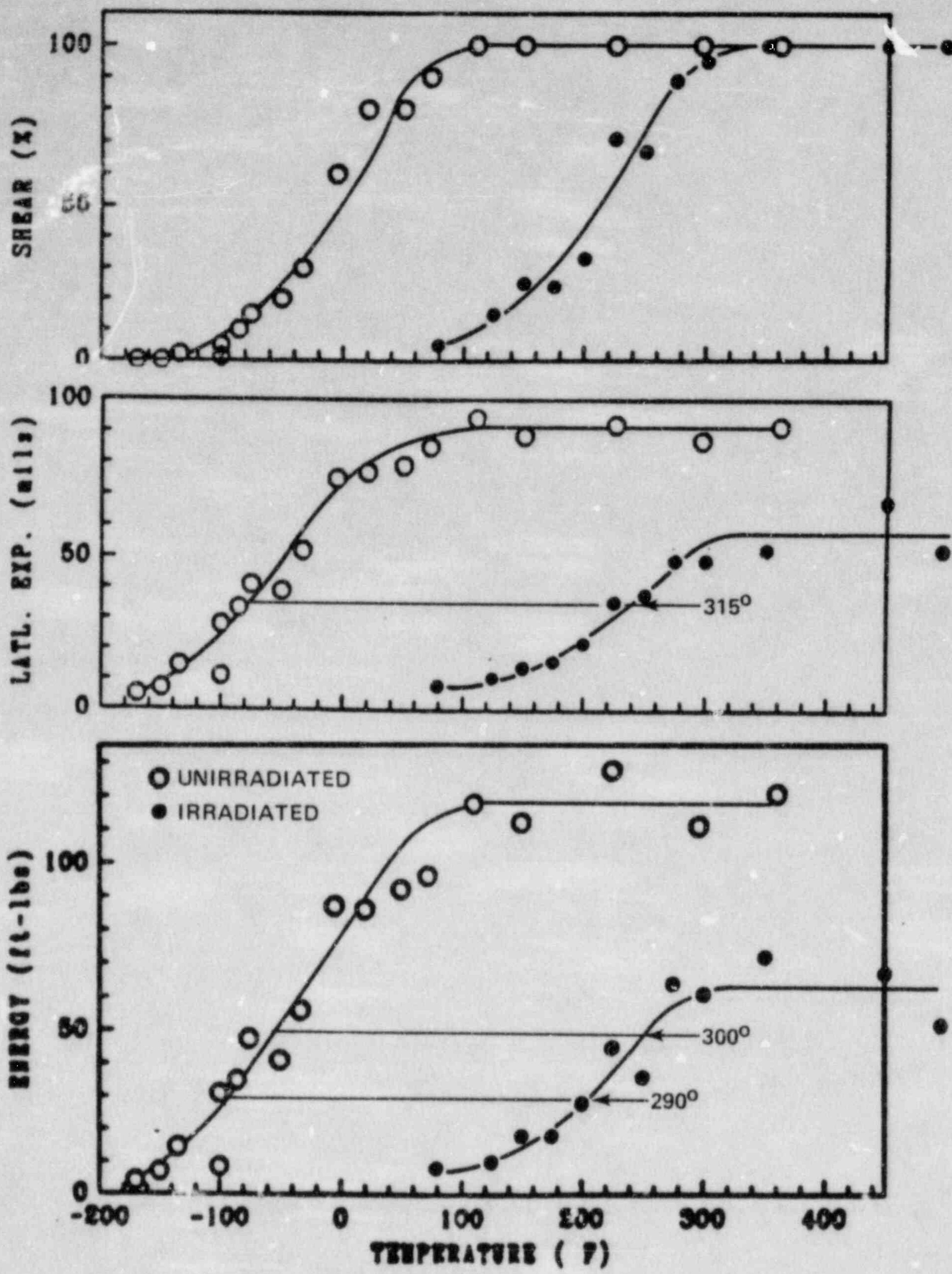

Figure 5-12. Irradiated Capsule Charpy V-Notch Impact Properties for Palisades Weld Metal

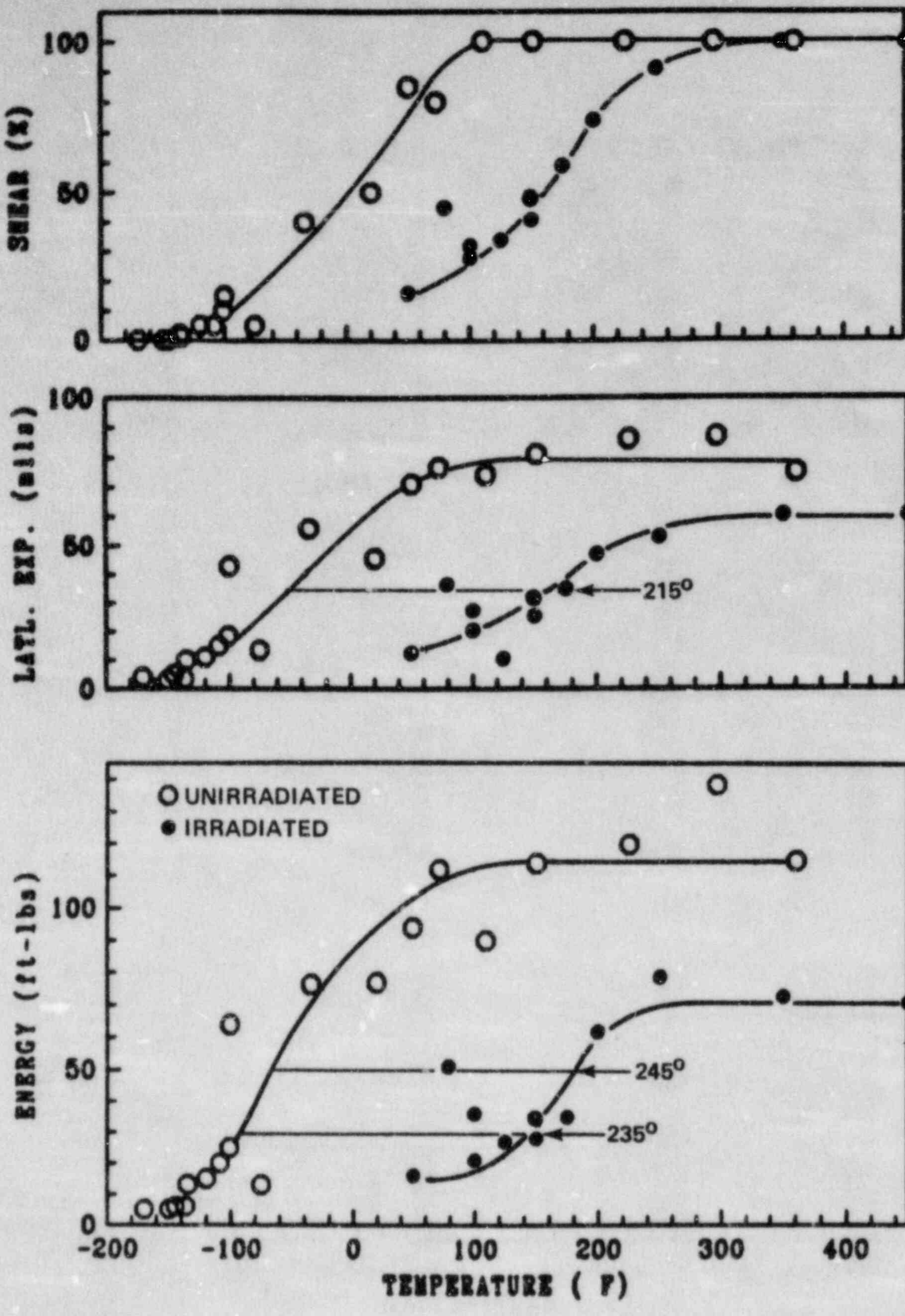

Figure 5-13. Irradiated Capsule V-Notch Impact Properties for Palisades Weld Heat Affected Zone Metal

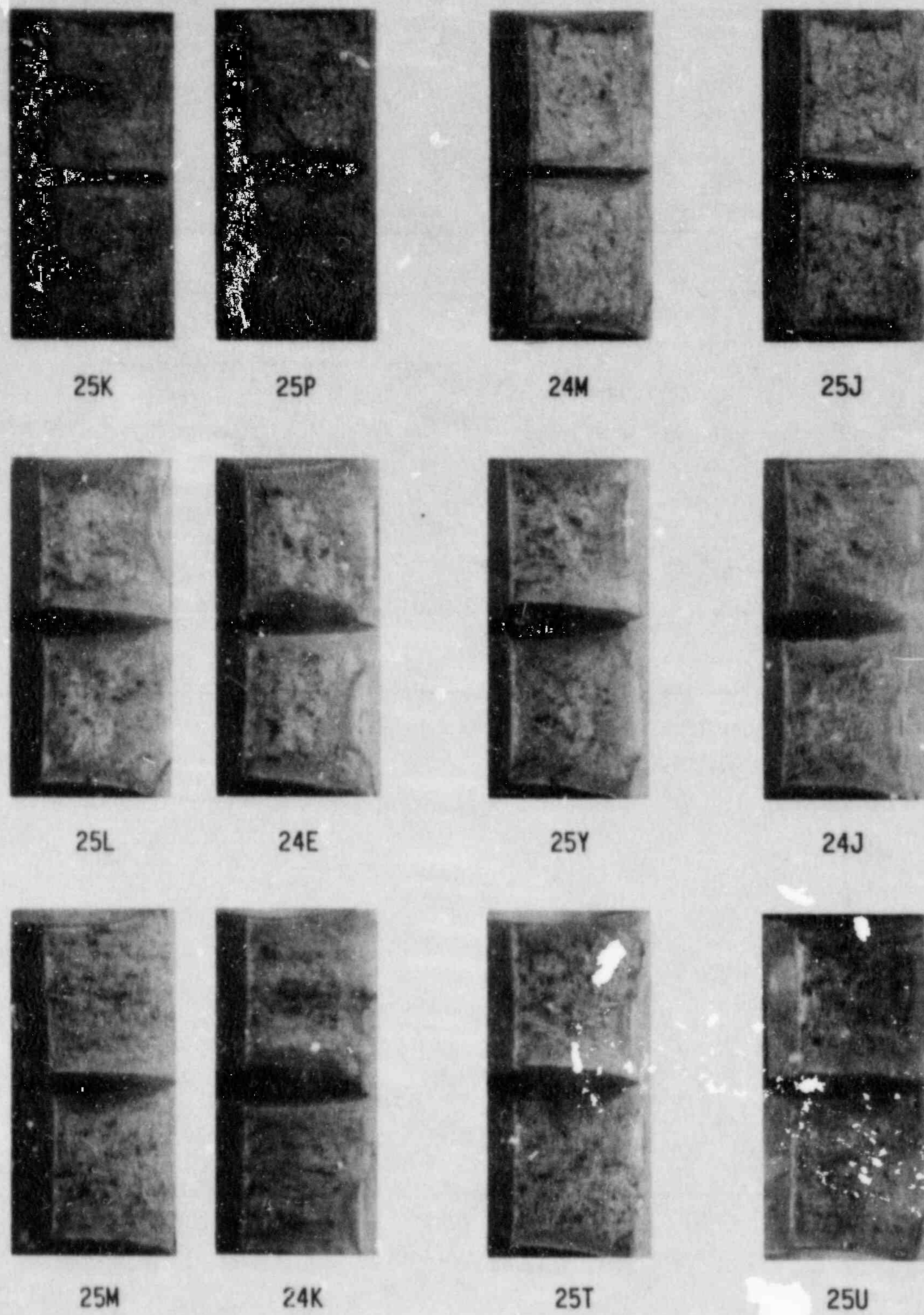

Figure 5-14. Irradiated Capsule Charpy (W-290) Impact Specimen Fracture Surfaces for Palisades Intermediate Shell Plate D-3803-1 (Transverse Orientation)

IMAGE EVALUATION
TEST TARGET (MT-3)

150mm

6″

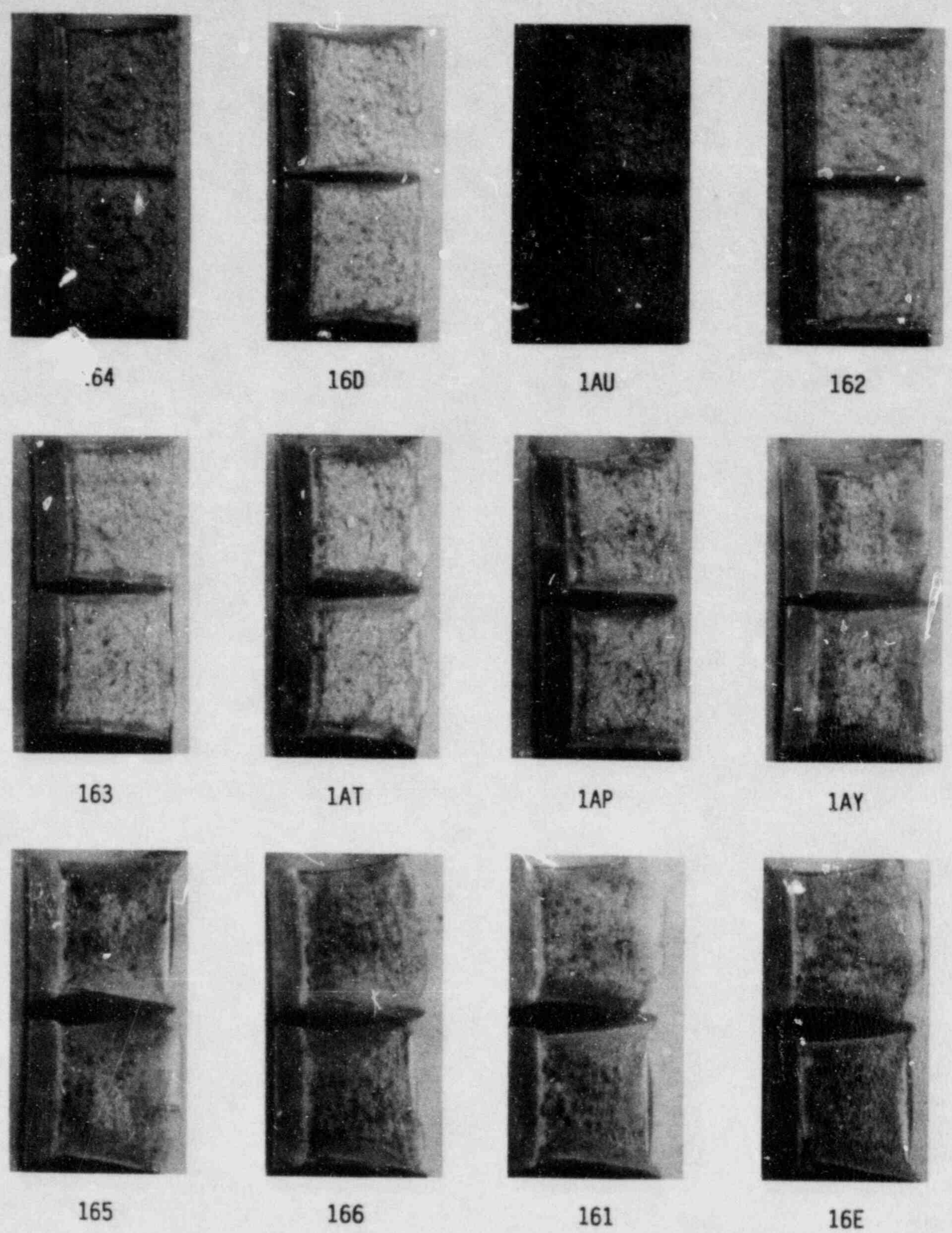

Figure 5-15. Irradiated Capsule (W-290) Charpy Impact Specimen Fracture Surfaces for Palisades Intermediate Shell Plate D-3803-1 (Longitudinal Orientation)

10644-13

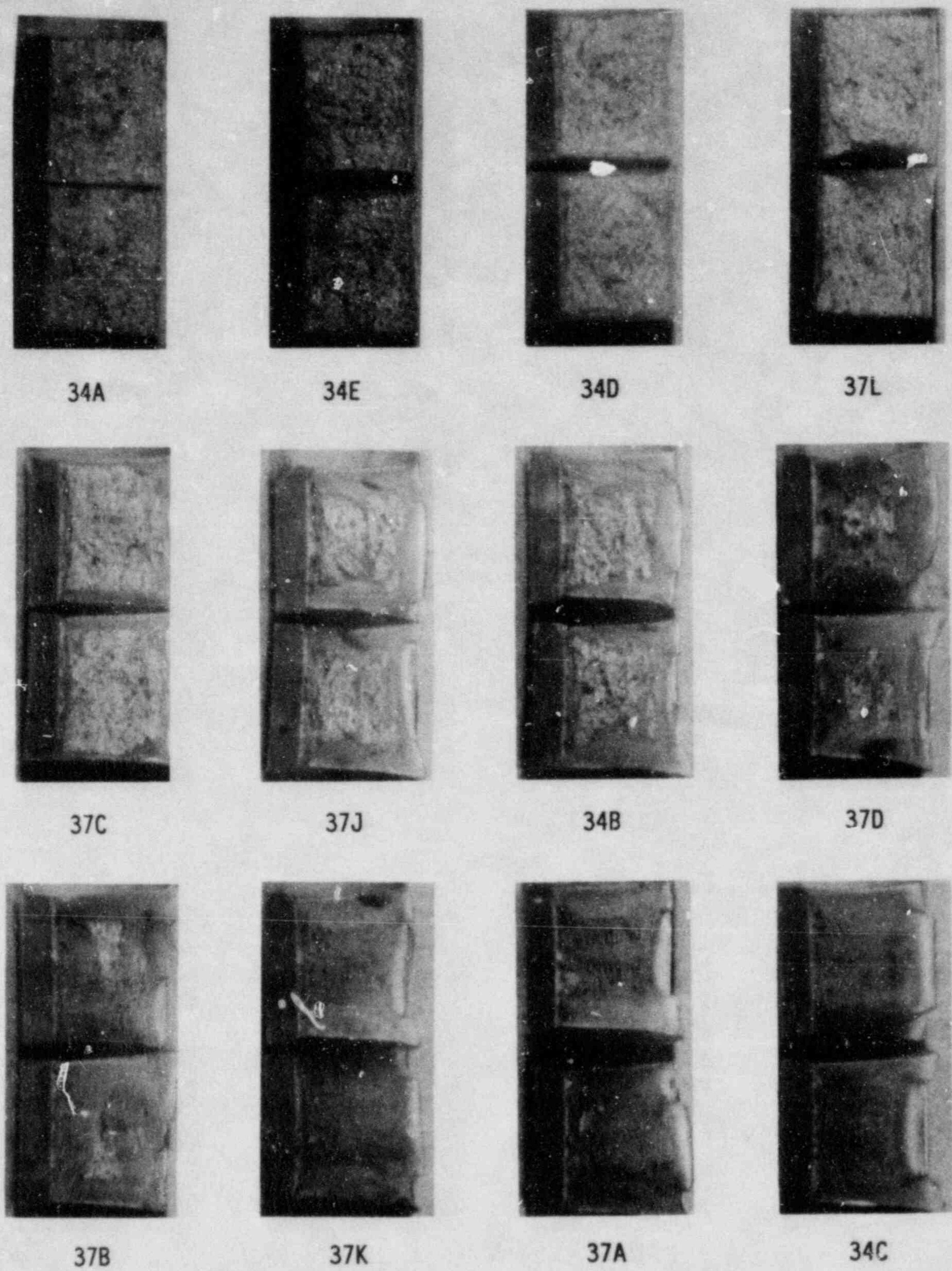

Figure 5-16. Irradiated Capsule (W-290) Charpy Impact Specimen Fracture Surfaces for Palisades Weld Metal

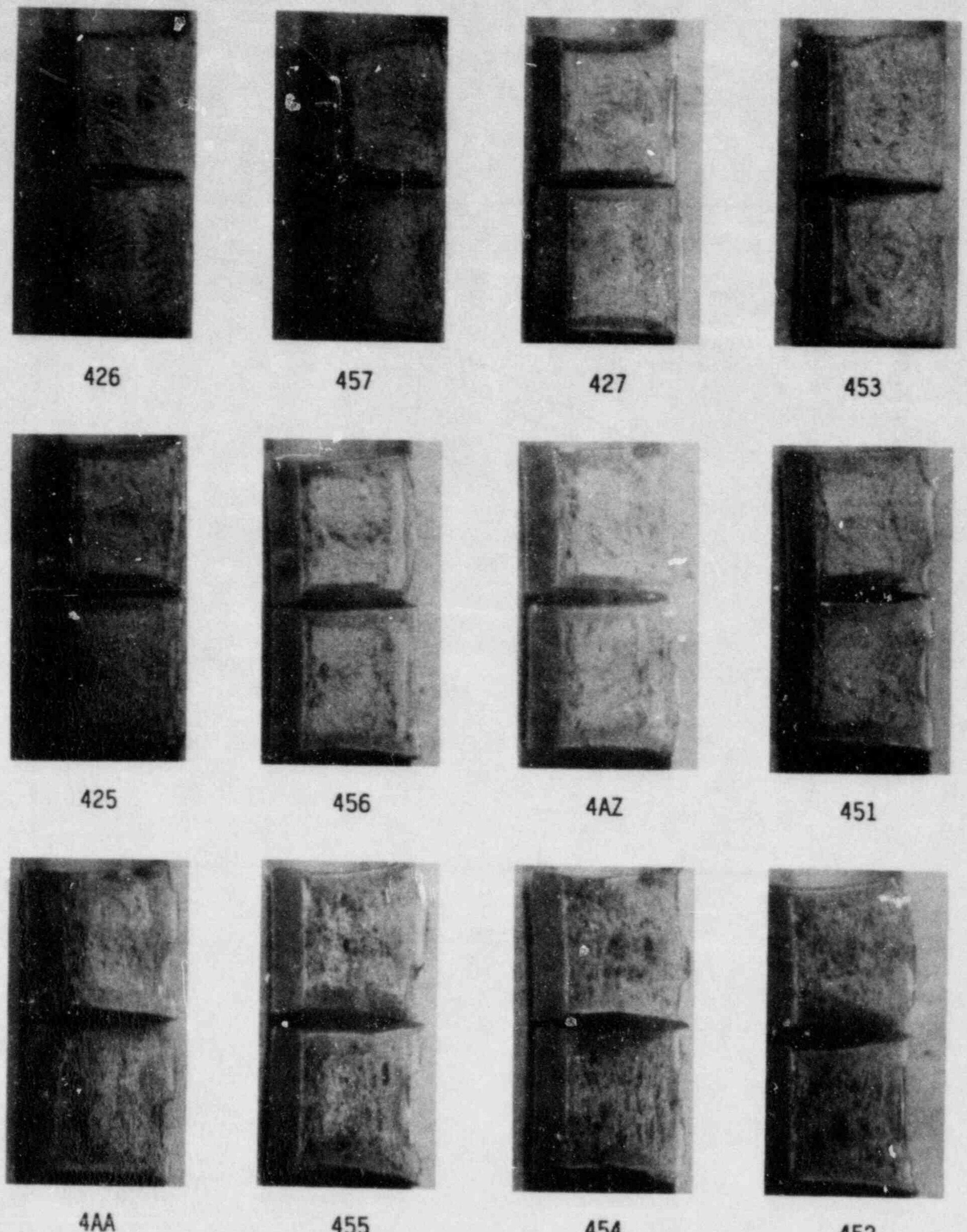

Figure 5-17. Irradiated Capsule (W-290) Charpy Impact Specimen Fracture Surfaces for Palisades Weld Metal Heat Affected Zone Metal

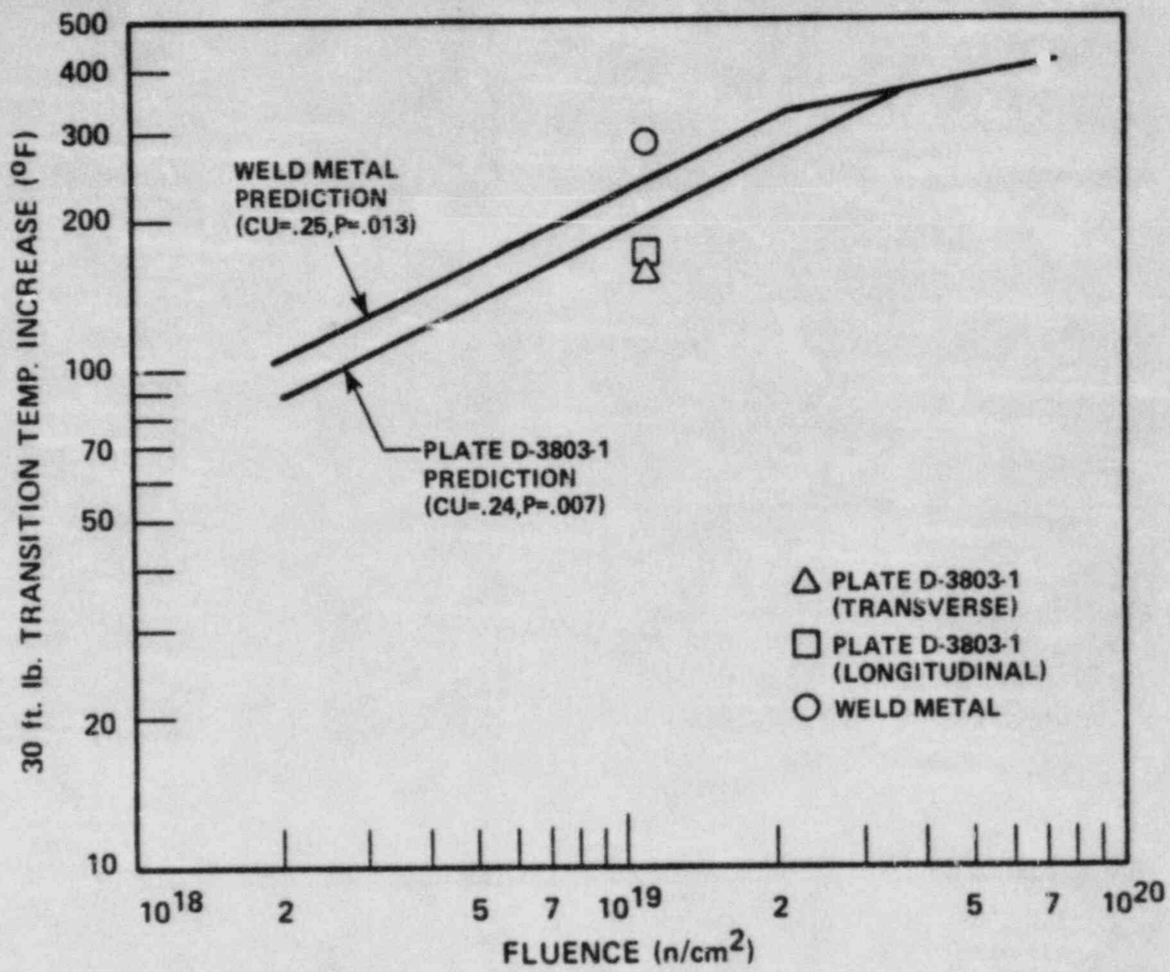

Figure 5-18. Comparison of Actual versus Predicted 30 ft-lb Transition Temperature Increases for the Palisades Surveillance Weld Material, Based on the Prediction Methods of Regulatory Guide 1.99 Revision 1

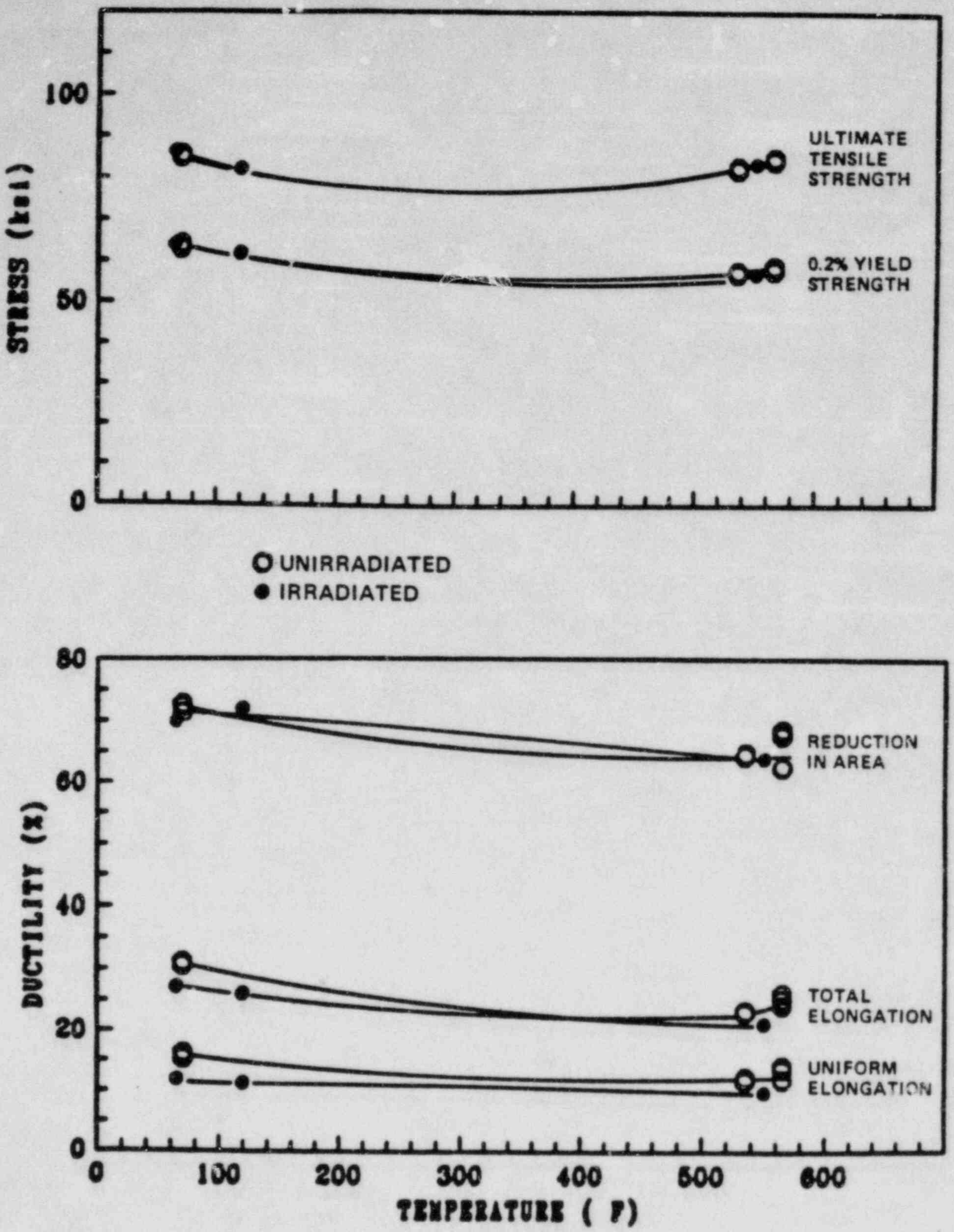

Figure 5-19. Thermal Capsule Tensile Properties for Palisades Intermediate Shell Plate D-3803-1 (Longitudinal Orientation)

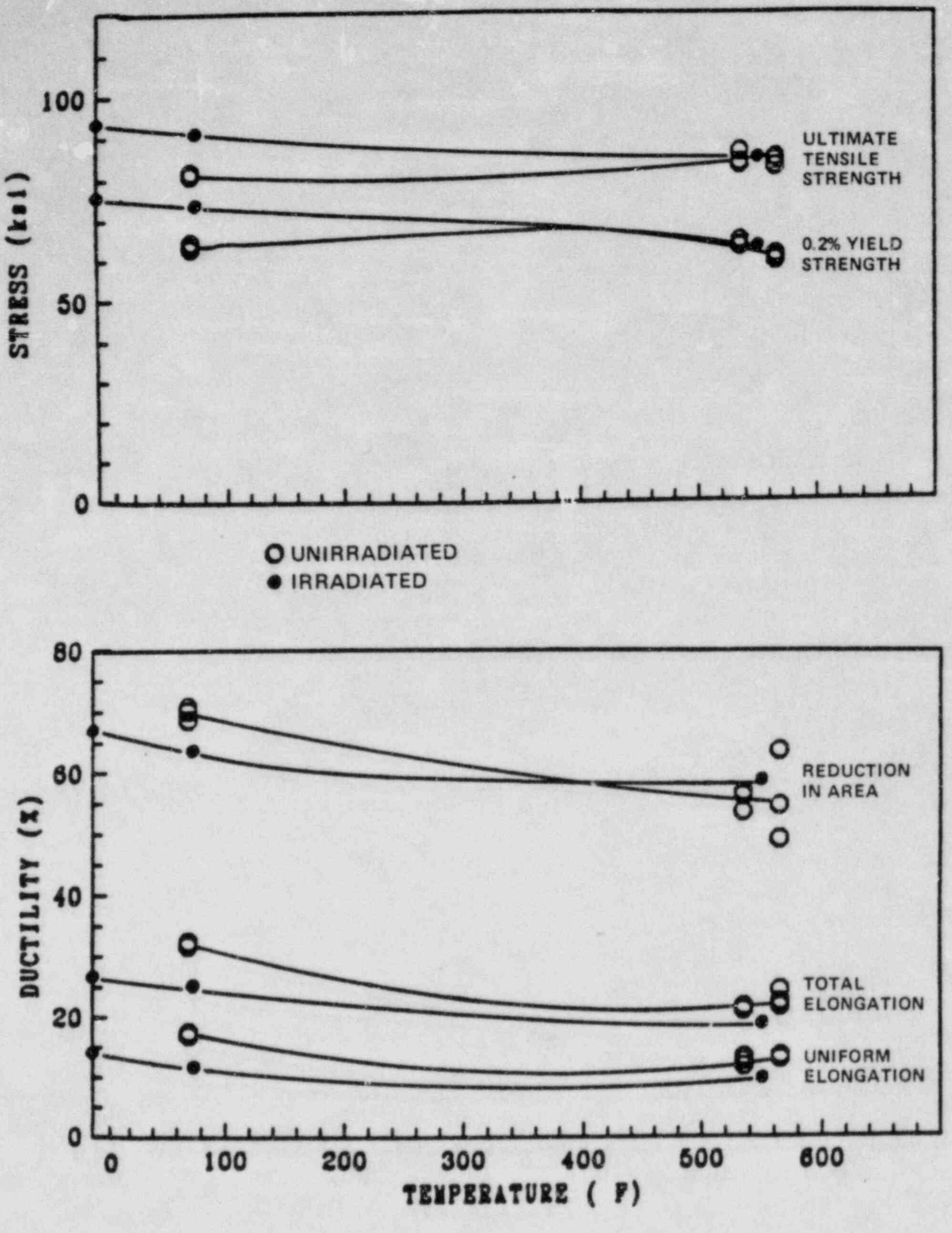

Figure 5-20. Thermal Capsule Tensile Properties for Palisades Weld Metal

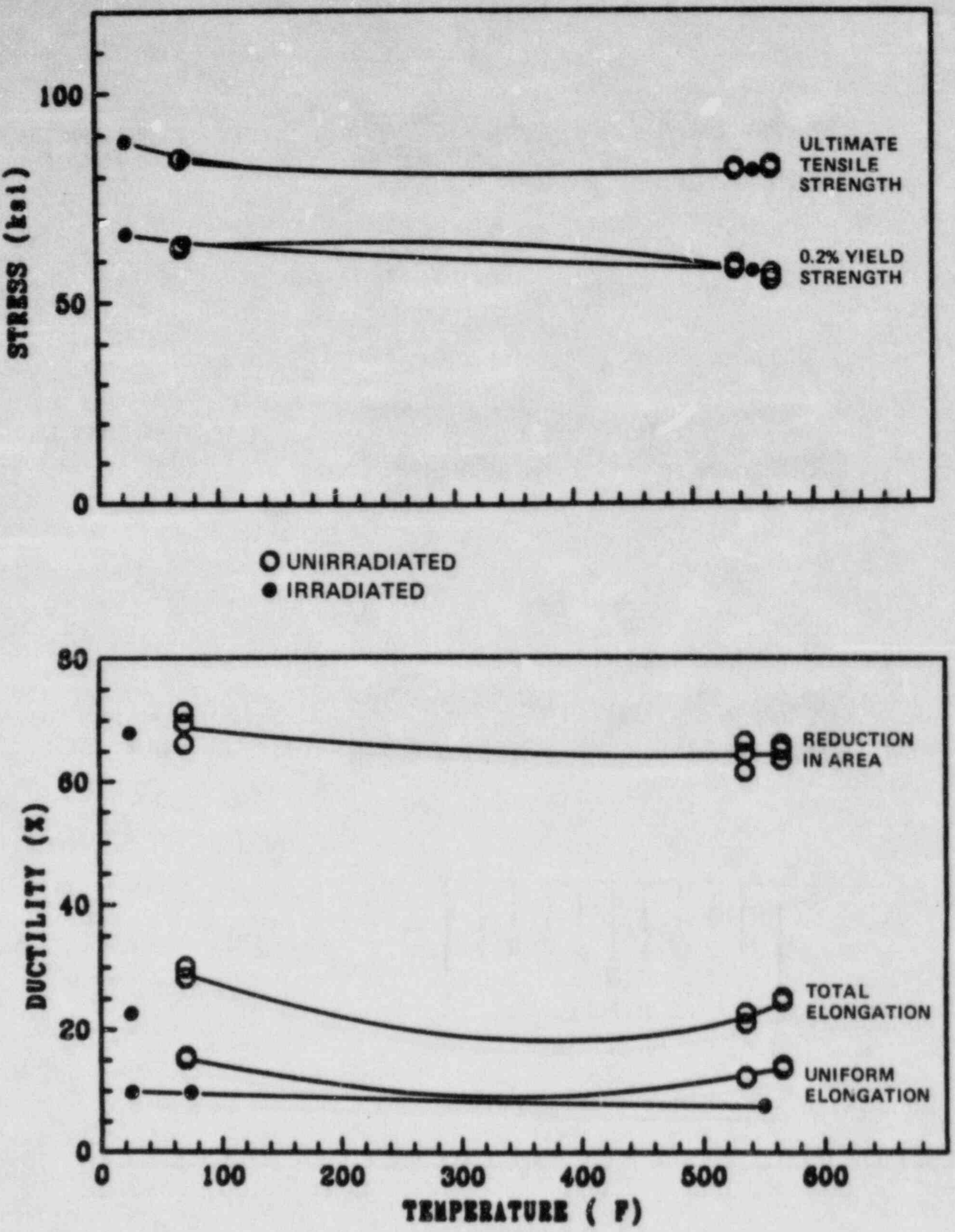

Figure 5-21. Thermal Capsule Tensile Properties for Palisades Weld Heat Affected Zone Metal

10644-1

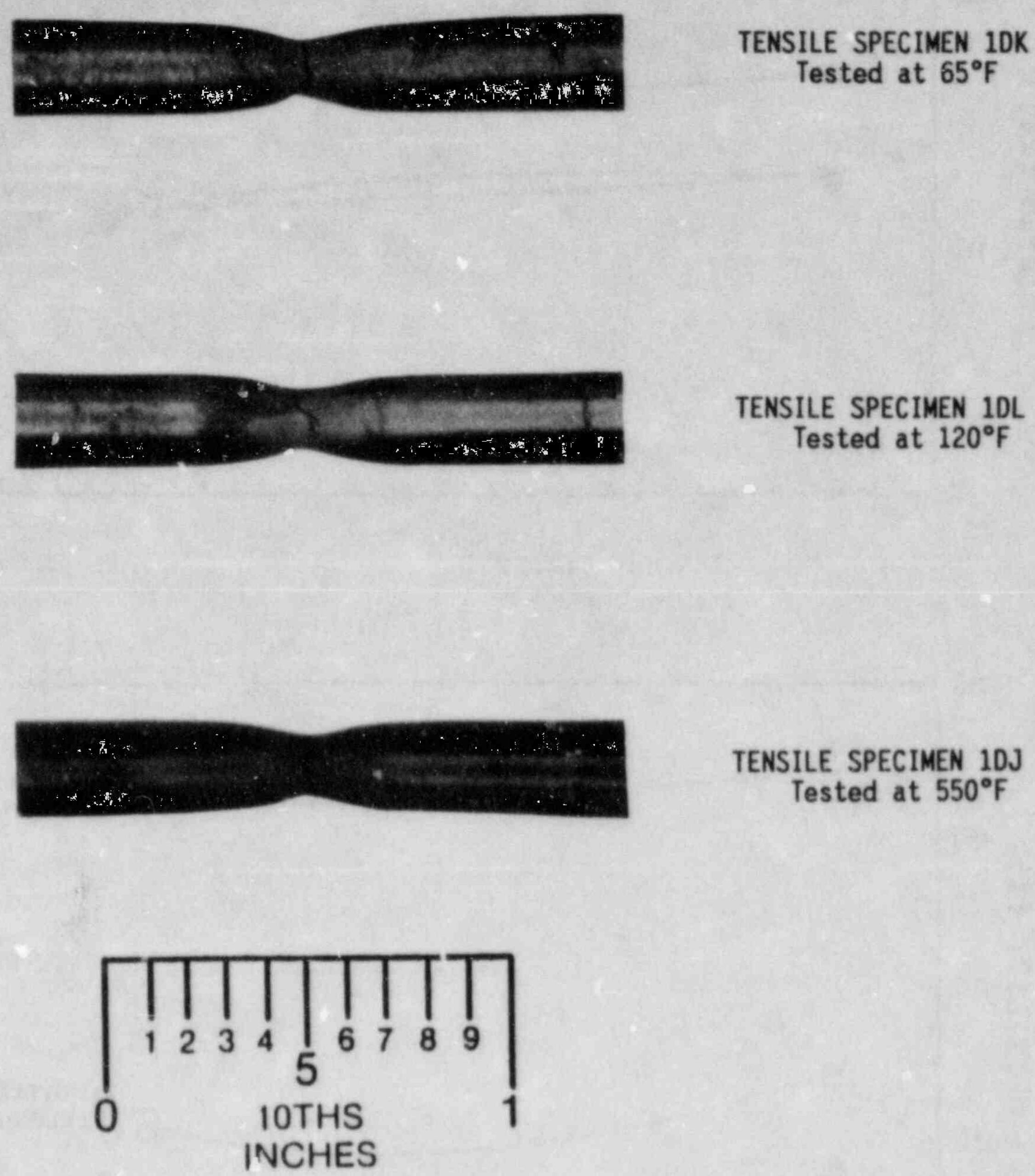

Figure 5-22. Fractured Thermal Capsule Tensile Specimens of Palisades Intermediate Shell Plate D-3803-1 (Longitudinal Orientation)

10644-2

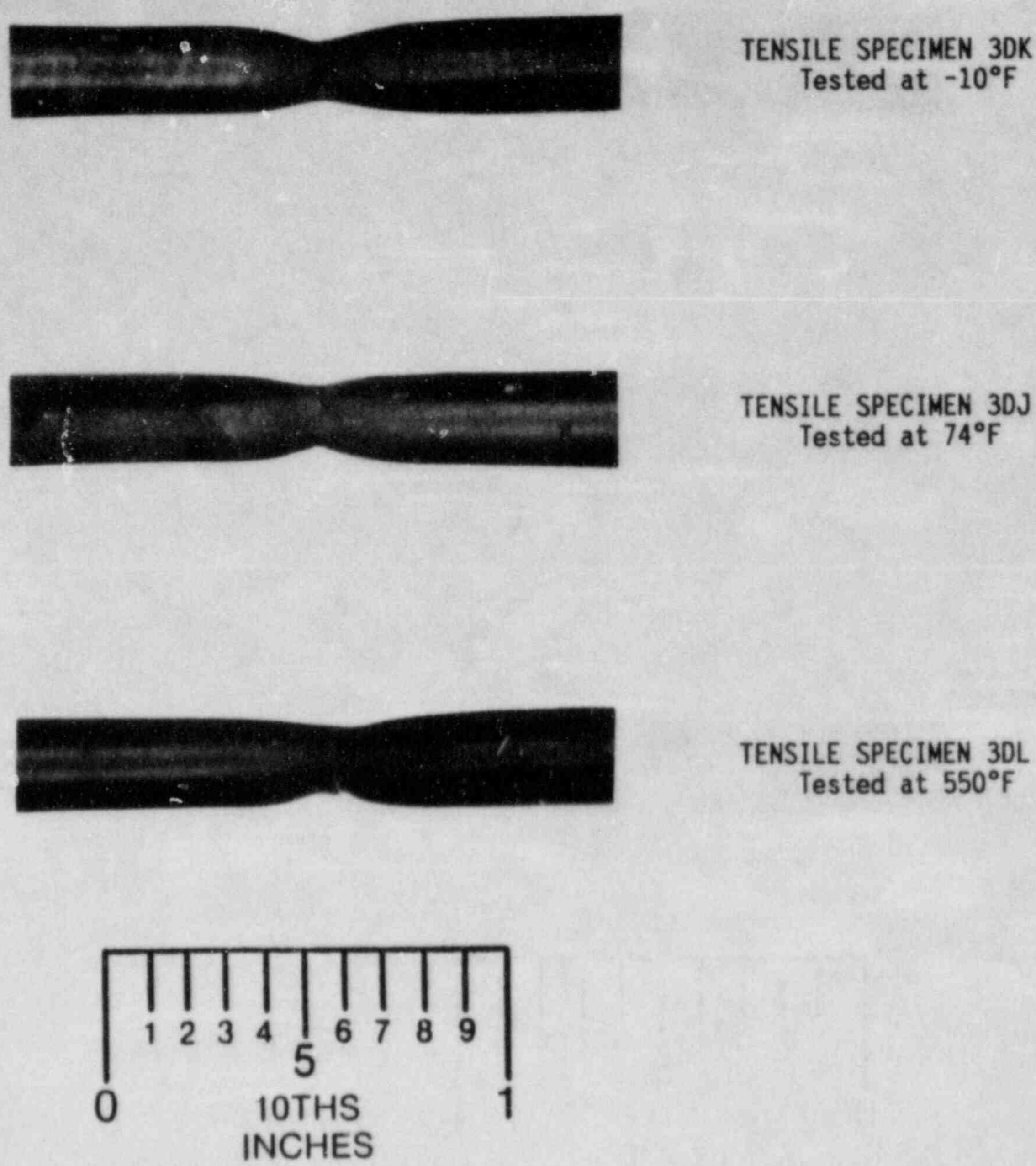

Figure 5-23. Fractured Thermal Capsule Tensile Specimens of Palisades Weld Metal

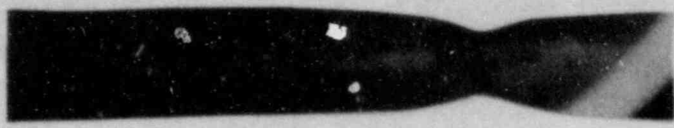

TENSILE SPECIMEN 4DK
Tested at 25°F

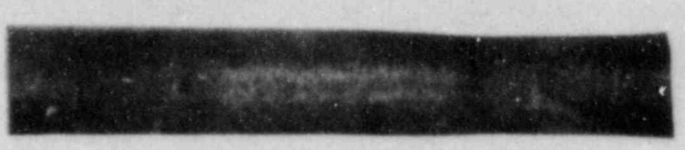

TENSILE SPECIMEN 4DJ
Tested at 74°F

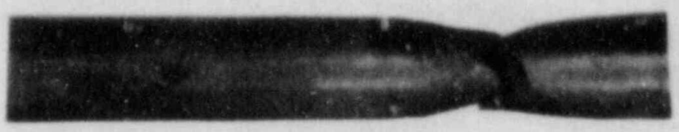

TENSILE SPECIMEN 4DL
Tested at 550°F

Figure 5-24. Fractured Thermal Capsule Tensile Specimens of Palisades Weld Heat Affected Zone Metal

FIGURE 5-25

Typcial Stress-Strain Curve for Tension Specimens

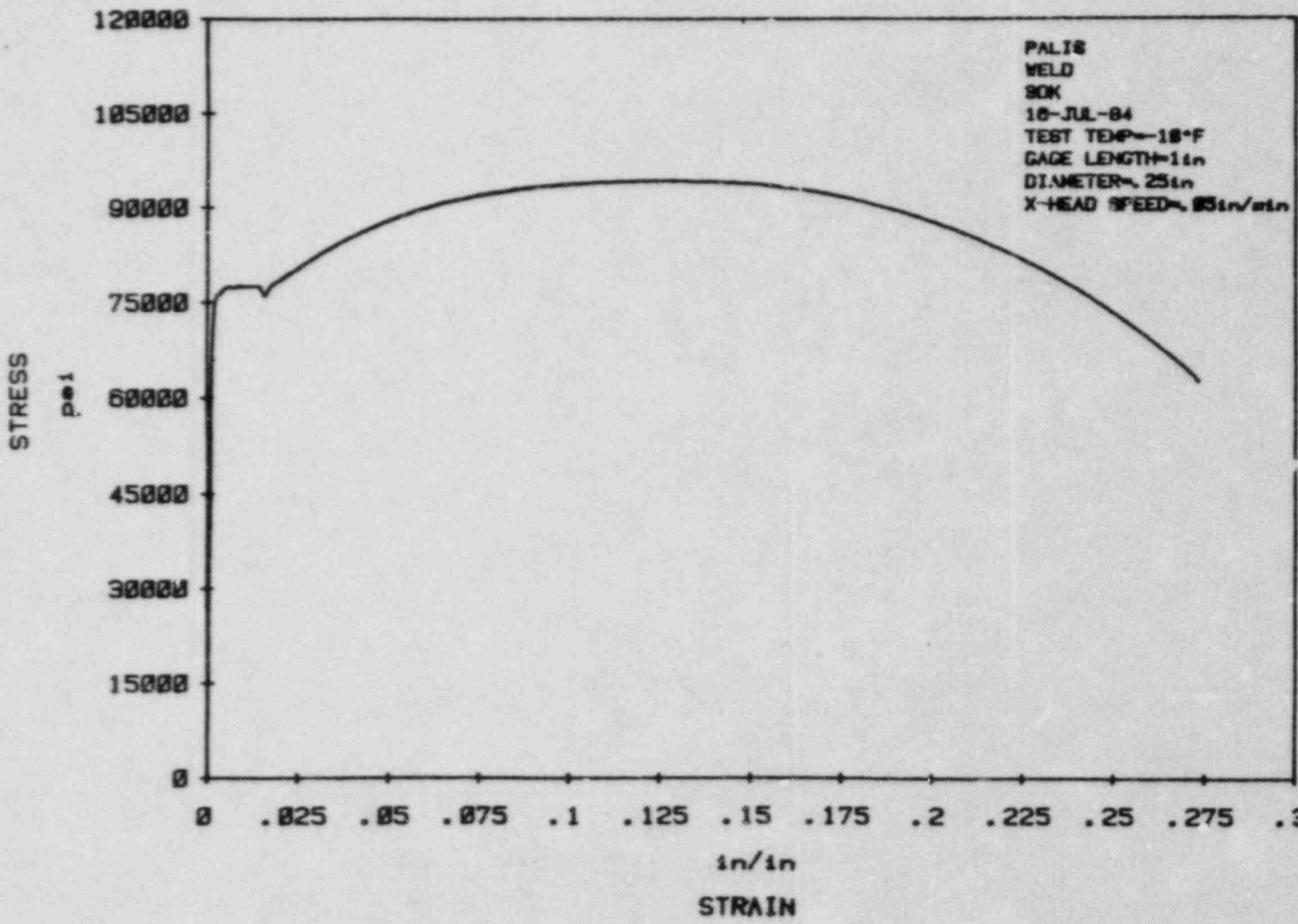

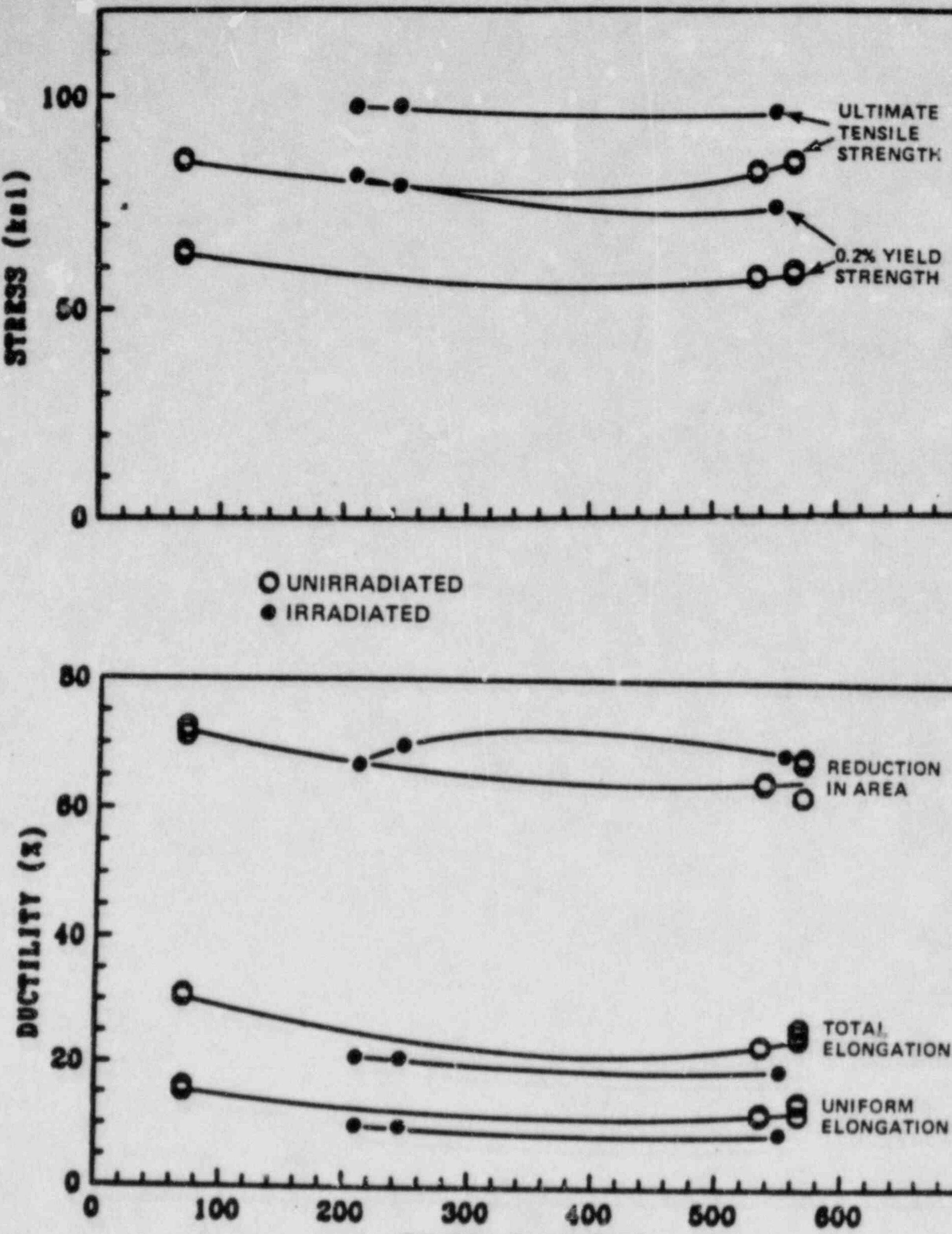

Figure 5-26. Irradiated Capsule Tensile Properties for Palisades Intermediate Shell Plate D-3803-1 (Longitudinal Orientation)

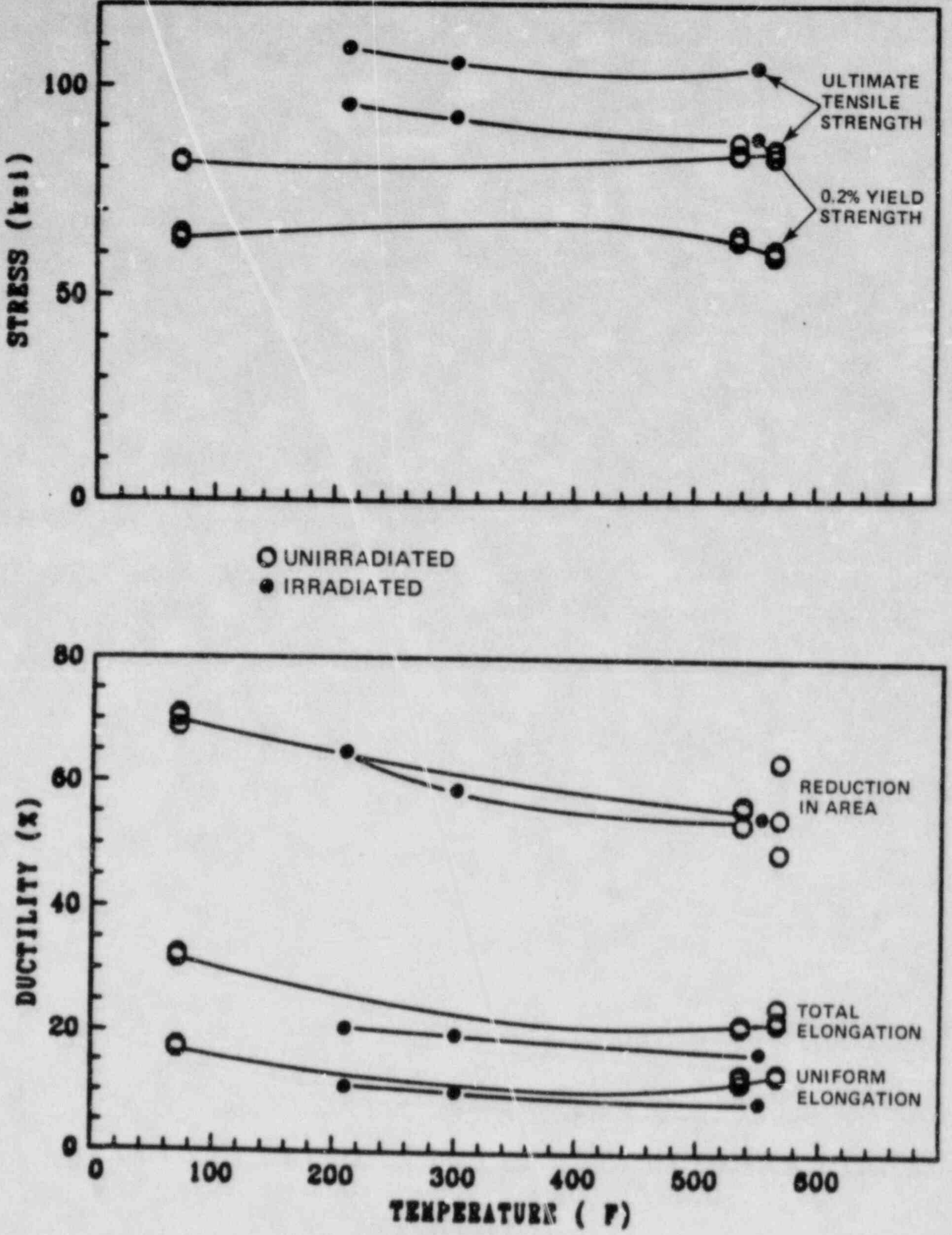

Figure 5-27. Irradiated Capsule Tensile Properties for Palisades Weld Metal

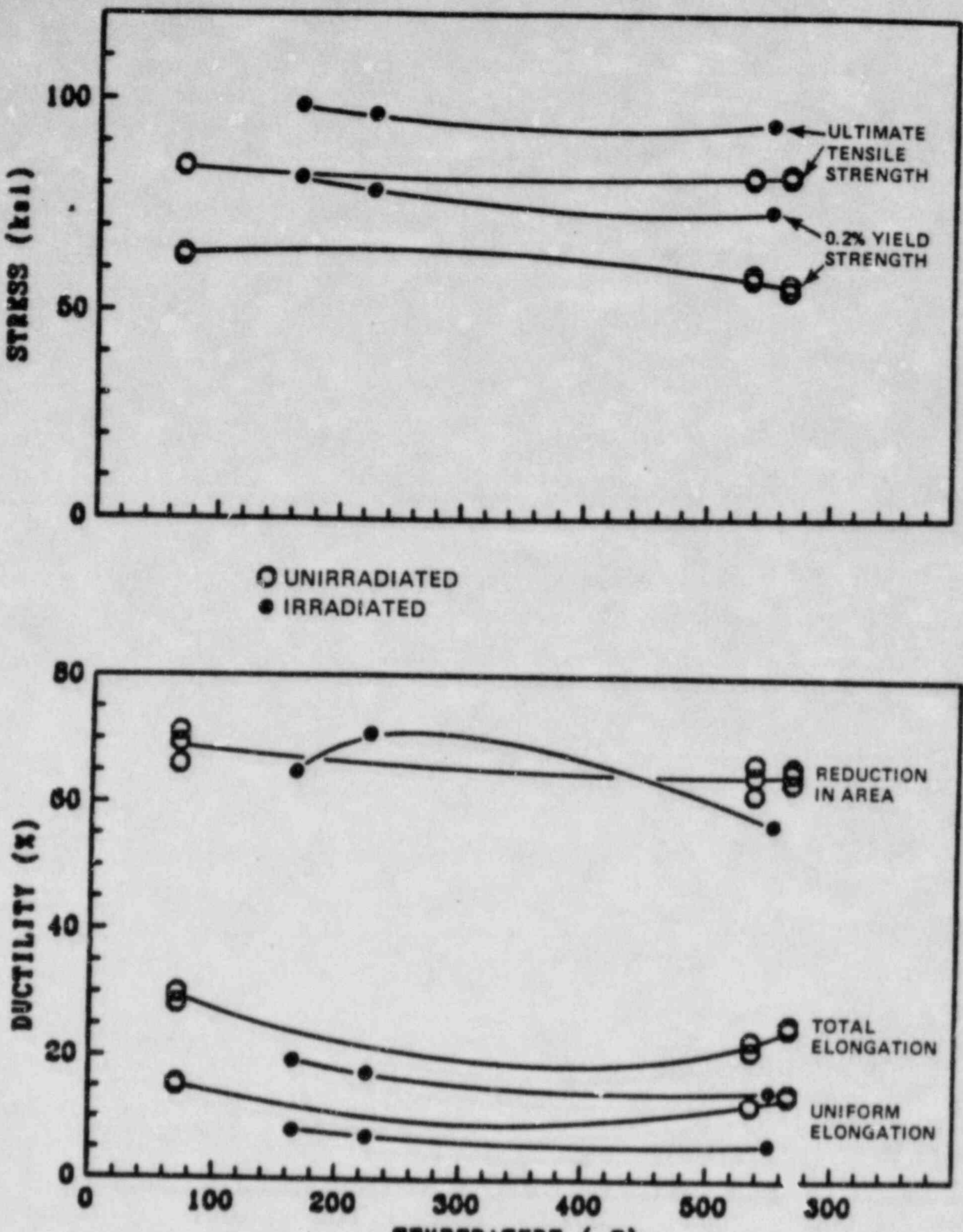

Figure 5-28. Irradiated Capsule Tensile Properties for Palisades Weld Heat Affected Zone Metal

10644-4

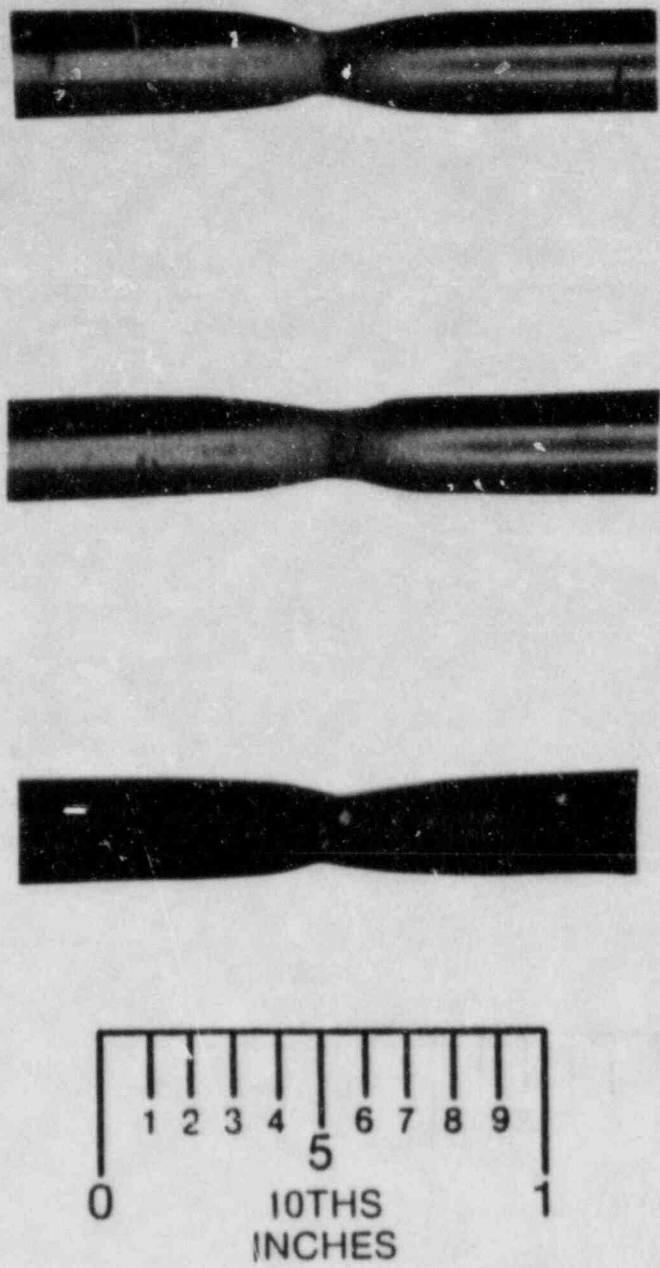

TENSILE SPECIMEN 1EL
Tested at 210°F

TENSILE SPECIMEN 1EM
Tested at 245°F

TENSILE SPECIMEN 1EK
Tested at 550°F

Figure 5-29. Fractured Irradiated Capsule Tensile Specimens of Palisades Intermediate Shell Plate D-3803-1 (Longitudinal Orientation)

10644-5

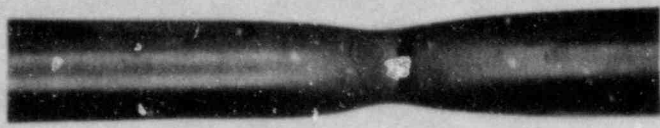

TENSILE SPECIMEN 3J6
Tested at 210°F

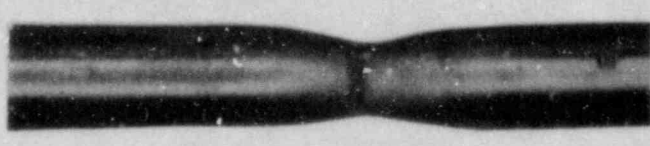

TENSILE SPECIMEN 3J1
Tested at 300°F

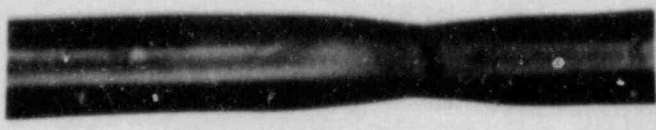

TENSILE SPECIMEN 3J7
Tested at 550°F

Figure 5-30. Fractured Irradiated Capsule Tensile Specimens of Palisades Weld Metal

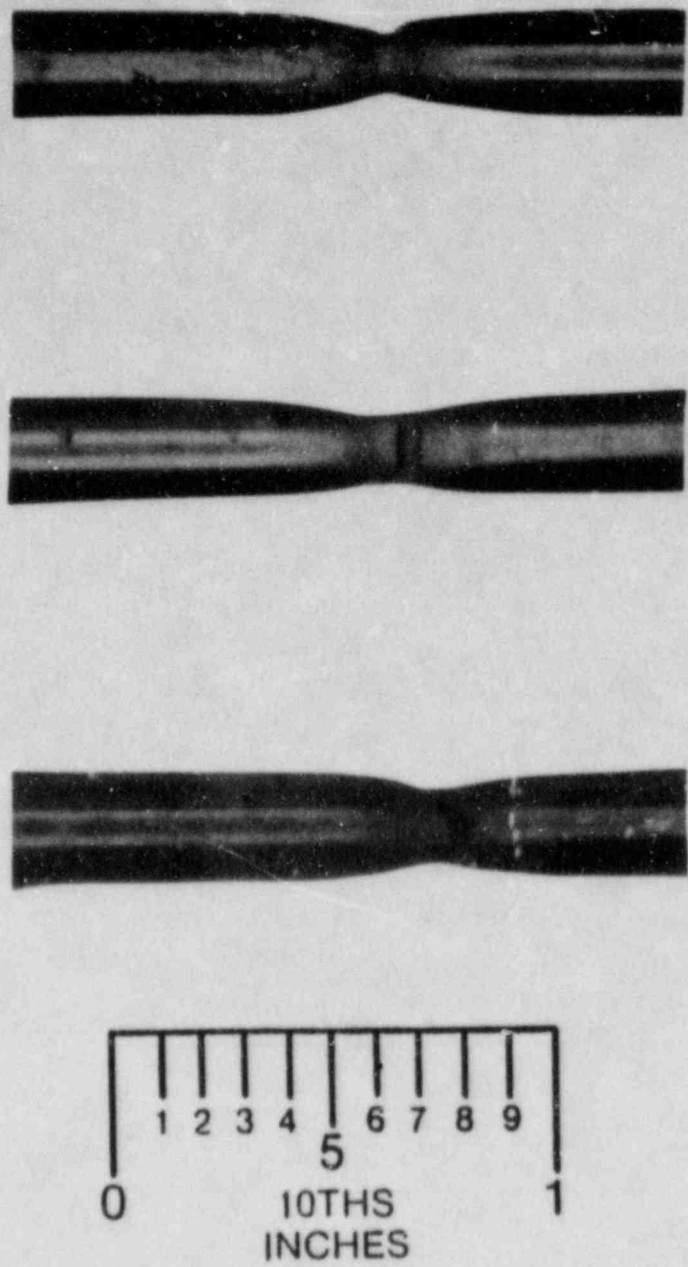

TENSILE SPECIMEN 4EL
Tested at 165°F

TENSILE SPECIMEN 4EM
Tested at 225°F

TENSILE SPECIMEN 4EK
Tested at 550°F

Figure 5-31. Fractured Irradiated Capsule Tensile Specimens of Palisades Weld Heat Affected Zone Metal

SECTION 6

RADIATION ANALYSIS AND NEUTRON DOSIMETRY

6-1. INTRODUCTION

Knowledge of the neutron environment within the pressure vessel/surveillance capsule geometry is required as an integral part of LWR pressure vessel surveillance programs for two reasons. First, in the interpretation of radiation-induced properties changes observed in materials test specimens the neutron environment (fluence, flux) to which the test specimens were exposed must be known. Second in relating the changes observed in the test specimens to the present and future condition of the reactor pressure vessel, a relationship must be established between the environment at various positions within the reactor vessel and that experienced by the test specimens. The former requirement is normally met by employing a combination of rigorous analytical techniques and measurements obtained with passive neutron flux monitors contained in the surveillance capsule. The latter information is derived solely from bench-marked analyses.

This section describes a discrete ordinates S_n transport analysis performed for the Palisades reactor to determine the fast neutron (E > 1.0 MeV) flux and fluence as well as the neutron energy spectra within the reactor vessel and surveillance capsule. The analytical data were then used to develop a lead factor for use in relating neutron exposure of the pressure vessel to that of the surveillance capsule. Based on spectrum-averaged reaction cross sections derived from this calculation, the analysis of the neutron dosimetry contained in Capsule W-290 is discussed and comparisons with analytical predictions are presented.

6.2. DISCRETE ORDINATES ANALYSIS

A plan view of Palisades reactor geometry at core midplane is shown in Figure 6-1. Since the reactor exhibits 1/8 th core symmetry, only a zero to 45 degree sector is depicted. Six wall capsules attached to the reactor vessel are included in the design to constitute the reactor vessel surveillance

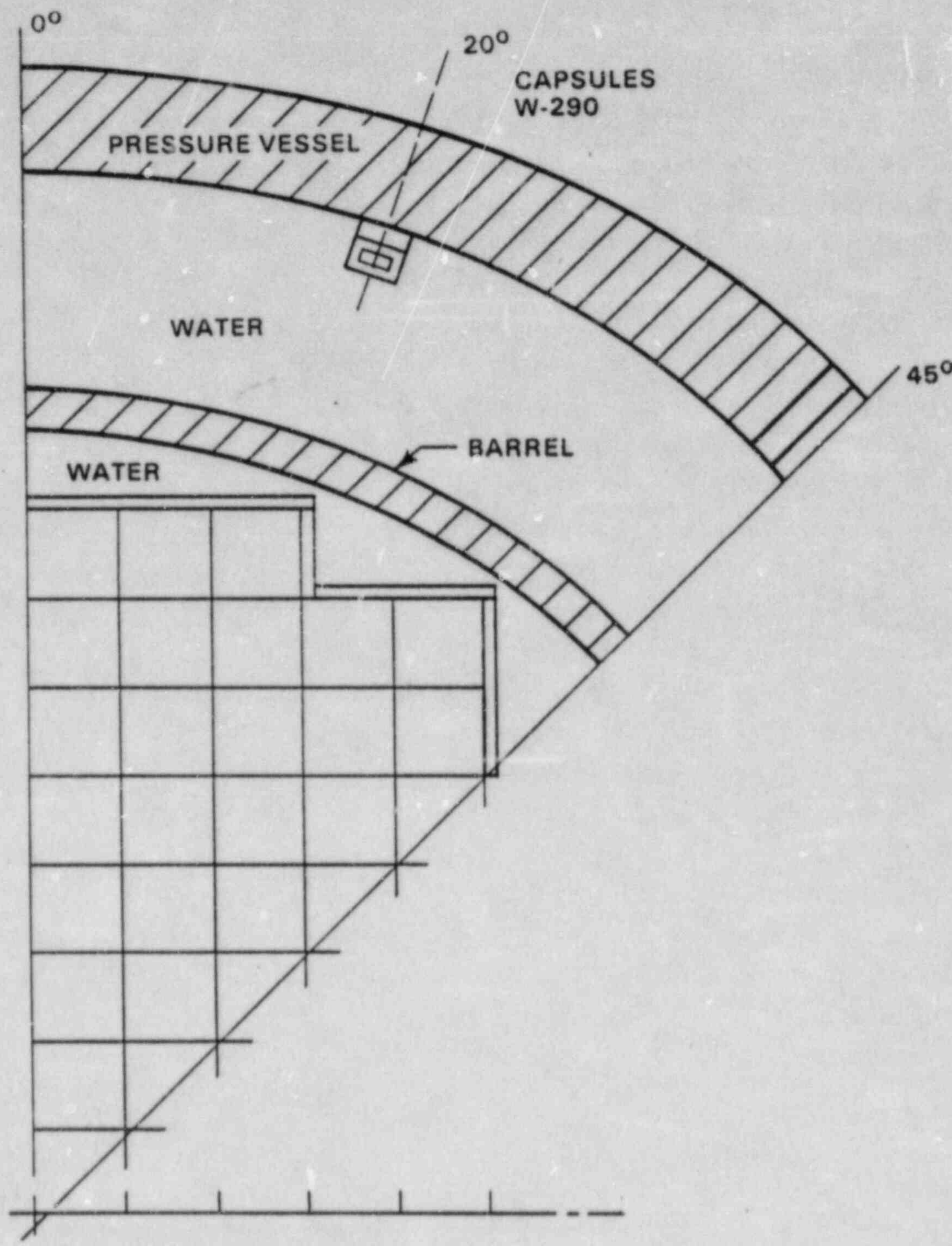

Figure 6-1. Palisades Reactor Geometry

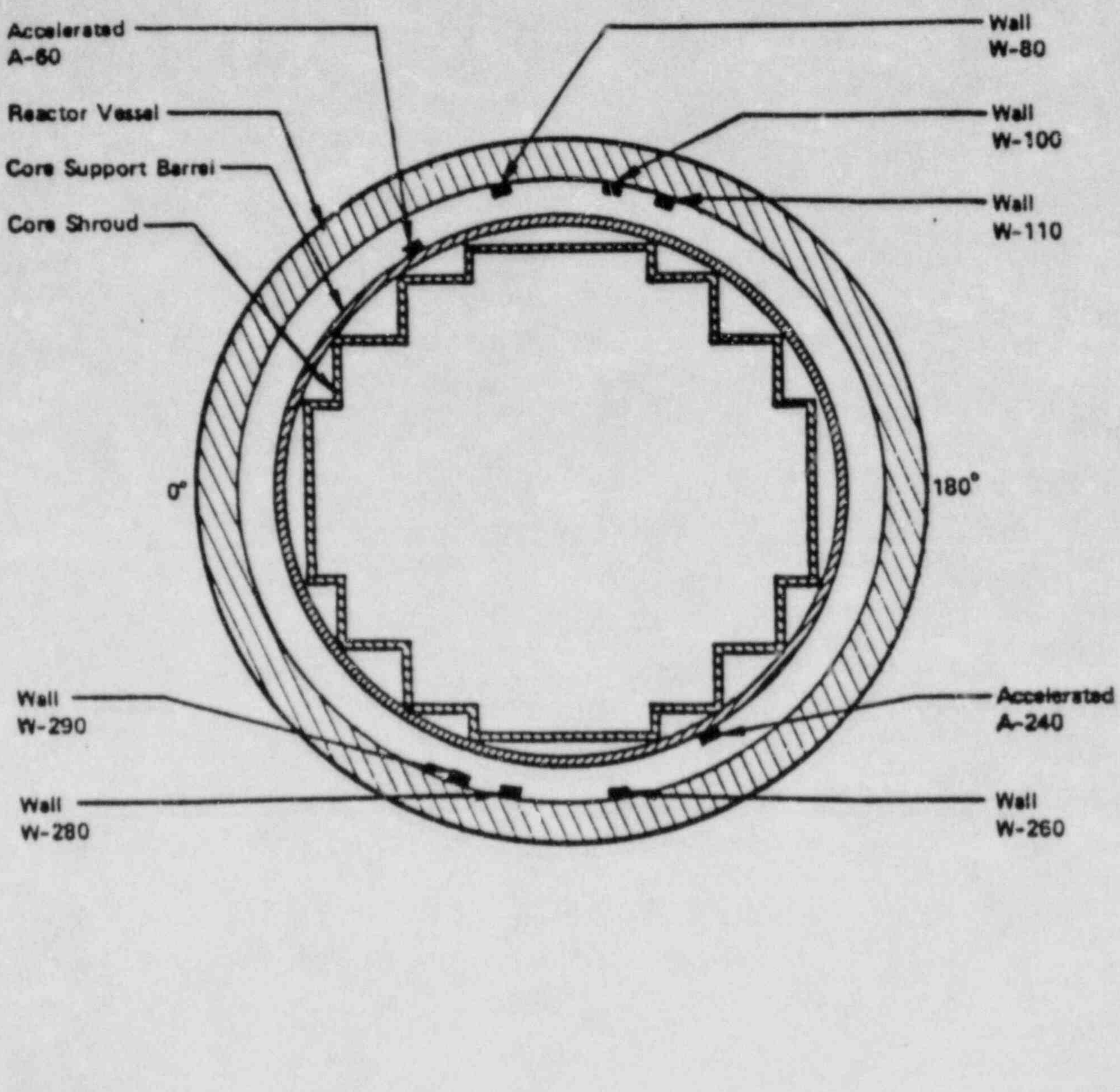

Figure 6-2A. Plan View of Palisades Wall Capsules

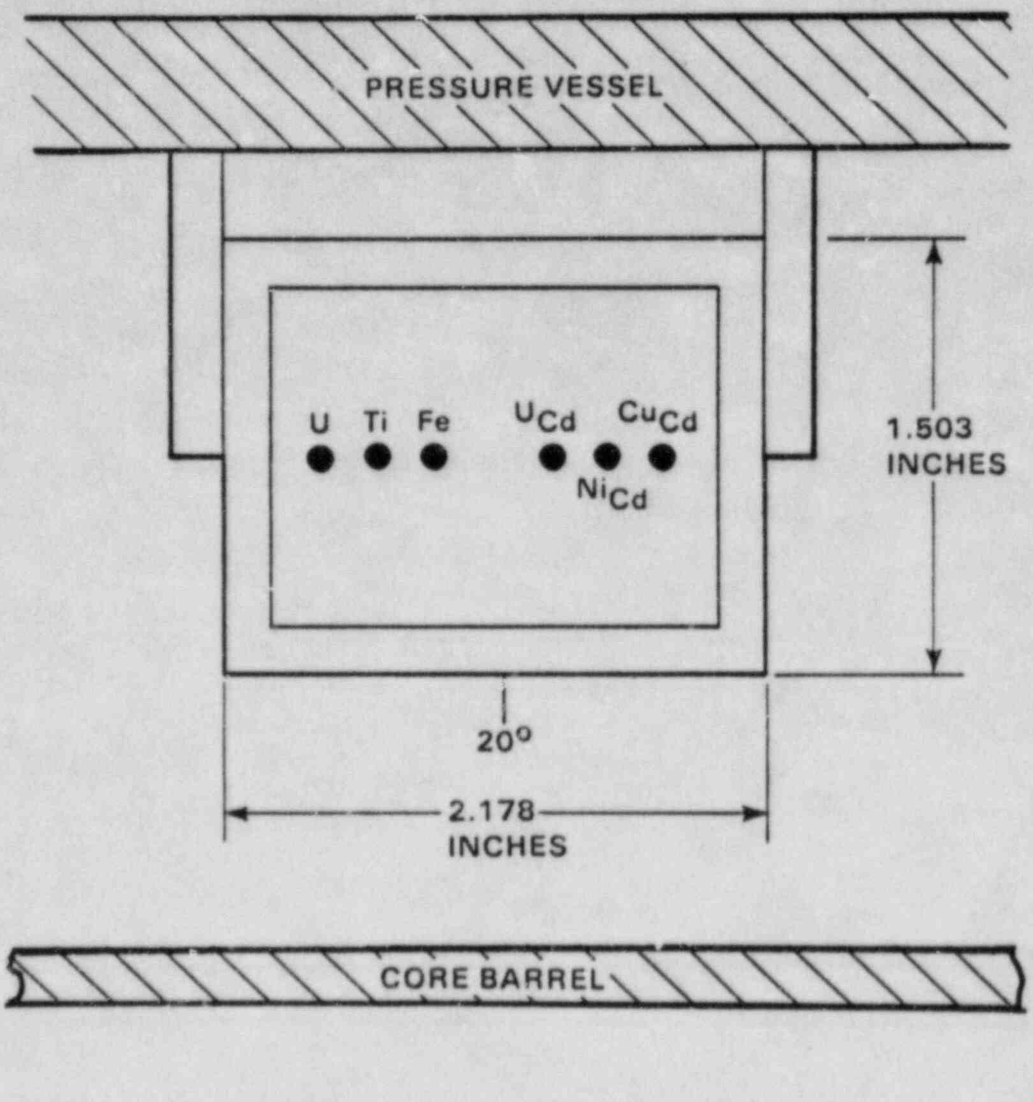

Figure 6-2B. Plan View of a Reactor Vessel Surveillance Capsule

TABLE 6-1

26 GROUP ENERGY STRUCTURE

Group	Lower Energy (MeV)	Group	Lower Energy (MeV)
1	14.19[a]	25	0.183
2	12.21	26	0.111
3	10.00		
4	8.61		
5	7.41		
6	6.07		
7	4.97		
8	3.68		
9	3.01		
10	2.73		
11	2.47		
12	2.37		
13	2.35		
14	2.23		
15	1.92		
16	1.65		
17	1.35		
18	1.00		
19	0.821		
20	0.743		
21	0.608		
22	0.498		
23	0.369		
24	0.298		

a. The upper energy of group 1 is 17.33 MeV.

program. A plan view of the surveillance capsules attached to the reactor vessel is shown in Figure 6-2A. As seen in Figure 6-2B, the stainless steel capsule holder is basically a 1.503-inch by 2.178-inch rectangular tube with a 0.12 inch wall. The monitors are embedded in carbon steel.

From a neutronic standpoint, the surveillance capsule structures are significant. In fact, as is shown later, they have a marked effect on the distributions of neutron flux and energy spectra in the water annulus between the core barrel and the reactor vessel. Thus, in order to properly ascertain the neutron environment at the test specimen locations, the capsules themselves must be included in the analytical model. Use of at least a two-dimensional computation is therefore mandatory.

In the analysis of the neutron environment within the Palisades reactor geometry, predictions of neutron flux magnitude and energy spectra were made with the DOT[4] two-dimensional discrete ordinates code. The radial and azimuthal distributions were obtained from an R,θ computation wherein the geometry shown in Figure 6-1 was described in the analytical model.

The R,θ analyses employed 26 neutron energy groups and a P_3 expansion of the scattering cross sections. The cross sections used in the analyses were obtained from the SAILOR cross section library[5] which was developed specifically for light water reactor applications. The neutron energy group structure used in the analysis is listed in Table 6-1.

A key input parameter in the analysis of the integrated fast neutron exposure of the reactor vessel is the core power distribution. For this analysis, Palisades Cycle 5 power distributions were employed. These input distributions include rod-by-rod spatial variations for all peripheral fuel assemblies.

Having the results of the R,θ calculation and an axial peaking factor, three-dimensional variations of neutron flux may be approximated by assuming that the following relation holds for the applicable regions of the reactor.

$$\phi(R,Z,\theta,E_g) = \phi(R,\theta,E_g) \times 1.2 \quad (6\text{-}1)$$

where

$\phi(R,Z,\theta,E_g)$ = neutron flux at point R,Z,θ within energy group g

$\phi(R,\theta,E_g)$ = neutron flux at point R,θ within energy group g obtained from the R,θ calculation

1.2 = axial peaking factor for the midplane of the core

6-3. NEUTRON DOSIMETRY

The passive neutron flux monitors included in Capsule W-290 of Palisades are listed in Table 6-2. The first five reactions in Table 6-2 are used as fast neutron monitors to relate neutron fluence (E > 1.0 MeV) to measured material property changes.

TABLE 6-2

NUCLEAR CONSTANTS FOR NEUTRON FLUX MONITORS CONTAINED IN THE PALISADES SURVEILLANCE CAPSULE

Monitor Material	Reaction of Interest	Target Weight Fraction	Product Half-life	Fission Yield (%)
Copper[a]	Cu^{63} (n,α) Co^{60}	0.6917	5.27 years	
Iron	Fe^{54} (n,p) Mn^{54}	0.0585	314 days	
Nickel[a]	Ni^{58} (n,p) Co^{58}	0.6777	71.4 days	
Uranium-238[a]	U^{238} (n,f) Cs^{137}	1.0	30.2 years	6.3
Titanium	Ti^{46} (n,p) Sc^{46}	0.0825	83.8 days	
Uranium	U^{238} (n,f) Cs^{137}	1.0	30.2 years	6.3

a. Denotes that monitor is cadmium-shielded

The relative locations of the various monitors within the surveillance capsule are shown in Figure 6-2.

The use of passive monitors such as those listed in Table 6-2 does not yield a direct measure of the energy-dependent flux level at the point of interest. Rather, the activation or fission process is a measure of the integrated effect that the time- and energy-dependent neutron flux has on the target material over the course of the irradiation period. An accurate assessment of the average neutron flux level incident on the various monitors may be derived from the activation measurements only if the irradiation parameters are well known. In particular, the following variables are of interest.

- The operating history of the reactor
- The energy response of the monitor
- The neutron energy spectrum at the monitor location
- The physical characteristics of the monitor

The analysis of the passive monitors and subsequent derivation of the average neutron flux requires completion of two operations. First, the disintegration rate of product isotope per unit mass of monitor must be determined. Second, in order to define a suitable spectrum-averaged reaction cross section, the neutron energy spectrum at the monitor location must be calculated.

The specific activity of each of the monitors is determined using established ASTM procedures.[7,8,9,10,11] Following sample preparation, the activity of each monitor is determined by means of a lithium-drifted germanium, Ge(Li), gamma spectrometer. The overall standard deviation of the measured data is a function of the precision of sample weighing, the uncertainty in counting, and the acceptable error in detector calibration. For the samples removed from Palisades, the overall 2σ deviation in the measured data is determined to be plus or minus 10 percent. The neutron energy spectra are determined analytically using the method described in paragraph 6-1.

Having the measured activity of the monitors and the neutron energy spectra at the locations of interest, the calculation of the neutron flux proceeds as follows. The reaction product activity in the monitor is expressed as

$$R = \frac{N_o}{A} f_i \, Y \int_E \sigma(E)\phi(E)dE \sum_{j=1}^{n} \frac{P_j}{P_{max}} (1-e^{-\lambda t_j}) \, e^{-\lambda t_d} \qquad (6\text{-}2)$$

where

R = induced product activity

N_o = Avogadro's number

A = atomic weight of the target isotope

f_i = weight fraction of the target isotope in the target material

Y = number of product atoms produced per reaction

$\sigma(E)$ = energy dependent reaction cross section

$\phi(E)$ = energy dependent neutron flux at the monitor location with the reactor at full power

P_j = average core power level during irradiation period j

P_{max} = maximum or reference core power level

λ = decay constant of the product isotope

t_j = length of irradiation period j

t_d = decay time following irradiation period j

Because neutron flux distributions are calculated using multigroup transport methods and, further, because the prime interest is in the fast neutron flux above 1.0 MeV, spectrum-averaged reaction cross sections are defined such that the integral term in equation (6-2) is replaced by the following relation.

$$\int_E \sigma(E)\phi(E)dE = \bar{\sigma}\ \phi\ (E > 1.0\ \text{MeV})$$

where

$$\bar{\sigma} = \frac{\int_0^{\infty} \sigma(E)\phi(E)dE}{\int_{1.0\ \text{MeV}}^{\infty} \phi(E)dE} = \frac{\sum_{g=1}^{N} \sigma_g \phi_g}{\sum_{g=g_{1.0\ \text{MeV}}}^{N} \phi_g}$$

Thus, equation (6-2) is rewritten

$$R = \frac{N_o}{A} f_i\ Y\ \bar{\sigma}\ \phi\ (E > 1.0\ \text{MeV}) \sum_{j=1}^{N} \frac{P_j}{P_{max}} (1-e^{-\lambda t_j})\ e^{-\lambda t_d}$$

or, solving for the neutron flux,

$$\phi(E > 1.0 \text{ MeV}) = \frac{R}{\frac{N_o}{A} f_i \, Y \, \bar{\sigma} \sum_{j=1}^{n} \frac{P_j}{P_{max}} (1-e^{-\lambda t_j}) \, e^{-\lambda t_d}} \quad (6\text{-}3)$$

The total fluence above 1.0 MeV is then given by

$$\Phi(E> 1.0 \text{ MeV}) = \phi(E> 1.0 \text{ MeV}) \sum_{j=1}^{n} \frac{P_j}{P_{max}} t_j \quad (6\text{-}4)$$

where

$\sum_{j=1}^{n} \frac{P_j}{P_{max}} t_j$ = total effective full power seconds of reactor operation up to the time of capsule removal

6-4. TRANSPORT ANALYSIS RESULTS

Results of the S_n transport calculations for the Palisades reactor are summarized in Figures 6-3 through 6-10 and in Tables 6-3 and 6-4. In Figure 6-3, the calculated maximum neutron flux levels at the surveillance capsule centerline, pressure vessel inner radius, 1/4 thickness location, and 3/4 thickness location are presented as a function of azimuthal angle. The influence of the surveillance capsules on the fast neutron flux distribution is clearly evident. In Figure 6-4, the radial distribution of maximum fast neutron flux (E > 1.0 MeV) through the thickness of the reactor pressure vessel is shown.

Figure 6-5, presents the radial variations of fast neutron flux within surveillance capsule W-290. This data, in conjunction with the maximum vessel flux, are used to develop a lead factor for capsule W-290. Here the lead factor is defined as the ratio of the fast neutron flux (E > 1.0 MeV) at the capsule center to the maximum fast neutron flux at the pressure vessel inner radius. The lead factor for Capsule W-290 is 1.28.

Figures 6-6 through 6-10 present the calculated variation of fast neutron flux monitor saturated activity within capsule W-290.

TABLE 6-3

CALCULATED NEUTRON ENERGY SPECTRA ABOVE 0.1 MeV AT THE CENTER OF PALISADES CAPSULE

Group No.	ϕ (n/cm^2-sec)	GROUP No.	ϕ (n/cm^2-sec)
1	3.71×10^{7}	14	3.11×10^{9}
2	1.35×10^{8}	15	7.70×10^{9}
3	4.55×10^{8}	16	8.24×10^{9}
4	8.26×10^{8}	17	1.13×10^{10}
5	1.38×10^{9}	18	1.67×10^{10}
6	3.24×10^{9}	19	1.04×10^{10}
7	4.47×10^{9}	20	5.21×10^{9}
8	7.83×10^{9}	21	1.48×10^{10}
9	5.67×10^{9}	22	1.04×10^{10}
10	4.26×10^{9}	23	1.31×10^{10}
11	4.79×10^{9}	24	1.16×10^{10}
12	2.38×10^{9}	25	1.45×10^{10}
13	6.40×10^{8}	26	1.41×10^{10}

TABLE 6-4

SPECTRUM-AVERAGED REACTION CROSS SECTIONS AT THE CENTER OF PALISADES SURVEILLANCE CAPSULES

Reaction	$\bar{\sigma}$ (barns)[a]
Fe^{54} (n,p) Mn^{54}	0.12700
Cu^{63} (n,α) Co^{60}	0.00129
Ni^{58} (n,p) Co^{58}	0.16130
Ti^{46} (n,p) Sc^{46}	0.02300
U^{238}(n,f) Cs^{137}	0.43700

a. $$\bar{\sigma} = \frac{\int_0^\infty \sigma(E)\phi(E)dE}{\int_{1\ MeV}^\infty \phi(E)dE}$$

TABLE 6-5

IRRADIATION HISTORY OF PALISADES

SURVEILLANCE CAPSULE W-290

Month	Year	P_j (MW)	P_{max} (MW)	P_j/P_{max}	Irradiation Time (Days)	Decay Time[a] (Days)
12	1971	26	2530	.010	1	4561
1	1972	209	2530	.083	31	4530
2	1972	24	2530	.009	29	4501
3	1972	332	2530	.131	31	4470
4	1972	722	2530	.285	30	4440
5	1972	0	2530	.000	31	4409
6	1972	951	2530	.376	30	4379
7	1972	900	2530	.356	31	4348
8	1972	1065	2530	.421	31	4317
9	1972	681	2530	.269	30	4287
10	1972	983	2530	.388	31	4256
11	1972	767	2530	.303	30	4226
12	1972	1440	2530	.569	31	4195
1	1973	897	2530	.355	31	4164
2	1973	0	2530	.000	28	4136
3	1973	1424	2530	.563	31	4105
4	1973	2152	2530	.851	30	4075
5	1973	1321	2530	.522	31	4044
6	1973	2192	2530	.866	30	4014
7	1973	2062	2530	.815	31	3983
8	1973	640	2530	.253	31	3952
9	1973	0	2530	.000	30	3922
10	1973	0	2530	.000	31	3891
11	1973	0	2530	.000	30	3861
12	1973	0	2530	.000	31	3830

a. Decay time is referenced to 6/27/84.

TABLE 6-5 (Cont)

IRRADIATION HISTORY OF PALISADES

SURVEILLANCE CAPSULE W-290

Month	Year	P_j (MW)	P_{max} (MW)	P_j/P_{max}	Irradiation Time (Days)	Decay Time[a] (Days)
1	1974	0	2530	.000	31	3799
2	1974	0	2530	.000	28	3771
3	1974	0	2530	.000	31	3740
4	1974	0	2530	.000	30	3710
5	1974	0	2530	.000	31	3679
6	1974	0	2530	.000	30	3649
7	1974	0	2530	.000	31	3618
8	1974	0	2530	.000	31	3587
9	1974	0	2530	.000	30	3557
10	1974	384	2530	.152	31	3526
11	1974	8	2530	.003	30	3496
12	1974	0	2530	.000	31	3465
1	1975	0	2530	.000	31	3434
2	1975	0	2530	.000	28	3406
3	1975	0	2530	.000	31	3375
4	1975	1263	2530	.499	30	3345
5	1975	1699	2530	.672	31	3314
6	1975	1115	2530	.441	30	3284
7	1975	1338	2530	.529	31	3253
8	1975	874	2530	.346	31	3222
9	1975	1277	2530	.505	30	3192
10	1975	1450	2530	.573	31	3161
11	1975	1597	2530	.631	30	3131
12	1975	598	2530	.236	31	3100
1	1976	0	2530	.000	31	3069
2	1976	0	2530	.000	29	3040
3	1976	0	2530	.000	31	3009

a. Decay time is referenced to 6/27/84.

TABLE 6-5 (Cont)

IRRADIATION HISTORY OF PALISADES

SURVEILLANCE CAPSULE W-290

Month	Year	P_j (MW)	P_{max} (MW)	P_j/P_{max}	Irradiation Time (Days)	Decay Time[a] (Days)
4	1976	0	2530	.000	30	2979
5	1976	707	2530	.279	31	2948
6	1976	2086	2530	.825	30	2918
7	1976	11	2530	.005	31	2887
8	1976	1636	2530	.647	31	2856
9	1976	1961	2530	.775	30	2826
10	1976	1605	2530	.634	31	2795
11	1976	1507	2530	.595	30	2765
12	1976	2063	2530	.816	31	2734
1	1977	1870	2530	.739	31	2703
2	1977	2133	2530	.843	28	2675
3	1977	1983	2530	.784	31	2644
4	1977	2008	1530	.794	30	2614
5	1977	1360	2530	.538	31	2583
6	1977	2173	2530	.859	30	2553
7	1977	1975	2530	.780	31	2522
8	1977	1438	2530	.567	31	2491
9	1977	1880	2530	.743	30	2461
10	1977	2153	2530	.851	31	2430
11	1977	1954	2530	.772	30	2400
12	1977	2176	2530	.860	31	2369
1	1978	343	2530	.135	31	2338
2	1978	0	2530	.000	28	2310
3	1978	0	2530	.000	31	2279
4	1978	482	2530	.191	30	2249
5	1978	1206	2530	.477	31	2218
6	1978	1574	2530	.622	30	2188

a. Decay time is referenced to 6/27/84.

TABLE 6-5 (Cont)

IRRADIATION HISTORY OF PALISADES

SURVEILLANCE CAPSULE W-290

Month	Year	P_j (MW)	P_{max} (MW)	P_j/P_{max}	Irradiation Time (Days)	Decay Time[a] (Days)
7	1978	1603	2530	.633	31	2157
8	1978	1254	2530	.496	31	2126
9	1978	680	2530	.269	30	2096
10	1978	1454	2530	.575	31	2065
11	1978	2249	2530	.889	30	2035
12	1978	1092	2530	.432	31	2004
1	1979	2275	2530	.899	31	1973
2	1979	2229	2530	.881	28	1945
3	1979	2277	2530	.900	31	1914
4	1979	1835	2530	.725	30	1884
5	1979	764	2530	.302	31	1853
6	1979	1695	2530	.670	30	1823
7	1979	2163	2530	.855	31	1792
8	1979	1979	2530	.782	31	1761
9	1979	410	2530	.162	30	1731
10	1979	0	2530	.000	31	1700
11	1979	0	2530	.000	30	1670
12	1979	0	2530	.000	31	1639
1	1980	0	2530	.000	31	1608
2	1980	0	2530	.000	29	1579
3	1080	0	2530	.000	31	1548
4	1980	0	2530	.084	30	1518
5	1980	213	2530	.084	31	1487
6	1980	2164	2530	.855	30	1457
7	1980	1516	2530	.599	31	1426
8	1980	1706	2530	.674	31	1395
9	1980	1763	2530	.697	30	1365

a. Decay time is referenced to 6/27/84.

TABLE 6-5 (Cont)

IRRADIATION HISTORY OF PALISADES

SURVEILLANCE CAPSULE W-290

Month	Year	P_j (MW)	P_{max} (MW)	P_j/P_{max}	Irradiation Time (Days)	Decay Time[a] (Days)
10	1980	2201	2530	.870	31	1334
11	1980	0	2530	.000	30	1304
12	1980	1194	2530	.472	31	1273
1	1981	2336	2530	.923	31	1242
2	1981	2426	2530	.959	28	1214
3	1981	2449	2530	.968	31	1183
4	1981	2390	2530	.945	30	1152
5	1981	2200	2530	.870	31	1122
6	1981	2089	2530	.826	30	1092
7	1981	799	2530	.316	31	1061
8	1981	1084	2530	.428	31	1030
9	1981	0	2530	.000	30	1000
10	1981	0	2530	.000	31	969
11	1981	0	2530	.000	30	939
12	1981	0	2530	.000	31	908
1	1982	1217	2530	.481	31	877
2	1982	246	2530	.097	28	849
3	1982	907	2530	.359	31	818
4	1982	0	2530.	.000	30	788
5	1982	481	2530	.190	31	757
6	1982	2203	2530	.871	30	727
7	1982	753	2530	.298	31	696
8	1982	0	2530	.000	31	665
9	1982	2129	2530	.841	30	635
10	1982	2222	2530	.878	31	604
11	1982	2484	2530	.982	30	574
12	1982	2471	2530	.977	31	543

a. Decay time is referenced to 6/27/84.

TABLE 6-5 (Cont)

IRRADIATION HISTORY OF PALISADES

SURVEILLANCE CAPSULE W-290

Month	Year	P_j (MW)	P_{max} (MW)	P_j/P_{max}	Irradiation Time (Days)	Decay Time[a] (Days)
1	1983	2324	2530	.918	31	512
2	1983	2468	2530	.975	28	484
3	1983	2470	2530	.976	31	453
4	1983	2345	2530	.927	30	423
5	1983	2222	2530	.878	31	392
6	1983	2367	2530	.936	30	362
7	1983	2222	2530	.878	31	331
8	1983	684	2530	.270	31	300
9	1983	0	2530	.000	16	284

EFPS = 1.57×10^8 sec

EFPY = 4.975

a. Decay time is referenced to 6/27/84.

In order to derive neutron flux and fluence levels from the measured disintegration rates, suitable spectum-averaged reaction cross sections are required. The neutron energy spectrum calculated to exist at the center of Palisades capsule is listed in Table 6-3. The associated spectrum-averaged cross sections for each of the fast neutron reactions are given in Table 6-4.

6-5. DOSIMETRY RESULTS

The irradiation history of the Palisades reactor up to the time of removal of Capsule W-290 is listed in Table 6-5. Comparisons of measured and calculated saturated activity of the flux monitors contained in Capsule W-290 based on the irradiation history shown in Table 6-5 are given in Table 6-6. The fast neutron (E > 1.0 MeV) flux and fluence levels derived for Capsule W-290 are presented in Table 6-7.

An examination of Table 6-7 shows that the fast neutron flux (E > 1.0 MeV) derived from the five threshold reactions ranges from 6.48×10^{10} to 7.84×10^{10} n/cm^2-sec, a total span of 30 percent. It may also be noted that the calculated flux value of 8.32×10^{10} n/cm^2-sec exceeds all of the measured values, with calculation to experimental ratios ranging from 1.06 to 1.28.

Comparisons of measured and calculated current fast neutron exposures for Capsule W-290 as well as for the inner radius of the pressure vessel are presented in Table 6-8. Measured values are given based on the $Fe^{54}(n,p)$ Mn^{54} reaction alone as well as for the average of all five threshold reactions. Based on the average data given in Table 6-8, the best estimate exposure of Capsule W-290 is

$$\Phi_T = 1.09 \times 10^{19} \ n/cm^2 \ (E > 1 \ MeV)$$

In addition, a fast neutron flux check was made of a fractured Charpy V-notch specimen from the thermal capsule, Capsule T-330. This analysis showed that Capsule T-330 was exposed to only a very minimal level of fast neutron flux, six orders of magnitude less than the exposure of Capsule W-290.

TABLE 6-6

COMPARISON OF MEASURED AND CALCULATD FAST NEUTRON FLUX MONITOR SATURATED ACTIVITIES FOR CAPSULE W-290

	Reaction and Z Location	R Location (CM)	Activity $(\frac{dis/s}{g})$		Saturated Activity $(\frac{dis/s}{g})$ Capsule W-290	Saturated Activity $(\frac{dis/s}{g})$ Calculated
	$Cu^{63}(n,d)Co^{60}$					
Top	84-1751	215.42	2.32E+05		6.87E+05	
Middle	84-1762	215.42	2.39E+05		7.08E+05	
Bottom	84-1773	215.42	2.07E+05		6.13E+05	
				Average	6.69E+05	7.11E+05
	$Fe^{54}(n,p)Mn^{54}$					
	84-1748	215.42	1.88E+06		5.76E+06	
	84-1754	215.42	1.77E+06		5.43E+06	
	84-1753	215.42	1.85E+06		5.67E+06	
Top	84-1754	215.42	1.89E+06		5.80E+06	
	84-1755	215.42	1.75E+06		5.37E+06	
	84-1756	215.42	1.95E+06		5.98E+06	
	84-1759	215.42	1.88E+06		5.76E+06	
	84-1763	215.42	1.86E+06		5.70E+06	
	84-1764A	215.42	1.86E+06		5.70E+06	
Middle	84-1765	215.42	1.75E+06		5.37E+06	
	84-1766	215.42	1.91E+06		5.86E+06	
	84-1767	215.42	1.66E+06		5.09E+06	
	84-1770	215.42	1.39E+06		4.26E+06	
	84-1774	215.42	1.67E+06		5.12E+06	
	84-1764B	215.42	1.66E+06		5.09E+06	
Bottom	84-1776	215.42	1.57E+06		4.81E+06	
	84-1777	215.42	1.74E+06		5.34E+06	
	84-1778	215.42	1.47E+06		4.51E+06	
				Average	5.37E+06	6.89E+06

TABLE 6-6 (Cont)

COMPARISON OF MEASURED AND CALCULATD FAST NEUTRON FLUX MONITOR SATURATED ACTIVITIES FOR CAPSULE W-290

	Reaction and Z Location	R Location	Activity		Saturated Activity	
	$Ni^{58}(n,p)Co^{58}$	(CM)	(dis/s / g)		(dis/s / g) Capsule W-290	(dis/s / g) Calculated
Top	84-1750	215.42	3.06E+06		7.72E+07	
Middle	84-1761	215.42	3.05E+06		7.70E+07	
Bottom	84-1772	215.42	2.90E+06		7.32E+07	
				Average	7.58E+07	9.43E+07
	$U^{238}(n,f)Cs^{137}$					
Top	84-1749	215.42	5.56E+05		5.52E+06	
Bottom	84-1771	215.42	5.36E+05		5.32E+06	
				Average	5.42E+06	5.79E+06
	$Ti^{46}(n,p)Sn^{46}$					
Top	84-1747	215.42	1.10E+05		1.78E+06	
Middle	84-1758	215.42	1.06E+05		1.71E+06	
Bottom	84-1769	215.42	1.01E+05		1.63E+06	
				Average	1.71E+06	2.07E+06

TABLE 6-7

RESULTS OF FAST NEUTRON DOSIMETRY FOR CAPSULE W-290

Reaction	$(\frac{dis/s}{g})$ Measured	$(\frac{dis/s}{g})$ Calculated	ϕ (E > 1.0 Mev) (n/cm^2-sec) Measured	ϕ (E > 1.0 Mev) (n/cm^2-sec) Calculated	Φ (E > 1.0 Mev) (n/cm^2) Measured	Φ (E > 1.0 Mev) (n/cm^2) Calculated
$Fe^{54}(n,p)Mn^{54}$	5.37×10^6	6.89×10^6	6.48×10^{10}	8.32×10^{10}	1.02×10^{19}	1.31×10^{19}
$Cu^{63}(n,\alpha)Co^{60}$	6.69×10^5	7.11×10^5	7.84×10^{10}	8.32×10^{10}	1.23×10^{19}	1.31×10^{19}
$Ni^{58}(n,p)Co^{58}$	7.58×10^7	9.43×10^7	6.68×10^{10}	8.32×10^{10}	1.05×10^{19}	1.31×10^{19}
$Ti^{46}(n,p)Sc^{46}$	1.71×10^6	2.07×10^6	6.68×10^{10}	8.32×10^{10}	1.08×10^{19}	1.31×10^{19}
$U^{238}(n,f)Cs^{137}$ (a)	4.77×10^6	5.79×10^6	6.85×10^{10}	8.32×10^{10}	1.07×10^{19}	1.31×10^{19}
				Average	1.09×10^{19}	

a. U^{238} adjusted saturated activity has been multiplied by 0.88 to correct for 350 ppm U^{235} impurity.

8148B:1b/092684

TABLE 6-8
SUMMARY OF NEUTRON DOSIMETRY RESULTS FOR CAPSULE W-290

Location	Current Φ (E > 1.0 mev) (n/cm^2)		EOL Φ (E > 1.0 mev) (n/cm^2)	
	Measured	Calculated	Measured	Calculated
Capsule W-290	1.09×10^{19}	1.31×10^{19}		
Vessel IR	8.52×10^{18}	1.02×10^{19}	5.48×10^{19}	6.56×10^{19}
Vessel 1/4T	5.37×10^{18}	6.45×10^{18}	3.45×10^{19}	4.15×10^{19}
Vessel 3/4T	9.93×10^{17}	1.19×10^{18}	6.39×10^{18}	7.65×10^{18}

Note: EOL fluences are based on operation at 2530 MWt for 32 effective full-power years.

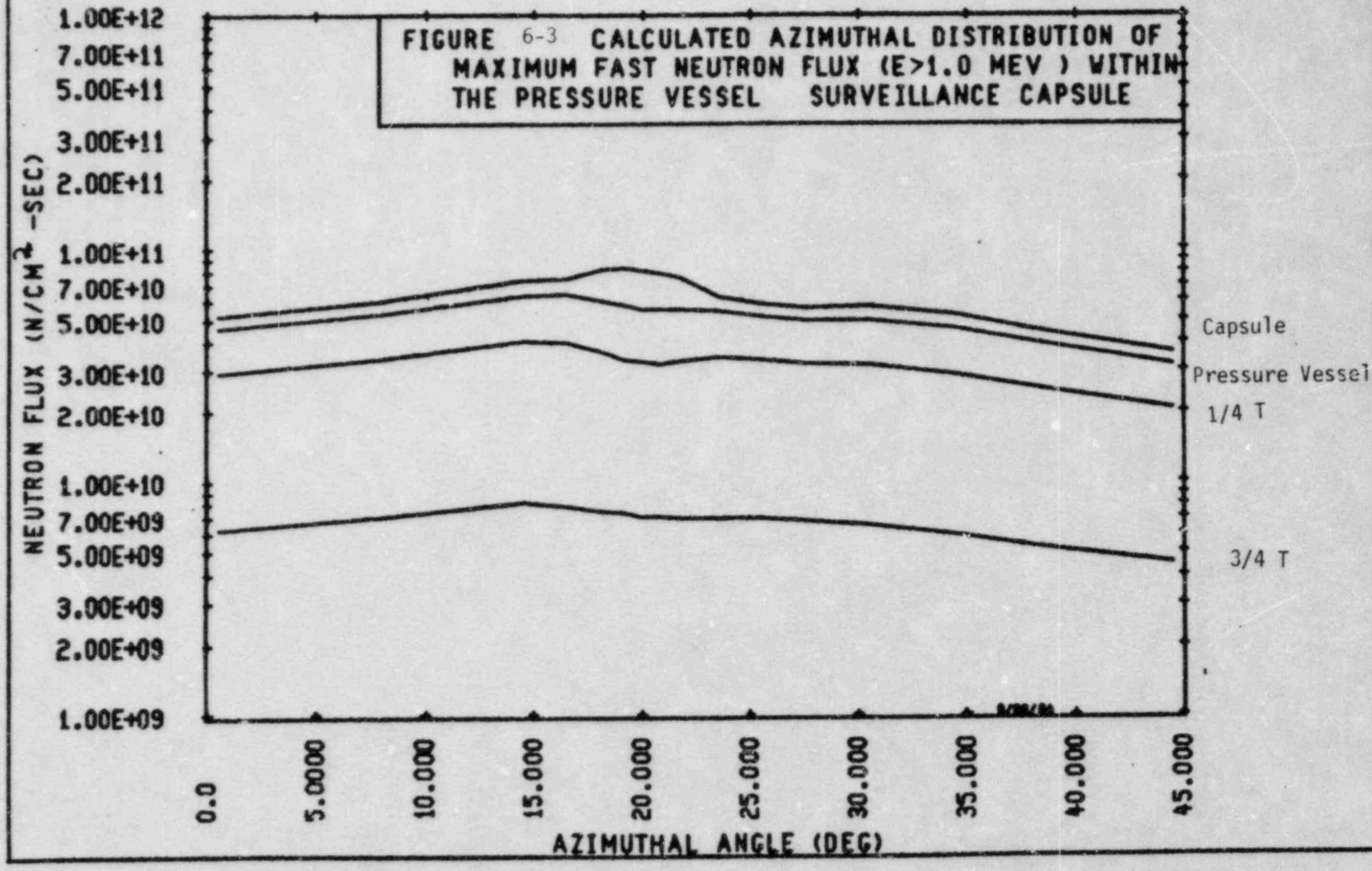

FIGURE 6-3 CALCULATED AZIMUTHAL DISTRIBUTION OF MAXIMUM FAST NEUTRON FLUX (E>1.0 MEV) WITHIN THE PRESSURE VESSEL SURVEILLANCE CAPSULE

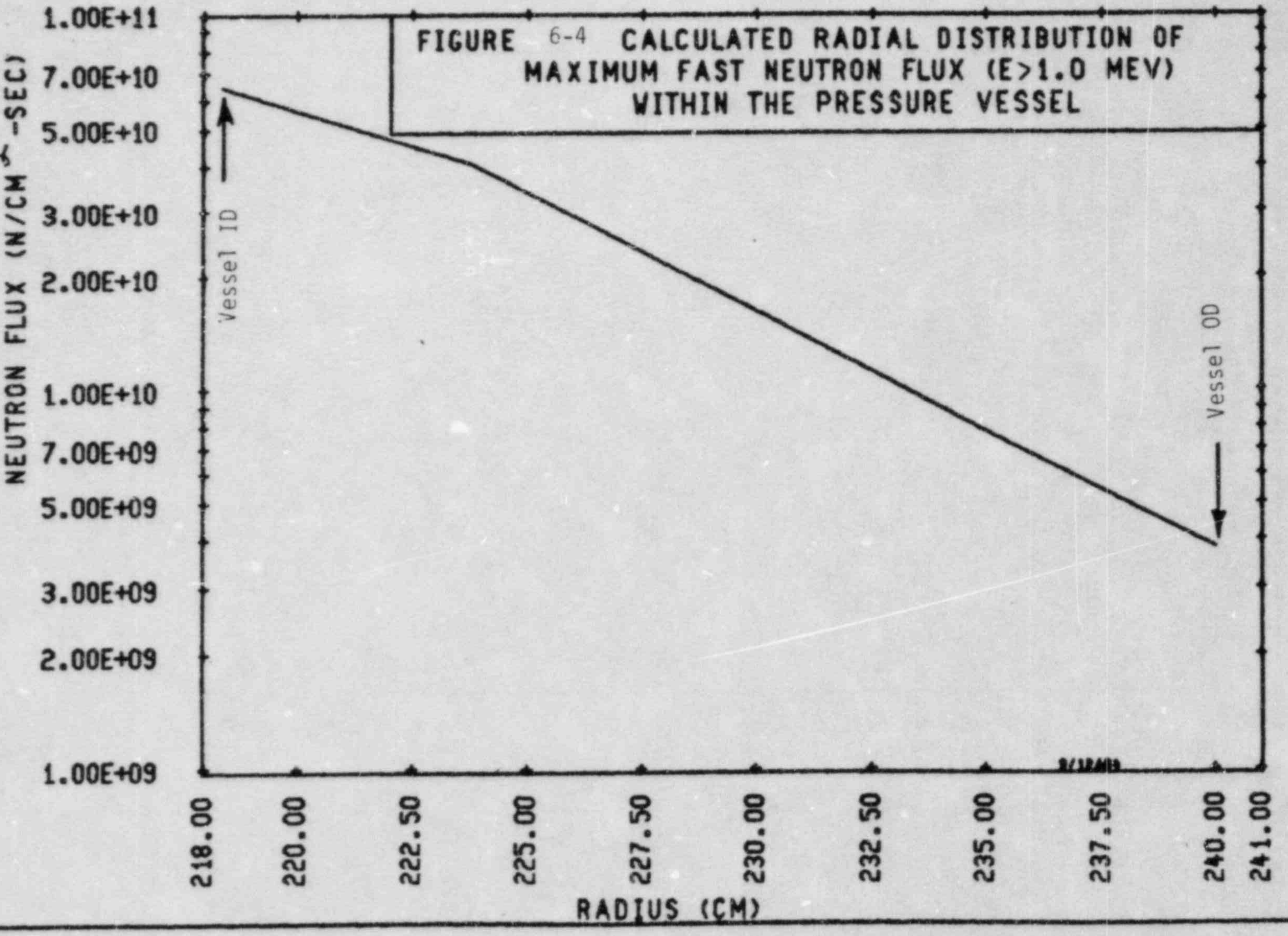

FIGURE 6-4 CALCULATED RADIAL DISTRIBUTION OF MAXIMUM FAST NEUTRON FLUX (E>1.0 MEV) WITHIN THE PRESSURE VESSEL

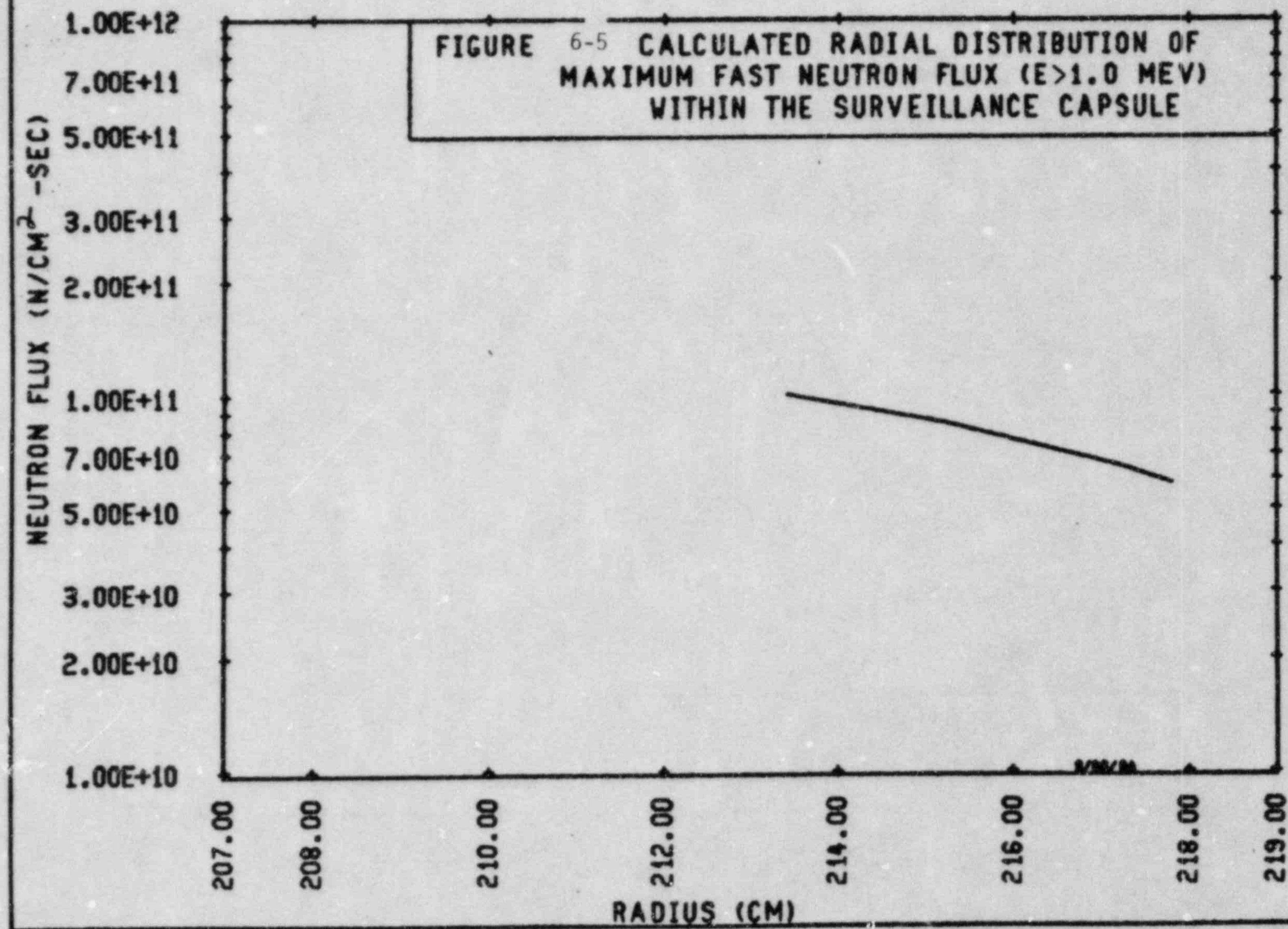

FIGURE 6-5 CALCULATED RADIAL DISTRIBUTION OF MAXIMUM FAST NEUTRON FLUX (E>1.0 MEV) WITHIN THE SURVEILLANCE CAPSULE

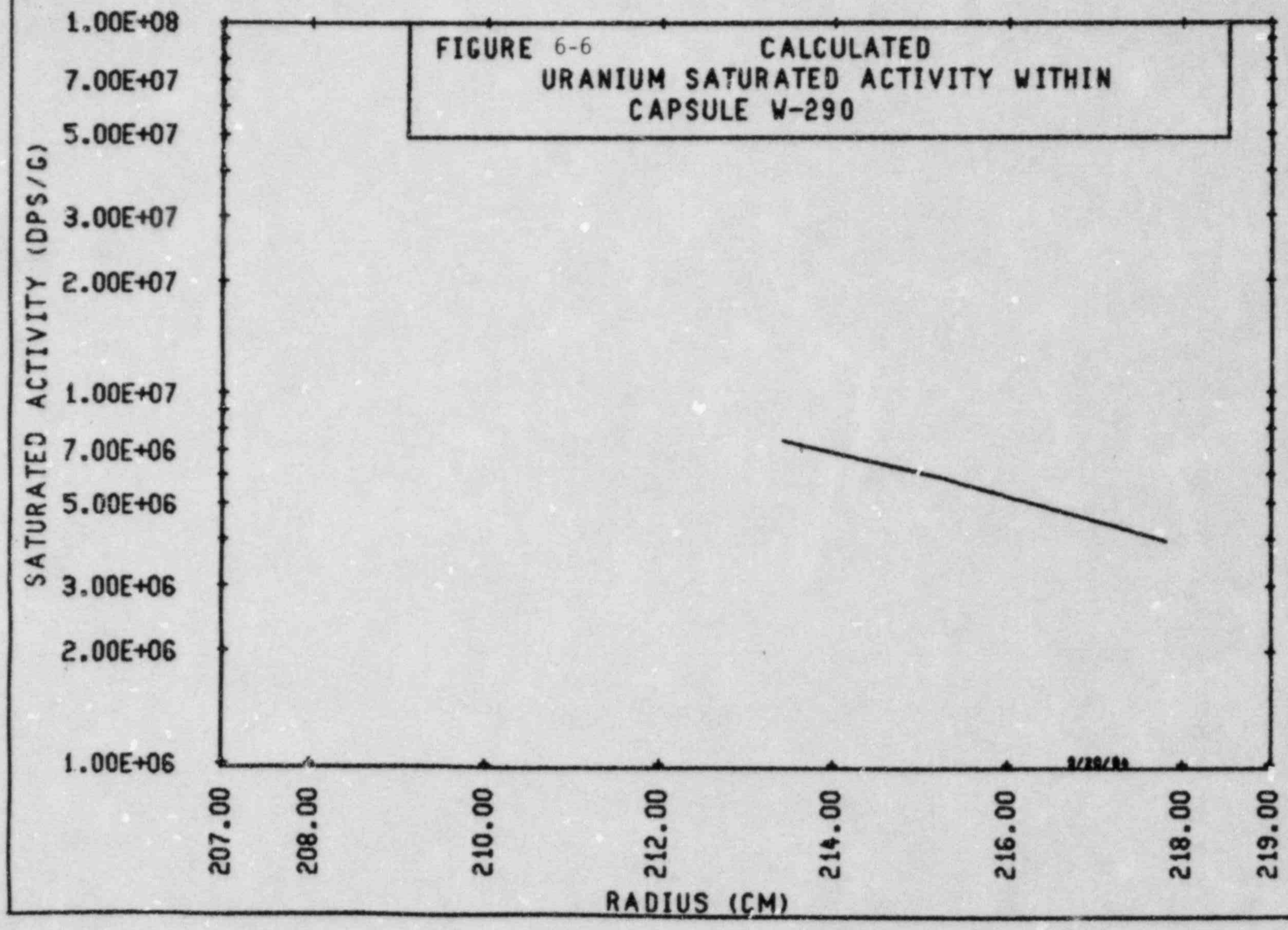

FIGURE 6-6 CALCULATED URANIUM SATURATED ACTIVITY WITHIN CAPSULE W-290

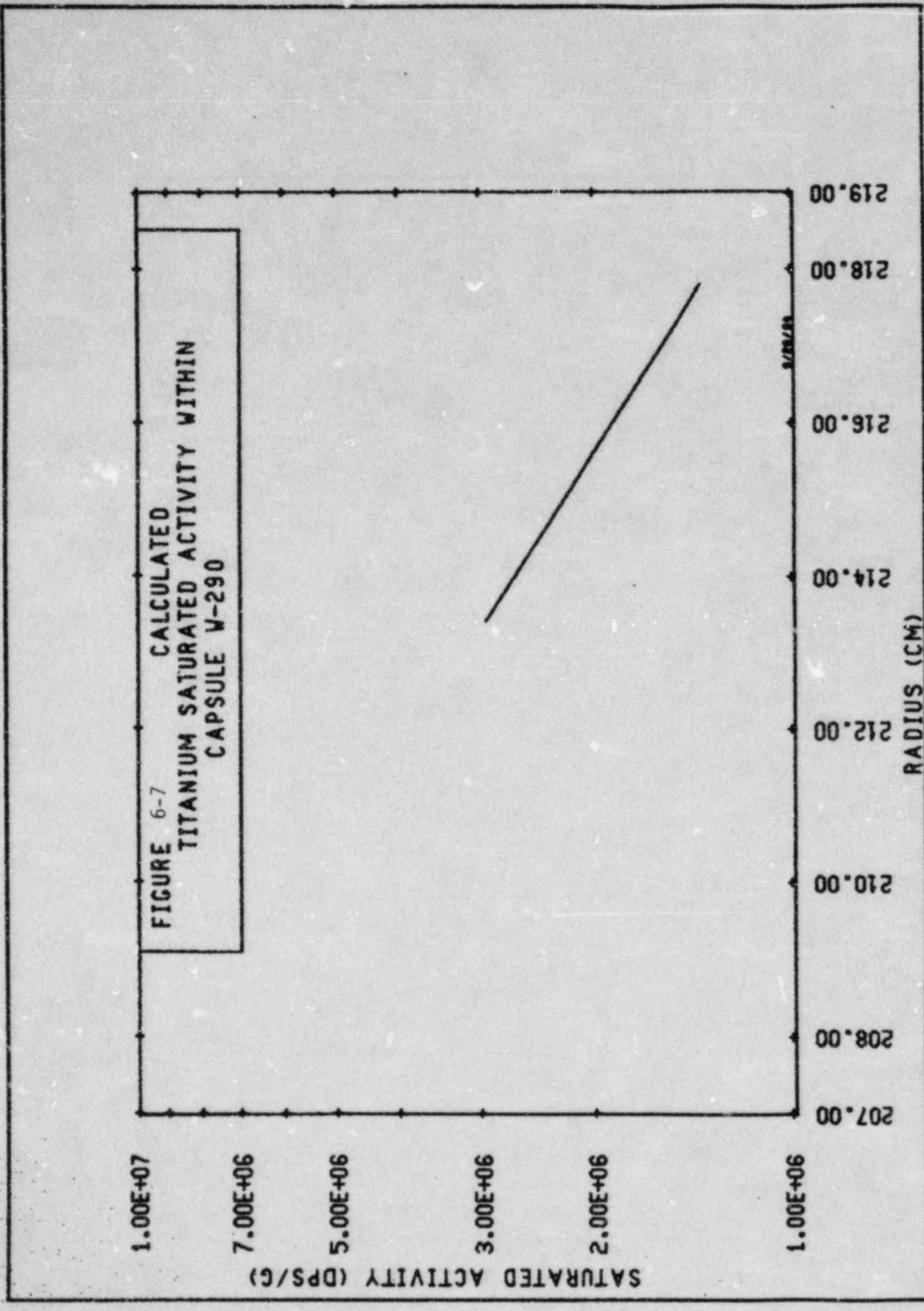

FIGURE 6-7 CALCULATED TITANIUM SATURATED ACTIVITY WITHIN CAPSULE W-290

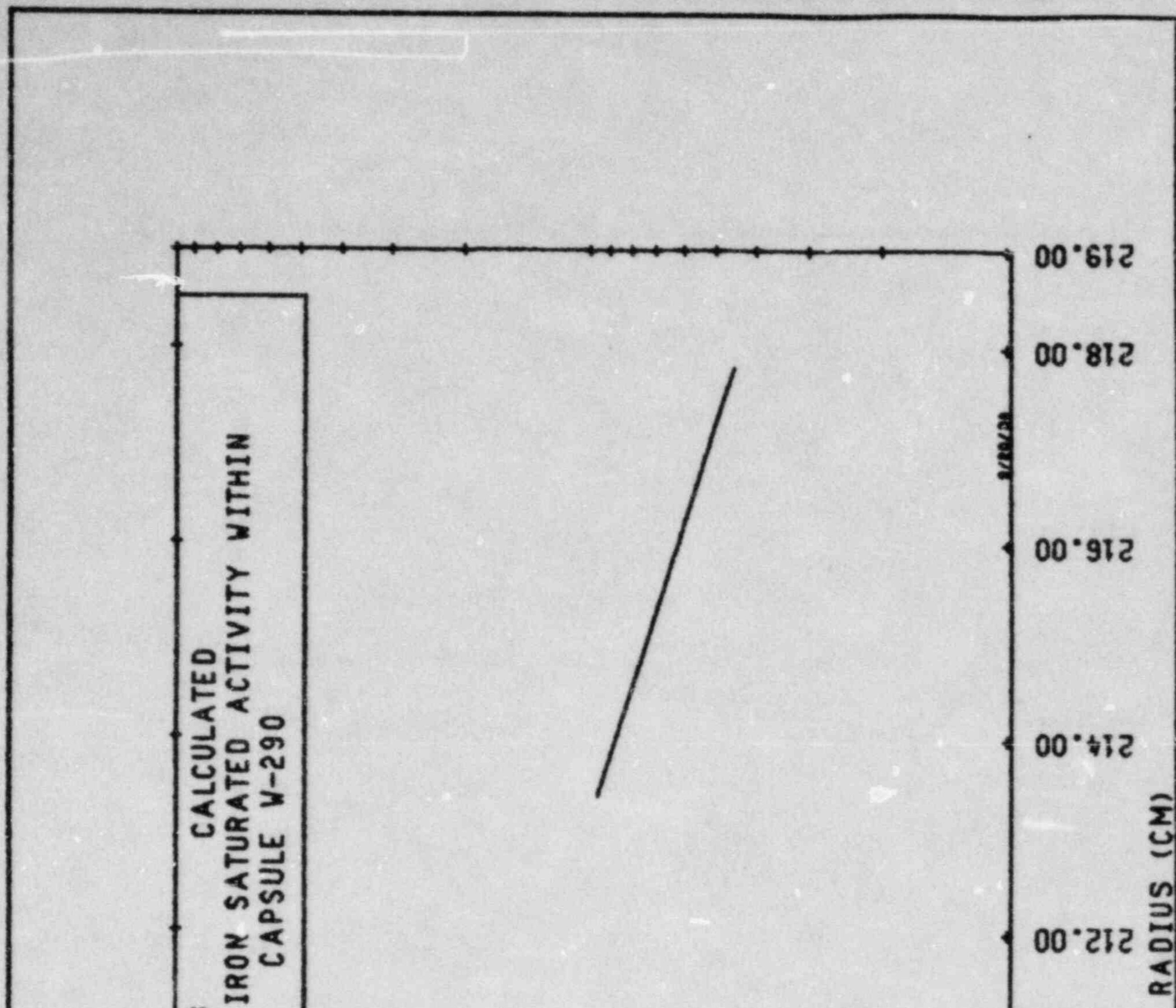
FIGURE 6-8 CALCULATED
IRON SATURATED ACTIVITY WITHIN
CAPSULE W-290
SATURATED ACTIVITY (DPS/G)
1.00E+08
7.00E+07
5.00E+07
3.00E+07
2.00E+07
1.00E+07
7.00E+06
5.00E+06
3.00E+06
2.00E+06
1.00E+06
RADIUS (CM)
207.00
208.00
210.00
212.00
214.00
216.00
218.00
219.00

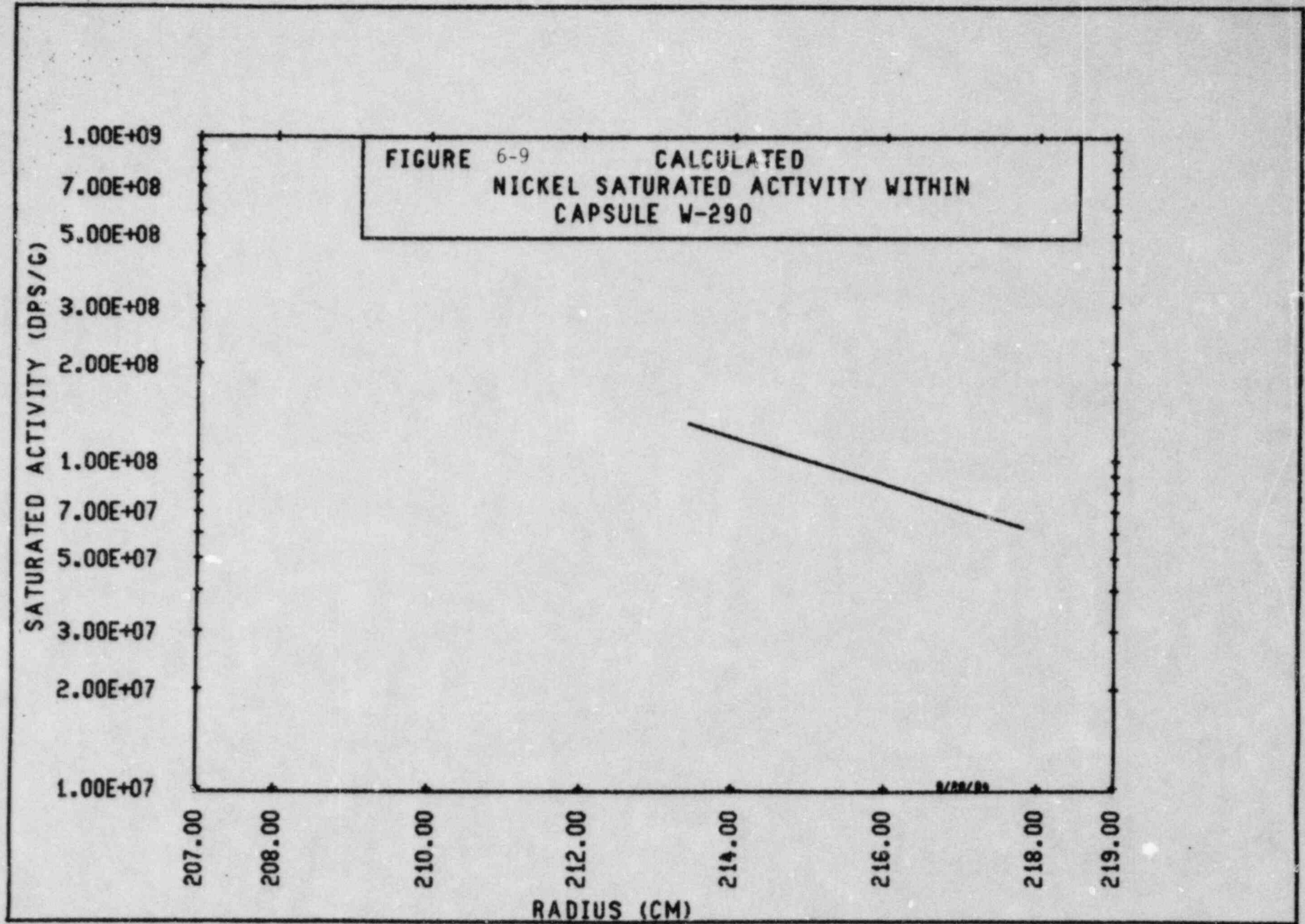
FIGURE 6-9 CALCULATED
NICKEL SATURATED ACTIVITY WITHIN
CAPSULE W-290
SATURATED ACTIVITY (DPS/G)
1.00E+09
7.00E+08
5.00E+08
3.00E+08
2.00E+08
1.00E+08
7.00E+07
5.00E+07
3.00E+07
2.00E+07
1.00E+07
207.00
208.00
210.00
212.00
214.00
216.00
218.00
219.00
RADIUS (CM)

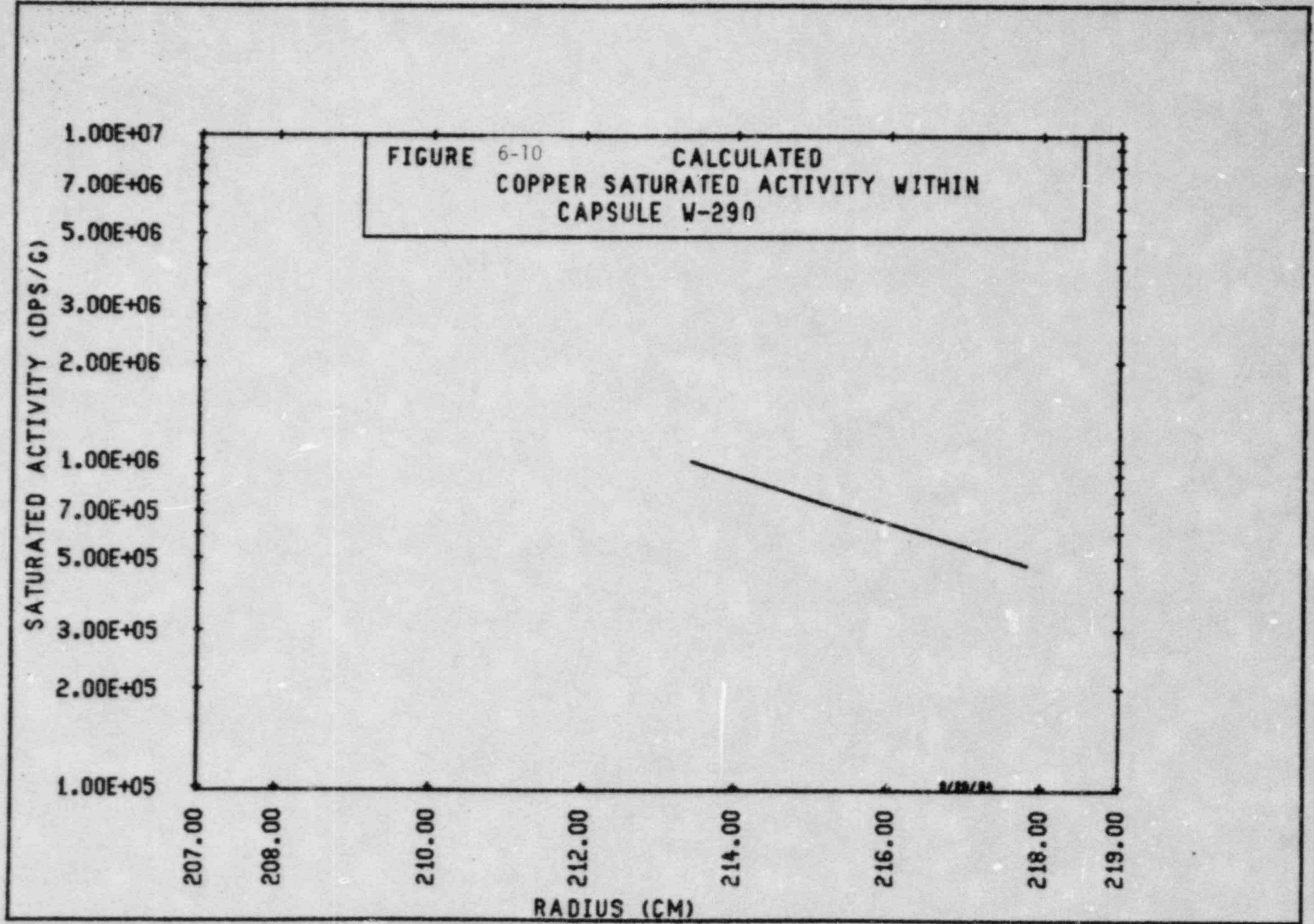
FIGURE 6-10 CALCULATED
COPPER SATURATED ACTIVITY WITHIN
CAPSULE W-290
SATURATED ACTIVITY (DPS/G)
1.00E+07
7.00E+06
5.00E+06
3.00E+06
2.00E+06
1.00E+06
7.00E+05
5.00E+05
3.00E+05
2.00E+05
1.00E+05
RADIUS (CM)
207.00
208.00
210.00
212.00
214.00
216.00
218.00
219.00

SECTION 7
REFERENCES

1. Groeschel, R. C., Summary Report on Manufacture of Test Specimens and Assembly of Capsules for Irradiation Surveillance of Palisades Reactor Vessel Materials, CE Report No. P-NLM-019, April 1, 1971.

2. Perrin, J. S., Farmelo, D. R. Jung, R. G., and Fromm, E. O., "Palisades Pressure Vessel Irradiation Capsule Program: Unirradiated Mechanical Properties", August 25, 1977.

3. Regulatory Guide 1.99, Revision 1, "Effects of Residual Elements on Predicted Radiation Damage to Reactor Vessel Materials," U.S. Nuclear Regulatory Commission, April 1977.

4. Soltesz, R. G., Disney, R. K., Jedruch, J., and Zeigler, S. L., "Nuclear Rocket Shielding Methods, Modification, Updating and Input Data Preparation. Vol. 5 - Vol. 5, August 1970.

5. SAILOR RSIC Data Library Collection "DLC-76," Coupled, Self-shielded, 47 Neutron, 20 Gamma-ray, P3, Cross Section Library for Light Water Reactors."

6. Benchmark Testing of Westinghouse Neutron Transport Analysis Methodology - to be published.

7. ASTM Designation E261-77, Standard Practice for Measuring Neutron Flux, Fluence, and Spectra by Radioactivation Techniques," in ASTM Standards (1981), Part 45, Nuclear Standards, pp. 915-926, American Society for testing and Materials, Philadelphia, Pa., 1981.

8. ASTM Designation E262-77, "Standard Method for Measuring Thermal Neutron Flux by Radioactivation Techniques," in ASTM Standards (1981), Part 45, Nuclear Standards, pp. 927-935, American Society for Testing and Materials, Philadelphia, Pa., 1981.

9. ASTM Designation E263-77, "Standard Method for Measuring Fast-Neutron Flux by Radioactivation of Iron," in ASTM Standards (1981), Part 45, Nuclear Standards, pp. 936-941, American Society for testing and Materials, Philadelphia, PA., 1981.

10. ASTM Designation E481-78, "Standard Method of Measuring Neutron-Flux Density by Radioactivation of Cobalt and Silver," in ASTM Standards (1981), Part 45, Nuclear Standards, pp. 1063-1070, American Society for Testing and Materials, Philadelphia, Pa., 1981.

11. ASTM Designation E264-77, "Standard Method for Measuring Fast-Neutron Flux by Radioactivation of Nickel," in ASTM Standards (1981), Part 45, Nuclear Standards, pp. 942-945, American Society for Testing and Materials, Philadephia, Pa., 1981.

ATTACHMENT II

PALISADES REACTOR PRESSURE VESSEL WELDS

2 PAGES

Palisades RPV Welds

WELD SEAM	LOCATION	WELD DEPOSIT
1-112 A/C	Upper Shell Long. Seams	RACO 3 #W5214 Linde 1092 #3617 Ni-200 #N-7753A E8018 Electrodes CBBF, JBFG (repair)
2-112 A/C	Intermediate Shell Long. Seams	RACO 3 #W5214 Linde 1092 #3617 Ni-200 #N-7753A E8018 Electrodes (none)
3-112 A/C	Intermediate Shell Long. Seams	RACO 3 #W5214 Linde 1092 #3692 RACO 3 #34B009 Linde 1092 #3692 Ni-200 #N-7753A E8018 Electrode CBBF (repair)
7-112	Upper Shell to Flange Girth Seam	RACO 3 #W5214 Linde 1092 #3692 9.8a. RACO 3 ~~#34B004~~ Linde 1092 #3692 #34B009 Ni-200 #N-7753A and #N-98674 E8018 Electrode COGG (backweld) E8018 Electrode DAGG (weld grindout)
8-112	Upper to Intermediate Shell Girth Seam	RACO 3 #34B009 Linde 1092 #3692 Ni-200 #N-98674 E8018 Electrode 7B-47B, COFC (back weld)
9-112	Intermediate to Lower Shell Girth Seam	MIL-B4 Mod. #27204 Linde 1092 #3714 E8018 Electrode JBFG (back weld) MIL-B4 Mod. #27204 Linde 124 #3687 (weld repair) E8018 Electrode LODG (first layer and back weld) (weld repair)
10-112	Lower Shell to Bottom Head Girth Seam	MIL-B4 Mod. #27204 Linde 1092 #3714 E8018 Electrode HAEG (first layer and back weld)
12-112	Seal Ledge to Flange Seam	RACO 3 #W5214 Linde 1092 #3617 E7018 Electrode HOHF (back weld and fillet) E7018 Electrode ABCG (ledge ring repair)

Palisades RPV Welds

WELD SEAM	LOCATION	WELD DEPOSIT
1-113 A/F	Bottom Head Torus Long. Seams	E8018 Electrode 6M10B E8018 Electrode 704B (weld repair)
4-113	Bottom Head Dome to Torus Girth Seam	MIL-B4 Mod. #12420 Linde 1092 #3708 E8018 Electrode CBB4 (back weld)
1-118 A/F	Closure Head Torus Long. Seams	RACO 3 #W5214 Linde 1092 #3617 Ni-200 #N-7753A
6-118 A/B	Closure Head Girth Seams	MIL-B4 Mod. #12420 Linde 1092 #3708 E8018 Electrode CBBF (back weld)
-	Surveillance Program Weld	RACO 3 #3277 Linde 1092 #3833 Ni-200 #N-0591A (face weld only) E8018 Electrode HADH (back weld, base metal repair)